Sequence-Space Jacobians of Life-Cycle Models

Bence Bardóczy*[1], Akshay Shanker†[2], and Mateo Velásquez-Giraldo‡[1]

[1]Board of Governors of the Federal Reserve, RS:MQS
[2]Econ-ARK & University of New South Wales, Sydney

June 12, 2026

Abstract

The sequence-space Jacobian (SSJ) method of Auclert et al. (2021a) has made heterogeneous-agent models far easier to solve, fueling an explosion of applications. But even SSJ strains against capacity constraints when state spaces grow very large, as in economies with overlapping generations of heterogeneous agents (HA-OLG). We show how to exploit the special properties of age—finite planning horizons and deterministic transitions between ages—to compute the Jacobians of a general class of HA-OLG models orders of magnitude faster. We provide rigorous proofs, age-specific Jacobians that decompose aggregate dynamics across cohorts, an application to the dynamic general-equilibrium effects of secularly declining birth rates, and an accessible cookbook for adopting our method.

Keywords: life cycle, heterogeneous-agent models, sequence-space Jacobian, population aging, R-star

JEL Codes: C61, C63, D15.

*bence.a.bardoczy@frb.gov
†a.shanker@unsw.edu.au
‡mateo.velasquezgiraldo@frb.gov

 Shanker gratefully acknowledges support from the Alfred P. Sloan Foundation (2025-79177).

Accompanying public code to this paper can be found in https://github.com/Mv77/LC-SSJ_public.

We thank Adrien Auclert, Marlon Azinovic-Yang, Christopher D. Carroll, Hess Chung, Cristina Fuentes-Albero, Matthew Rognlie, Ludwig Straub, Matthew N. White, and participants in CEF 2025 for helpful comments.

1 Introduction

Advances in perturbation methods have accelerated the adoption of heterogeneous-agent models in macroeconomics.[1] The literature identifies dimensions of household heterogeneity that matter for macro dynamics. Wealth, portfolios, and marginal propensities to consume are prominent examples and they all vary substantially over the life cycle. In addition to heterogeneity, aggregate demographic changes such as secular shifts in migration and birth rates, have large effects on macroeconomic outcomes like the natural rate of interest and the sustainability of public debt.[2] Yet most existing work in heterogeneous-agent macro relies on infinite-horizon models that abstract from life-cycle dynamics and demographics. One reason is computational cost. Existing perturbation methods can accommodate life-cycle dynamics by treating age as an additional state variable. However, without a tailored representation or solution algorithm, expanding a model with 75 possible years or 300 possible quarters of age can make it prohibitively expensive to solve.

Age, however, has special properties that solution methods can exploit. First, its transitions are limited. A 20-year-old cannot turn 38, he either turns 21 or dies. All the future information relevant to a 20-year-old at time t is therefore contained in the value function of a 21-year-old at time $t+1$, $v_{t+1}(21)$, he is not concerned with $v_{t+1}(38)$. Second, in models without explicit dynastic motives, agents care only about events within their own lifetime. Shocks in the distant future therefore have no effect on their current actions. The life-cycle literature has long exploited these properties, but they have not, to our knowledge, been built into a general-purpose solution method for equilibrium macro models.

This paper formalizes the special properties of age and provides a practical guide to exploiting them in the sequence-space Jacobian (SSJ) framework of Auclert et al. (2021a). The result is an efficient algorithm for computing the dynamic effects of macroeconomic and demographic shocks in general-equilibrium models with overlapping generations of heterogeneous agents (HA-OLG). Our leading example is a life-cycle version of the Krusell and Smith (1998) model with 75 distinct ages and population growth. We use it to study a permanent fall in births and the secular demographic transition it induces. Solving for the equilibrium paths of prices, macroeconomic aggregates, and population composition takes a few seconds on a modern laptop. Our method also makes it easy to isolate the responses of different age groups and cohorts, which is useful for analyzing the transition. In our model, we find that the working-age population becomes older and more productive before it starts to shrink, producing hump-shaped paths of capital and labor per capita alongside a fall in the natural rate of interest.

[1] For perturbation methods, see, for example, Reiter (2009), Boppart, Krusell, and Mitman (2018), Auclert et al. (2021a), and Bhandari et al. (2023). For the role of household heterogeneity in shaping aggregate fluctuations, see, for example, Kaplan, Moll, and Violante (2018), Auclert, Rognlie, and Straub (2024), Auclert (2019), and Luetticke (2021).

[2] Examples of papers that demonstrate that life-cycle dynamics matters for macroeconomic outcomes include Doepke and Schneider (2006), Auclert et al. (2021b), Peterman and Sager (2022), Platzer and Peruffo (2022), Bardóczy, Savoia, and Velásquez-Giraldo (2024), Beaudry, Cavallino, and Willems (2024), and Gruss et al. (2025).

Table 1: Costs of Augmenting a Household Model with Life-Cycle Dynamics

Model	Number of States	Cost of a Single Jacobian ($H = 300$) Time (Seconds)	Peak memory (GB)
Infinite Horizon	2,754	0.29	0.36
Large Infinite Horizon	206,550	234.25	26.65
Life Cycle (75 ages)	206,550	2.19	0.24
Cross-model ratios			
Large I.H. / I.H.	75	797.74	74.92
Life Cycle / I.H.	75	7.45	0.66

Notes: The life-cycle model that the table refers to is the one described in Section 6. The infinite-horizon model simply takes the parameters (income process, preferences) of the first period of the life-cycle model; we set its survival probability to 0.96 per year. We use exactly the same single-period solver and the same code to represent the law of motion for the three models. All the tests were performed using an AMD Ryzen 9 5950X 16-Core Processor. For Jacobians, the input is the interest rate and the output is consumption.

Table 1 demonstrates the advantages of using our algorithm. The first row establishes a benchmark: a canonical infinite-horizon Krusell-Smith model with 2,754 possible combinations of income and wealth states. Computing a Jacobian for a single input-output pair takes 0.3 seconds and uses 0.36 GB of memory. The second row considers a large-scale version of the same model, with an expanded income process that has 75 times as many states. Using the same algorithm as in the benchmark case, calculating a single Jacobian takes almost 800 times as long, going from two seconds to almost four minutes. Memory might also become a bottleneck with peak usage exceeding 26 GB. Adding another state variable or switching to quarterly frequency would push the solution of this model beyond the capacity of most personal computers. The third row considers a life-cycle version of the model, with an age-income-wealth grid that adds up to a total of 206,550 states, the same as in the large-scale infinite-horizon model. The time required to compute a Jacobian using our specialized algorithm is only 7.4 times greater than in the benchmark model, and requires only two thirds as much memory. Hence, in this example, the special properties of age reduce the time and memory needed to solve an HA-OLG model to less than a hundredth of the costs of solving an infinite-horizon model of the same size.

We formalize these properties of age in the context of a general representation of HA-OLG models that accommodates population growth with permanent shocks to the size of newborn cohorts; flows of agents that can represent, for example, migration; and dynastic links that can tie the wealth and productivity of a dying household to those of the newborns who replace it. Within this representation, we partition the state space by age and show that age-specific versions of policy functions, value functions, and state-transition kernels satisfy

the invariance and symmetry properties that make the fake news algorithm of Auclert et al. (2021a) so efficient. These invariance results are in fact broader in our setting, because households only react to shocks that occur within their finite lives.

Next, we derive first-order approximations of households' responses to shocks. The building blocks of these approximations are age-specific counterparts of the objects used in the infinite-horizon fake news algorithm: age-specific Jacobians, fake news matrices, and expectation vectors. Age-specific Jacobians isolate the dynamic responses of different age groups, making them powerful tools for understanding the propagation of shocks. Crucially, the properties of age described above make these objects sparse: in a model without dynastic links, 75-period lives, and shock horizons of up to 300 periods, only 2.1% of the entries in age-specific fake news matrices can differ from zero. We locate and characterize these non-zero entries.

We conclude the methodological sections by presenting the fake news algorithm adapted to HA-OLG models, Algorithm 1. Its efficiency comes from our characterization of the non-zero elements of age-specific fake news matrices: many operations can be skipped, and the algorithm skips them. It also constructs age-specific fake news matrices progressively, running one backward pass of the life-cycle problem at a time and using that pass to update the approximation before moving on to the next backward pass. This reduces the number of perturbed solutions held in memory at any point, dramatically lowering peak memory requirements. We express the algorithm in terms of objects and methods that most life-cycle implementations already have, which we hope will ease adoption.

For various applications, links between dying households and the agents that replace them can be important—these links can include a direct inheritance of their idiosyncratic wealth, productivity, or entrepreneurial ability.[3] These links scramble the practical separation of cohorts that our baseline algorithm exploits. An agent's reaction to a shock can have consequences after his death through its effects on his descendants. In Appendix B we present a version of our algorithm that allows for these dynastic links and requires no additional backward solutions of the life-cycle model. The main text omits these links for ease of exposition.

We illustrate the method through an application to the ongoing decline in birth rates. We calibrate the life-cycle version of the Krusell-Smith model to match the age pyramid and life-cycle profiles of income, wealth, and income risk in the U.S., and then simulate a permanent fall in the growth rate of newborn cohorts from 0.30% to zero. The resulting demographic transition takes 75 years—one full lifetime—and reshapes the age distribution unevenly: the share of young workers drops first and fastest, the share of middle-aged workers rises in a hump-shaped pattern that peaks after 37 years, and the share of retirees grows slowly and steadily. To track how these forces evolve over time, we extend the static asset supply and demand framework of Auclert et al. (2025b) to a dynamic setting, decomposing the entire transition path of equilibrium capital into the contributions of population aging, wages, taxes, and the interest rate. Aging drives asset demand up most strongly and most

[3]Such dynastic links feature, for example, in Castañeda, Díaz-Giménez, and Ríos-Rull (2003), Cagetti and De Nardi (2006), Iacoviello and Pavan (2013), and Guvenen et al. (2023).

quickly, because the age group with the fastest-falling population share—young workers—are the lowest savers. Wages rise more slowly as labor becomes scarce, reinforcing household savings. Working against these forces, the government raises income taxes to finance social security at a higher dependency ratio, and the interest rate falls to clear the asset market. Together, these channels deliver a substantial fall in the natural rate of interest along a non-monotonic transition path.

Related literature. Our method builds on the literature that solves heterogeneous-agent models with aggregate shocks by perturbing around the steady state (Reiter 2009; Boppart, Krusell, and Mitman 2018; Bhandari et al. 2023). We extend the sequence-space Jacobian approach of Auclert et al. (2021a) to economies with overlapping generations of heterogeneous agents. In doing so, we also contribute to an active literature developing computational methods for rich OLG models (Evans and Phillips 2014; Kübler and Scheidegger 2025; Azinovic-Yang and Žemlička 2025).

Our application connects to a large body of work on demographic change and the secular decline of real interest rates (Carvalho, Ferrero, and Nechio 2016; Bielecki, Brzoza-Brzezina, and Kolasa 2020; Gagnon, Johannsen, and López-Salido 2021; Blanchard 2023; Fernández-Villaverde, Ventura, and Yao 2025). Closest to our quantitative exercise are heterogeneous-agent OLG models that quantify these forces (Platzer and Peruffo 2022; Auclert et al. 2025b); we adapt the asset supply and demand framework of Auclert et al. (2025b) from a long-run, static comparison to the full dynamic transition path. Finally, our result that the arrival of larger cohorts initially lowers productivity-adjusted labor relates to Vandenbroucke (2021).

Outline. The rest of this paper is organized as follows. Section 2 presents a life-cycle version of the Krusell and Smith (1998) model that serves as a running example throughout the paper. Section 3 formalizes the class of life-cycle problems we consider and represents it in the SSJ framework. Section 4 defines age-specific sequence-space Jacobians and fake news matrices and characterizes their structure. Section 5 presents our algorithm for computing these objects. Section 6 applies the method to a permanent fall in birth rates, illustrating how to use age-specific Jacobian decompositions to analyze the resulting demographic transition in general equilibrium. Section 7 concludes.

2 Motivating Example

We begin by presenting a life-cycle version of the Krusell and Smith (1998) model. This model serves as a concrete example and reference point for the more general results developed in the following sections.[4] It also illustrates the key technical and economic complications introduced by life-cycle dynamics. The technical complications are the introduction of age as a state variable and the need to account for household entry and exit through births

[4]The general framework accommodates a far larger set of shocks, choices, constraints, and timing assumptions than those in this specific model.

and deaths. The economic complications are the inclusion of a pension system and bequest motives, which generate additional equilibrium constraints.

Time is discrete. The economy is inhabited by a mass of households that make consumption-saving decisions, a representative final goods firm that hires labor and capital in competitive markets, and a government that collects taxes and pays pensions.

Households. Households are heterogeneous in age, income, and wealth. They live for at most J periods, surviving from age j to $j+1$ with probability ψ_j. Working-age households ($j < J^{ret}$) supply labor inelastically and earn labor income $y_{j,t}(z) = w_t\, z$, where w_t is the market wage and z is the household's idiosyncratic labor productivity in efficiency units. Retirees ($j \geq J^{ret}$) do not work and receive pension income $y_{j,t}(z) = z$. The productivity state z evolves over the life cycle according to an age-specific Markov process that may combine deterministic and stochastic components. Households save in a single non-contingent asset with real return R_t, subject to a borrowing constraint. Those who die receive warm-glow utility $\phi(a)$ from bequeathing their assets a; bequests are pooled and redistributed homogeneously among surviving households.

The household block's micro dynamics are characterized by two operators: the Bellman equation and the law of motion of the distribution. We break each operator down into a sequence of stages. This representation makes timing assumptions transparent and allows aggregate outputs—for example, bequests and consumption—to be computed at the stages where they naturally arise. Each stage k has a value function $V^{(k)}$ and a distribution $D^{(k)}$. Chaining the stages together yields a representation of the form in (12), which we work with in the following sections.

Households aged $j \geq 1$ enter period t with states (z_{-1}, a_{-1}) inherited from the previous period; we denote their distribution by $D^{(0)}_{j,t}$. In the first stage, newborns enter with an exogenous distribution D^{entry}_t and the distribution becomes

$$D^{(1)}_{j,t}(z_{-1}, a_{-1}) = \begin{cases} D^{(0)}_{j,t}(z_{-1}, a_{-1}) & \text{for } j \geq 1, \\ D^{\text{entry}}_t(z_{-1}, a_{-1}) & \text{for } j = 0. \end{cases} \tag{1}$$

Since flow utility does not change in this stage, the value function satisfies $V^{(1)}_{j,t} = V^{(2)}_{j,t}$. The second stage captures mortality, which affects continuation values and therefore changes the value function:

$$V^{(2)}_{j,t}(z_{-1}, a_{-1}) = (1 - \psi_j)\, \phi(a_{-1}) + \psi_j\, V^{(3)}_{j,t}(z_{-1}, a_{-1}), \tag{2}$$

and the distribution becomes $D^{(2)}_{j,t} = \psi_j D^{(1)}_{j,t}$. Aggregate bequests are determined at this stage:

$$B_t = \sum_{j=0}^{J-1} \int (1 - \psi_j)\, a_{-1}\, dD^{(1)}_{j,t}(z_{-1}, a_{-1}). \tag{3}$$

In the third stage, households draw a new idiosyncratic productivity z from a discretized distribution $\Pi_j(z \mid z_{-1})$. The value function is obtained by taking expectations,

$$V^{(3)}_{j,t}(z_{-1}, a_{-1}) = \sum_{z} \Pi_j(z \mid z_{-1})\, V^{(4)}_{j,t}(z, a_{-1}), \tag{4}$$

while the distribution is rolled forward as

$$D^{(3)}_{j,t}(z, a_{-1}) = \sum_{z_{-1}} \Pi_j(z \mid z_{-1})\, D^{(2)}_{j,t}(z_{-1}, a_{-1}). \tag{5}$$

In the fourth and final stage, households receive income and choose consumption and savings. Cash on hand consists of the gross return on assets and inheritances received within the period, plus after-tax labor or pension income. For simplicity, inheritances are homogeneous across the population and denoted with I_t. The value function is

$$V^{(4)}_{j,t}(z, a_{-1}) = \max_{c,\, a \geq 0} u(c) + \beta\, \mathbb{E}_t\Big[V^{(1)}_{j+1,t+1}(z, a)\Big] \tag{6}$$

$$\text{s.t. } c + a = R_t\,(a_{-1} + I_t) + (1 - \tau_t)\, y_{j,t}(z). \tag{7}$$

Solving this Bellman equation yields a consumption policy $c_{j,t}(z, a_{-1})$ and a saving policy $a_{j,t}(z, a_{-1})$ which advances the distribution to the initial stage of the next period and age:

$$D^{(0)}_{j+1,t+1}(z, a) = \int D^{(3)}_{j,t}\big(z, a^{-1}_{j,t}(z, a)\big). \tag{8}$$

Aggregate consumption, savings, labor supply, population, and taxes net of transfers are computed at this stage as

$$\begin{aligned}
C_t &= \sum_{j=0}^{J-1} \int c_{j,t}(z, a_{-1})\, dD^{(3)}_{j,t}(z, a_{-1}), & A_t &= \sum_{j=0}^{J-1} \int a_{j,t}(z, a_{-1})\, dD^{(3)}_{j,t}(z, a_{-1}), \\
N_t &= \sum_{j=0}^{J^{ret}-1} \int z\, dD^{(3)}_{j,t}(z, a_{-1}), & P_t &= \sum_{j=0}^{J-1} \int dD^{(3)}_{j,t}(z, a_{-1}), \\
T_t &= \sum_{j=0}^{J-1} \int \tau_t y_{j,t}(z)\, dD^{(3)}_{j,t}(z, a_{-1}) - \sum_{j=J^{ret}}^{J-1} \int y_{j,t}(z)\, dD^{(3)}_{j,t}(z, a_{-1}).
\end{aligned} \tag{9}$$

Rest of the model. A representative firm produces output with Cobb-Douglas technology $Y_t = \Theta_t K^{\alpha}_{t-1} L^{1-\alpha}_t$, and perfect competition yields factor prices

$$w_t = (1 - \alpha)\, \frac{Y_t}{L_t}, \qquad R_t = \alpha\, \frac{Y_t}{K_{t-1}} + 1 - \delta, \tag{10}$$

where δ is the depreciation rate. Given an exogenous sequence of TFP and newborn distributions $\{\Theta_t, D^{\text{entry}}_t\}_{t \geq 0}$ and initial conditions $\{D^{(0)}_{j,0}\}_{j=1}^{J-1}$ and K_{-1}, a competitive equilibrium

is a sequence of allocations $\{C_t, A_t, P_t, B_t, I_t, N_t, T_t, Y_t, K_t, L_t\}_{t\geq 0}$ and prices $\{R_t, w_t, \tau_t\}_{t\geq 0}$ such that (a) households and firms optimize and (b) the government budget is balanced, per-capita inheritances are consistent with aggregate bequests, and goods, asset, and labor markets clear for all $t \geq 0$:

$$T_t = 0, \qquad B_t = I_t P_t, \qquad Y_t = C_t + K_t - (1-\delta)K_{t-1}, \qquad A_t = K_t, \qquad N_t = L_t. \tag{11}$$

Applying SSJ. This model cannot be solved with the current version of the published SSJ package because total population may change over time, outputs are defined at different stages, and shocks to the distribution of newborns do not propagate through the Bellman equation in the usual way.[5] These are practical rather than conceptual hurdles: the framework of Auclert et al. (2021a) does apply once age is included as an additional state variable, but, as Table 1 demonstrates, this naive approach is very costly. Sections 3–5 show how to exploit the life-cycle structure to compute Jacobians much more efficiently.

3 Life-Cycle Problems in Sequence Space

The SSJ framework represents macroeconomic models as collections of blocks. A block can represent, for example, households, firms, or a fiscal authority. Blocks interact through aggregate variables that they either take as given (an "input") or that they produce (an "output"). This section defines the generic HA-OLG block whose Jacobians we will study in the rest of the paper.

Heterogeneous-agent blocks. Blocks are functions that take a time path of aggregate inputs $\{\mathbf{X}_t\}_{t\geq 0}$ and return a time path of aggregate outputs $\{\mathbf{Y}_t\}_{t\geq 0}$. For a household block, inputs may include the interest and wage rates, while outputs may include aggregate consumption. The state space that agents inhabit within the block is discretized on a grid; individual-level outcomes $\mathbf{y}_t$, value functions $\mathbf{v}_t$, and distributions $\mathbf{D}_t$ are vectors whose ith entries correspond to the ith grid point. Letting $\mathbf{\Lambda}_t$ denote the transition matrix governing the evolution of the distribution, the heterogeneous-agent block is given by the following system:

$$\begin{aligned} \mathbf{v}_t &= v(\mathbf{v}_{t+1}, \mathbf{X}_t), \quad \mathbf{\Lambda}_t = \Lambda(\mathbf{v}_{t+1}, \mathbf{X}_t), \quad \mathbf{y}_t = y(\mathbf{v}_{t+1}, \mathbf{X}_t), \quad \mathbf{F}_{t+1} = F(\mathbf{v}_{t+2}, \mathbf{X}_{t+1}) \\ \mathbf{D}_{t+1} &= \mathbf{\Lambda}_t^\top \mathbf{D}_t + \mathbf{F}_{t+1} \qquad\qquad \mathbf{Y}_t = \mathbf{y}_t^\top \mathbf{D}_t. \end{aligned} \tag{12}$$

So far, this setup is just a slight generalization of that in Auclert et al. (2021a). Aggregate outputs integrate individual outcomes over $\mathbf{D}_t$. The distribution of agents over states advances from time t to $t+1$ through the transition matrix $\mathbf{\Lambda}_t$ and the external flows $\mathbf{F}_{t+1}$.

[5] The SSJ package is available at https://pypi.org/project/sequence-jacobian/. Version 1.0 assumes a specific timing of events (agents make decisions after all shocks have been realized), and constructs the law of motion from the Bellman equation that rules out non-trivial entry and exit.

Agents are forward-looking: v, Λ, and y depend on contemporaneous inputs $\mathbf{X}_t$ and the continuation value $\mathbf{v}_{t+1}$, reflecting Bellman's principle. The flow function F may also depend on the continuation value. For example, if $\mathbf{F}_{t+1}$ represents net migration, it may depend on the future income that an agent may expect if he enters the economy. The incoming distribution $\mathbf{m}_t := \mathbf{D}_t - \mathbf{F}_t$ is predetermined in each t: it is carried in from period $t-1$, before the exogenous flow $\mathbf{F}_t$ enters. Given $\mathbf{m}_0$ fixed at its steady-state value, (12) defines a mapping from input sequences to output sequences,

$$f(\{\mathbf{X}_t\}_{t\geq 0}) = \{\mathbf{Y}_t\}_{t\geq 0}. \tag{13}$$

Life-cycle structure. We now impose a life-cycle structure on (12). Age, denoted j, takes J distinct values, $\{0, 1, \ldots, J-1\}$. The vectors in (12) partition into age-specific sub-vectors,

$$\begin{aligned}
\mathbf{v}_t^\mathsf{T} &= \left[\mathbf{v}_t^\mathsf{T}(0)\ , ..., \mathbf{v}_t^\mathsf{T}(J-1)\right], \\
\mathbf{D}_t^\mathsf{T} &= \left[\mathbf{D}_t^\mathsf{T}(0)\ , ..., \mathbf{D}_t^\mathsf{T}(J-1)\right], \\
\mathbf{F}_t^\mathsf{T} &= \left[\mathbf{F}_t^\mathsf{T}(0)\ , ..., \mathbf{F}_t^\mathsf{T}(J-1)\right], \\
\mathbf{y}_t^\mathsf{T} &= \left[\mathbf{y}_t^\mathsf{T}(0)\ , ..., \mathbf{y}_t^\mathsf{T}(J-1)\right],
\end{aligned} \tag{14}$$

and aggregate output decomposes additively into cohort contributions,

$$\mathbf{Y}_t = \sum_{j=0}^{J-1} \mathbf{y}_t(j)^\mathsf{T} \mathbf{D}_t(j).$$

We could perform this partition for any idiosyncratic state. What we call a "life-cycle structure" is a set of restrictions that we impose on this partition and which age as a state variable satisfies in a wide range of applications. These restrictions fall into two groups. The first concerns the law of motion of this age partition. The second concerns the information agents use to make decisions.

We start with the transition equation. Our assumption is that an age-j agent either survives and advances to age $j+1$ or dies and is replaced by a mass of newborn agents. We capture these transitions with two matrices: $\mathcal{L}_t(j)$ maps age-j agents into age-$(j+1)$ agents incorporating survival probabilities, and $\Omega_t(j)$ maps age-j agents into newborns incorporating death probabilities.

Assumption 1. *The matrices $\mathbf{\Lambda}_t$ that govern the evolution of the distribution of agents in (12) have the structure*

$$\mathbf{\Lambda}_t = \begin{bmatrix}
\Omega_t(0) & \mathcal{L}_t(0) & \mathbf{0} & ... & \mathbf{0} \\
\Omega_t(1) & \mathbf{0} & \mathcal{L}_t(1) & ... & \mathbf{0} \\
\vdots & \vdots & \vdots & ... & \vdots \\
\Omega_t(J-2) & \mathbf{0} & \mathbf{0} & ... & \mathcal{L}_t(J-2) \\
\Omega_t(J-1) & \mathbf{0} & \mathbf{0} & ... & \mathbf{0}
\end{bmatrix}, \tag{15}$$

which implies the law of motion

$$\mathbf{D}_{t+1}(j) = \begin{cases} \sum_{l=0}^{J-1} \Omega_t(l)^\mathsf{T} \mathbf{D}_t(l) + \mathbf{F}_{t+1}(0), & j = 0 \\ \mathcal{L}_t(j-1)^\mathsf{T} \mathbf{D}_t(j-1) + \mathbf{F}_{t+1}(j), & 0 < j \leq J-1. \end{cases} \tag{16}$$

At a steady state, this law of motion yields:

Claim 1 (Steady-state distribution)**.** *If a steady state exists, then it satisfies*

$$\mathbf{D}_{ss}(j) = \begin{cases} \sum_{l=0}^{J-1} \Omega_{ss}(l)^\mathsf{T} \mathbf{D}_{ss}(l) + \mathbf{F}_{ss}(0), & j = 0 \\ \mathcal{L}_{ss}(j-1)^\mathsf{T} \mathbf{D}_{ss}(j-1) + \mathbf{F}_{ss}(j), & 0 < j \leq J-1. \end{cases}$$

Proof of Claim 1. See Appendix A.1.

The representation in (15) can accommodate several popular setups in the life-cycle and overlapping-generations literatures. Death can be exogenous or depend on each agent's idiosyncratic states. An agent's idiosyncratic state can influence that of his offspring: they can inherit, for example, his productivity or wealth.[6] As the following examples will show, it can also represent population growth with rich transitional dynamics.

Consider two special cases of the model in Section 2 as examples.

Example (A: Exogenous constant newborn distribution)**.** *Assume an exogenous, constant newborn distribution η, no population growth, and no migration. Since newborns do not inherit assets or productivity from their parents, dying agents simply exit the system: $\Omega(j) = \mathbf{0}$ for all j. Newborns enter as a constant flow $\mathbf{F}_{t+1}(0) = \eta$, with $\mathbf{F}_{t+1}(j) = \mathbf{0}$ for $j > 0$. The law of motion becomes*

$$\mathbf{D}_{t+1}(j) = \begin{cases} \eta, & j = 0 \\ \mathcal{L}_t(j-1)^\mathsf{T} \mathbf{D}_t(j-1), & 0 < j \leq J-1. \end{cases} \tag{17}$$

Example (B: Demographic shifts)**.** *Continue to assume exogenous births ($\Omega(j) = \mathbf{0}$), but allow for migration and let the mass of newborns, n_{t+1}, fluctuate and grow over time according to a scalar growth factor Υ_{t+1}. Assuming that the distribution of newborns across idiosyncratic states remains fixed at η, the law of motion is*

$$\mathbf{D}_{t+1}(j) = \begin{cases} n_{t+1}\, \eta, & j = 0 \\ \mathcal{L}_t(j-1)^\mathsf{T} \mathbf{D}_t(j-1) + \mathbf{F}_{t+1}(j), & 0 < j \leq J-1. \end{cases} \tag{18}$$

If n_{t+1} grows over time, then so does the distribution $\mathbf{D}_t$. We restore stationarity by scaling the distribution and the migration flows by the size of the newborn cohort: $\hat{\mathbf{D}}_t := \mathbf{D}_t / n_t$ and

[6] The representation does rule out, however, inter vivos transfers as in Straub (2019).

$\hat{\mathbf{F}}_t := \mathbf{F}_t/n_t$.[7] *Using* $n_{t+1} = n_t\Upsilon_{t+1}$, *the stationary law of motion can be written as*

$$\hat{\mathbf{D}}_{t+1}(j) = \begin{cases} \eta, & j = 0 \\ \frac{1}{\Upsilon_{t+1}}\mathcal{L}_t(j-1)^\intercal \hat{\mathbf{D}}_t(j-1) + \hat{\mathbf{F}}_{t+1}(j), & 0 < j \leq J-1. \end{cases} \tag{19}$$

To conform with (16), *we define* $\hat{\mathcal{L}}_t(j-1) := 1/\Upsilon_{t+1} \cdot \mathcal{L}_t(j-1)$.

Now we impose restrictions on agents' behavior that finalize our life-cycle structure. We require that the actions and transitions of age-j agents at time t depend on the future only through the value function of age-$(j+1)$ agents at time $t+1$.

Assumption 2 (Recursive structure)**.** *There exist functions* $\{v[j], y[j], \mathcal{L}[j], \Omega[j], F[j]\}_{j=0}^{J-1}$ *such that for each* $0 \leq j < J-1$ *and* $t \geq 0$,

$$\begin{aligned} \mathbf{v}_t(j) &= v[j]\left(\mathbf{v}_{t+1}\left(j+1\right), \mathbf{X}_t\right), \\ \mathbf{y}_t(j) &= y[j]\left(\mathbf{v}_{t+1}\left(j+1\right), \mathbf{X}_t\right), \\ \mathcal{L}_t(j) &= \mathcal{L}[j]\left(\mathbf{v}_{t+1}\left(j+1\right), \mathbf{X}_t\right), \\ \Omega_t(j) &= \Omega[j]\left(\mathbf{v}_{t+1}\left(j+1\right), \mathbf{X}_t\right), \\ \mathbf{F}_t(j) &= F[j]\left(\mathbf{v}_{t+1}\left(j+1\right), \mathbf{X}_t\right) \end{aligned} \tag{20}$$

and $\mathbf{v}_t(J-1) = v[J-1]\left(\mathbf{X}_t\right)$, $\mathbf{y}_t(J-1) = y[J-1]\left(\mathbf{X}_t\right)$, $\Omega_t(J-1) = \Omega[J-1]\left(\mathbf{X}_t\right)$, *and* $\mathbf{F}_t(J-1) = F[J-1](\mathbf{X}_t)$.

This is a typical restriction satisfied by finite-horizon problems that can be expressed in recursive Bellman form. Even behavioral assumptions like quasi-hyperbolic discounting (Laibson 1997) can satisfy this restriction. What the restriction rules out is the dependence of agent's actions on events that occur outside of their lifetimes. For example, in our demonstration in Section 6, agents will derive utility from bequeathing their wealth. This wealth could go directly to the newborn that might replace the agent as he dies, through the $\Omega_t(j)$ matrices. The agent, however, cannot consider the path of interest rates and wages that his descendant will experience in deciding how much wealth to bequeath to them.

We now turn to the dynamic effects of changes in inputs. We concentrate on shocks to a single input that changes it for a single period s by a fixed small amount dx. To first order, the response of the household sector to any change in the paths of any combination of inputs is a linear function of these basis responses. We extend the SSJ notation for these shocks to our age partition and examine the symmetry and invariance properties that our assumptions afford.

[7] We assume that normalized flows $\hat{\mathbf{F}}_t$ are stationary: when inputs are constant at their steady-state value, non-normalized flows grow at a factor Υ_{ss}.

Shocks to the life-cycle block. The system starts from a steady state with constant inputs $\mathbf{X}_{ss}$. For shock size dx, let $\mathbf{X}^s$ denote the input sequence that equals $\mathbf{X}_{ss} + dx$ in period s and $\mathbf{X}_{ss}$ otherwise. At time 0, agents unexpectedly learn that the future path of inputs will be $\{\mathbf{X}_t^s\}_{t\geq 0}$ instead of their assumed $\{\mathbf{X}_{ss}\}_{t\geq 0}$. Vectors and matrices $\{\mathbf{v}_t^s, \mathbf{D}_t^s, \mathbf{y}_t^s, \mathbf{\Lambda}_t^s\}_{t\geq 0}$ are the solution to (12) under $\mathbf{X}^s$, with age-specific counterparts $\{\mathbf{v}_t^s(j), \mathbf{D}_t^s(j), \mathbf{y}_t^s(j), \mathcal{L}_t^s(j), \Omega_t^s(j), \mathbf{F}_t^s(j)\}_{t\geq 0}$ for $0 \leq j \leq J-1$. For any vector or variable Z, $dZ := Z - Z_{ss}$ and $dZ(j) := Z(j) - Z_{ss}(j)$.

The SSJ method is fast because it exploits three properties of one-time shocks. The next three lemmas record them in the life-cycle setting (proofs in Appendix A.1). Together they say that $(\mathbf{y}, \mathcal{L}, \Omega, \mathbf{F})$ at (t, j) depend on the shock arrival date s only through the gap $s - t$, and equal their steady-state values whenever this gap falls outside the cohort's planning window $[0,\, J-1-j]$. This restriction is tighter than in the infinite-horizon version of the algorithm, where the planning window is $[0,\, \infty)$.

First, once the shock lies in the past, policies, transition matrices and flows return to their steady-state values.

Lemma 1 (Invariance to past shocks)**.** *If $t > s$, then*

$$\mathbf{y}_t^s(j) = \mathbf{y}_{ss}(j), \quad \mathcal{L}_t^s(j) = \mathcal{L}_{ss}(j), \quad \Omega_t^s(j) = \Omega_{ss}(j), \quad \textit{and} \quad \mathbf{F}_t^s(j) = \mathbf{F}_{ss}(j).$$

Second, for any fixed age, responses depend only on the time until the shock arrives, not on calendar dates.

Lemma 2 (Time-shift symmetry)**.** *For all $t \geq 0$, we have*

$$\mathbf{y}_t^s(j) = \mathbf{y}_{t+k}^{s+k}(j), \quad \mathcal{L}_t^s(j) = \mathcal{L}_{t+k}^{s+k}(j), \quad \Omega_t^s(j) = \Omega_{t+k}^{s+k}(j), \quad \textit{and} \quad \mathbf{F}_t^s(j) = \mathbf{F}_{t+k}^{s+k}(j) \quad \forall k \geq 0.$$

And third, cohorts do not respond to shocks that will arrive after their certain death.

Lemma 3 (Truncated horizon)**.** *If $s - t > (J-1) - j$, then*

$$\mathbf{y}_t^s(j) = \mathbf{y}_{ss}(j), \quad \mathcal{L}_t^s(j) = \mathcal{L}_{ss}(j), \quad \Omega_t^s(j) = \Omega_{ss}(j), \quad \textit{and} \quad \mathbf{F}_t^s(j) = \mathbf{F}_{ss}(j).$$

These three properties sharply reduce the set of (t, s, j) combinations for which we need to calculate a numerical response when constructing the age-specific sequence-space Jacobians that underpin our method. We define these objects in the following section.

4 Age-Specific Jacobians and Fake News Matrices

The Jacobian $\mathcal{J}$ of the block in (12) represents the first-order effects of a perturbation to $\mathbf{X}_s$ on $\mathbf{Y}_t$ for all combinations of s and t,

$$\mathcal{J}_{t,s} = \frac{df_t(\{\mathbf{X}_\tau\}_{\tau=0}^{\infty})}{d\mathbf{X}_s} = \frac{d\mathbf{Y}_t}{d\mathbf{X}_s} \tag{21}$$

around $\{\mathbf{X}_{ss}\}_{\tau=0}^{\infty}$. Block Jacobians are the cornerstone of the SSJ framework. They can be used to compute first-order impulse responses, assess local determinacy, evaluate likelihood functions, and even improve nonlinear perfect-foresight solutions of general-equilibrium models (Auclert et al. 2021a; Boehl 2023; Auclert et al. 2025a). The main difficulty is calculating the Jacobians of heterogeneous agent blocks. For this purpose, Auclert et al. (2021a) provide an efficient method called the "fake news algorithm" which exploits the structure of (12). Our contribution is a version that further exploits life-cycle structure (Lemmas 1–3) to reduce computation time and memory.

The first step is to decompose aggregate Jacobians into the contribution of all the cohorts that live in a given year:

$$\begin{aligned}\mathcal{J}_{t,s}dx = d\mathbf{Y}_t^s &= d\left(\sum_{j=0}^{J-1}\mathbf{y}_t^s(j)^\intercal \mathbf{D}_t^s(j)\right)\\ &= \sum_{j=0}^{J-1}\left\{d\mathbf{y}_t^s(j)^\intercal \mathbf{D}_{ss}(j) + \mathbf{y}_{ss}(j)^\intercal d\mathbf{D}_t^s(j)\right\} =: \sum_{j=0}^{J-1}\mathcal{J}_{t,s}(j)dx.\end{aligned} \tag{22}$$

The age-specific Jacobian for age j, $\mathcal{J}(j)$, has entries such that $\mathcal{J}_{t,s}(j)dx := d\mathbf{y}_t^s(j)^\intercal \mathbf{D}_{ss}(j) + \mathbf{y}_{ss}(j)^\intercal d\mathbf{D}_t^s(j)$. In the aggregate Jacobian, entry $\mathcal{J}_{t,s}$ measures the change in output $\mathbf{Y}$ at time t from a shock to $\mathbf{X}$ announced at time 0 and realized at time s; its age-specific component $\mathcal{J}_{t,s}(j)$ isolates the contribution of the cohort with age j at time t.

Age-specific Jacobians have two immediate uses. First, since $\mathcal{J} = \sum_{j=0}^{J-1}\mathcal{J}(j)$, they construct the aggregate Jacobian that is required to solve for equilibrium dynamics in the SSJ framework. Second, they trace cohort-level responses: the dynamic response of the cohort of agents that had age j at time 0 to a shock at time s is $\{\mathcal{J}_{t,s}(j+t)\}_{t=0}^{J-1-j}$. The rest of this section and the next derive our method to calculate age-specific Jacobians.

Our method is an adaptation of the fake news algorithm of Auclert et al. (2021a). As such, it requires age-specific analogs of many of the objects defined in that paper. Among these objects, the most important are fake news matrices, which measure the difference between the time t response to a time s shock, and the time $t-1$ response to a time $s-1$ shock.

Definition 1 (Age-Specific Fake News Matrices)**.** *For $t, s \geq 0$ and $j \in \{0, \ldots, J-1\}$, define $\{\mathcal{F}(j)\}_{j=0}^{J-1}$ by*

$$\mathcal{F}_{t,s}(j) = \begin{cases}\mathcal{J}_{t,s}(j), & \text{if } t = 0 \text{ or } s = 0,\\ \mathcal{J}_{t,s}(j) - \mathcal{J}_{t-1,s-1}(j), & \text{otherwise.}\end{cases}$$

Definition 1 implies

$$\mathcal{J}_{t,s}(j) = \sum_{k=0}^{\min\{t,s\}}\mathcal{F}_{t-k,s-k}(j). \tag{23}$$

and

$$\mathcal{F} = \sum_{j=0}^{J-1} \mathcal{F}(j), \tag{24}$$

where $\mathcal{F}$ is defined as $\mathcal{F}_{t,s} = \mathcal{J}_{t,s} - \mathcal{J}_{t-1,s-1}$ for $t, s \geq 1$, and $\mathcal{F}_{t,s} = \mathcal{J}_{t,s}$ if $t = 0$ or $s = 0$. It is clear, therefore, that if we had age-specific fake news matrices $\{\mathcal{F}(j)\}_{j=0}^{J-1}$, we would be able to construct age-specific and aggregate Jacobians $\{\mathcal{J}(j)\}_{j=0}^{J-1}$ and $\mathcal{J}$. Before presenting our method for calculating these age-specific fake news matrices, we characterize them in terms of simpler objects.

4.1 Building Blocks of Age-Specific Fake News Matrices

Our main result, Theorem 1, writes each entry of age-specific fake news matrices $\mathcal{F}_{t,s}(j)$ in terms of objects that are age-specific specializations of their infinite-horizon counterparts in Auclert et al. (2021a): expectation vectors, policy shifts, and distributional shifts (Definitions 2–4). We now construct these objects.

Definition 2 (Age-Specific Expectation Vectors)**.** *For $j \in \{0, \ldots, J-1\}$ and $t \in \{0, \ldots, J-1-j\}$, set*

$$\mathcal{E}_0(j) \;:=\; \mathbf{y}_{ss}(j), \qquad \mathcal{E}_t(j) \;:=\; \mathcal{L}_{ss}(j)\,\mathcal{E}_{t-1}(j+1) \quad (t \geq 1).$$

Equivalently,

$$\mathcal{E}_t(j) \;=\; \mathcal{L}_{ss}(j)\,\mathcal{L}_{ss}(j+1)\cdots\mathcal{L}_{ss}(j+t-1)\,\mathbf{y}_{ss}(j+t).$$

These vectors help us transform distributions of agents into their future expected contribution to the outcome of interest. The m-th entry of $\mathcal{E}_t(j)$ is the expected steady-state outcome t periods from now for an agent at grid point m whose age is j today, conditional on surviving t further periods (so the agent ends at age $j+t$).[8] Hence, if the current distribution of age-j agents is $\mathbf{D}(j)$, we know their contribution to the aggregate outcome $\mathbf{Y}$ in t periods will be $\mathcal{E}_t(j)'\mathbf{D}(j)$.

The next two objects capture the initial effect of shocks on agent's actions and their distribution. Age-specific policy shifts capture the effect of a date-s shock on policies at time 0, and age-specific distributional shifts capture its effect on the distribution at time 1.

Definition 3 (Policy and Distributional Shifts)**.** *For $0 \leq j \leq J-1$ and shock date $s \geq 0$:*

(i) the age-specific policy shift *is*

$$d\mathbf{y}_0^s(j) \;:=\; \mathbf{y}_0^s(j) - \mathbf{y}_{ss}(j);$$

(ii) the age-specific distributional shift *is*

$$d\mathbf{D}_1^s(j) \;:=\; \mathbf{D}_1^s(j) - \mathbf{D}_{ss}(j).$$

[8] "Today" is the vector's own reference time and is decoupled from the paper's calendar time; only the start age j and the forward horizon t enter the formula. The vector is defined for $j + t \leq J - 1$.

Two mechanisms can shift the distribution $\mathbf{D}_1^s(j)$. First, there can be changes in the distribution of agents coming from time 0, caused by shifts in $\mathcal{L}_0(j-1)$ and $\mathbf{F}_0(j-1)$ for $j \geq 1$, or shifts in $\{\Omega_0(j_0), \mathbf{F}_0(j_0)\}_{j_0=0}^{J-1}$ for $j = 0$. Second, there can be contemporaneous changes in exogenous net flows $\mathbf{F}_1^s(j)$. The next object isolates the former component of distributional shifts.

Definition 4 (Endogenous Distributional Shifts)**.** *For shock date $s \geq 0$ and $j \in \{0, \ldots, J-1\}$, the endogenous distributional shift is*

$$\boldsymbol{\Xi}^s(j) \;:=\; d\mathbf{D}_1^s(j) - d\mathbf{F}_1^s(j).$$

$\boldsymbol{\Xi}^s(j)$ is the time-1 change in the age-j distribution net of the direct response of the exogenous age-j inflow. For ages $j \geq 1$, we know $\boldsymbol{\Xi}^s(j)$ must come from those who were age $j-1$ at time 0. For newborns ($j = 0$), if we allow for dynastic links, $\boldsymbol{\Xi}^s(0)$ comes from their parents, who might have had any age $0 \leq j_0 \leq J-1$ at time 0. With no dynastic links, $\boldsymbol{\Xi}^s(0) = \mathbf{0}$, as exogenous flows are the only source of newborn agents. This represents a major fork in our derivations and algorithm, and the version without dynastic links is far more intuitive. Hence, we shut down dynastic links for the remainder of the main text and present our derivations with dynastic links in Appendix B.

Assumption 3 (Absence of dynastic links)**.** *For the remainder of our exposition in the main text,*

$$\Omega_t^s(j) = \Omega_{ss}(j) = \mathbf{0}, \quad \forall\; t,\, s,\, j.$$

Appendix B relaxes this assumption.

The next lemma characterizes $\boldsymbol{\Xi}^s(j)$.

Lemma 4 (Distributional Shifts Without Dynastic Links)**.** *For $s \geq 0$:*

(i) For $1 \leq j \leq J-1$,

$$\boldsymbol{\Xi}^s(j) \;=\; d\mathcal{L}_0^s(j-1)^\mathsf{T}\mathbf{D}_{ss}(j-1) \;+\; \mathcal{L}_{ss}(j-1)^\mathsf{T} d\mathbf{F}_0^s(j-1). \tag{25}$$

(ii) For $j = 0$,

$$\boldsymbol{\Xi}^s(0) \;=\; \mathbf{0}. \tag{26}$$

Moreover, $\boldsymbol{\Xi}^s(j) = \mathbf{0}$ for $j > J - s$ (with $1 \leq j \leq J-1$).

Proof of Lemma 4. See Appendix A.2.

Cases (i) and (ii) of Lemma 4 follow directly from differentiating the transition equation (16). Its final condition says there is no distributional shift if $j - 1 + s > J - 1$, for this inequality implies that the relevant cohort to the distributional shift (those aged $j-1$ at time 0) will be dead when the shock arrives. Hence, their transitions and flows do not shift.

These building blocks are sufficient to characterize age-specific fake news matrices.

4.2 Structure of Fake News Matrices

Our main result expresses every entry of age-specific fake news matrices in terms of expectation vectors, policy shifts, and distributional shifts. It also shows that a large fraction of these entries are zero.

Theorem 1 (Structure of Age-Specific Fake News Matrices)**.** *Let* $t, s, j \in \{0, \ldots, J-1\}$*. If* $0 \leq j - t \leq J - 1 - s$*, then*

$$\mathcal{F}_{t,s}(j) = \begin{cases} d\mathbf{y}_0^s(j)^\intercal \mathbf{D}_{ss}(j) \;+\; \mathbf{y}_{ss}(j)^\intercal d\mathbf{F}_0^s(j), & \text{if } t = 0, \\ \mathcal{E}_{t-1}(j-t+1)^\intercal \boldsymbol{\Xi}^s(j-t+1), & \text{if } t \geq 1, \end{cases} \tag{27}$$

otherwise, $\mathcal{F}_{t,s}(j) = 0$*.*

Proof of Theorem 1. See Appendix A.2.

To interpret Theorem 1, remember that $\mathcal{F}_{t,s}(j)$ is linked to the incremental time-t response from the cohort of age j to a shock that is scheduled to arrive at time s and was announced at time 0. This cohort has age $j-t$ when the shock is announced and age $j-t+s$ when the shock arrives.

The condition $j - t \leq J - 1 - s$ isolates cohorts that will be alive when the shock arrives: cohorts who know they won't be alive do not react. The first case ($t = 0$) captures the instantaneous reaction to the shock's announcement: the endogenous start-of-period distribution is fixed, but policy functions and flows may change. The second case ($t \geq 1$) captures the effect of these reactions on future periods. The time 0 reaction shifts the distribution of agents over states in time 1, generating $\boldsymbol{\Xi}^s(j-t+1)$, and these shifts propagate forward to time t via the expectation vector.

The condition $0 \leq j - t$ isolates cohorts that were alive when the shock was announced. Without dynastic links, past shocks can not shift the distribution of newborn agents over states. Announcing a shock at time 0 and withdrawing it at time 1[9] leaves the distribution and actions of cohorts born starting on period 1 (those with $t > j$) unchanged, other than through time-1 flows. With dynastic links, this ceases to be true as past shock announcements change newborn distributions through the reactions of their ancestors. In Appendix B, we show that this creates non-zero entries in the $t > j$ region, but leaves the other cases unchanged.

Remark 1 (The bounds on t and s follow from finite lifespans). The index ranges $t, s \in \{0, \ldots, J-1\}$ do not discard any non-zero entries, as Lemmas 3 and 4 already make every entry with $t \geq J$ or $s \geq J$ vanish. A time-t entry with $t \geq 1$ carries the shift $\boldsymbol{\Xi}^s(j-t+1)$, and by Lemma 4 this shift can be non-zero only when $1 \leq j-t+1 \leq J-s$, since $\boldsymbol{\Xi}^s(0) = \mathbf{0}$ and $\boldsymbol{\Xi}^s(j') = \mathbf{0}$ for $j' > J-s$. The lower bound $1 \leq j-t+1$ with $j \leq J-1$ forces $t \leq J-1$, and the upper bound $j-t+1 \leq J-s$ forces $s \leq J-1$. Moreover, the $t = 0$ entry vanishes once $j > J-1-s$ by Lemma 3, which again forces $s \leq J-1$. The non-zero entries therefore lie in the leading $J \times J$ block, with the row $t = J-1$ and the column $s = J-1$ both live.

[9] This is the interpretation that Auclert et al. (2021a) give to entries of the fake news matrix.

Example (A (continued))**.** *Continuing Example A, suppose the shock changes household decisions and survivor transitions but leaves the exogenous newborn inflows unchanged. This implies* $d\mathbf{F}_0^s(j) = \mathbf{0}$ *for all* j *and reduces fake news matrices to*

$$\mathcal{F}_{t,s}(j) = \begin{cases} d\mathbf{y}_0^s(j)^\mathsf{T}\mathbf{D}_{ss}(j), & \text{if } t = 0 \\ \mathcal{E}_{t-1}(j-t+1)^\mathsf{T}\boldsymbol{\Xi}^s(j-t+1), & \text{if } t \geq 1 \end{cases}$$

if $0 \leq j - t \leq J - 1 - s$ *and* $\mathcal{F}_{t,s}(j) = 0$ *otherwise.*

Theorem 1 applies directly to our model with demographic shifts and migration (Example B) with the newborn-weighted law of motion (19) for shocks to standard inputs like the wage or interest rate. The only necessary addition is a Jacobian for the growth factor of newborn cohorts, Υ. This shock does not fit our ongoing assumptions because, through its newborn re-weighting, it can shift the initial net-of-flow distribution $\hat{\mathbf{D}}_0 - \hat{\mathbf{F}}_0$, which so far we have assumed to be fixed. Hence, fake news matrices with respect to this input have a peculiar but very simple form that we now derive. Because Υ enters the law of motion as a divisor, we have found that defining Jacobians with respect to $(1/\Upsilon)$ yields more precise results.[10]

Example (B (continued))**.** *Continuing Example B, consider shocks to the inverse of the newborn growth factor* $d(1/\Upsilon)$*. The age-specific fake news matrices of a generic output* $\hat{\mathbf{Y}}$ *with respect to these shocks have all their non-zero elements in their first columns (*$\mathcal{F}_{t,s}(j) = 0$ *for* $s \geq 1$*). Furthermore, the first columns are*

$$\mathcal{F}_{t,0}(j) = \begin{cases} \Upsilon_{ss} \cdot \mathcal{E}_t(j-t)^\mathsf{T}\left(\hat{\mathbf{D}}_{ss}(j-t) - \hat{\mathbf{F}}_{ss}(j-t)\right), & \text{if } j \geq t+1 \\ \mathbf{0}, & \text{otherwise.} \end{cases}$$

Here $\mathcal{E}_t$ *is built as in Definition 2 from the normalized survival transitions* $(1/\Upsilon_{ss})\,\mathcal{L}_{ss}$ *of* (19)*. This implies that the fake news matrix for newborns,* $\mathcal{F}(0)$*, is zero for this shock.*

Proof. See Claim 4 in Appendix A.3 for the proof.

Age-specific fake news matrices for newborn growth shocks can, therefore, be calculated directly from the steady-state solution. The reason is that they operate through the model's law of motion and generate no direct changes in policy functions or (non-normalized) transition matrices. Under the newborn-weighted measure, a shock to the number of newborns simply re-weighs incumbent cohorts. The effects of this re-weighing are propagated to future outputs through expectation vectors. As our application in Section 6 will show, this mathematically humble shock can generate rich transition dynamics as cohorts of changing sizes move through the life cycle.

Theorem 1 and the previous examples reveal the remarkable sparsity of age-specific fake news matrices. To ground this implication, consider a model with $\Omega_t(j) = 0$ like the examples

[10] The law of motion is linear with respect to $(1/\Upsilon)$ but non-linear with respect to Υ.

above. Non-zero entries of age-specific fake news matrices satisfy $0 \leq j - t \leq J - 1 - s$; Figure D.1 of Appendix D depicts this restriction. For a maximum shock horizon of 300 and a model with 75 possible ages, only 2% of all possible $300 \times 300 \times 75$ combinations of (t, s, j) satisfy this restriction.[11] Knowing that we can skip most of these combinations is a large contributor to the efficiency of our algorithm. The other contributing factor is that we use the properties in Lemmas 1–3 to find the required building blocks of the fake news matrices with as few model solutions as possible. The next section describes our scheme to do so.

5 Computing Age-Specific Fake News Matrices

This section explains our algorithm to efficiently compute $\{\mathcal{F}(j)\}_{j=0}^{J-1}$. To make the algorithm accessible, we also provide a "cookbook" that gives concrete examples and visualizations of the objects in the algorithm and is accompanied by public code that reproduces every step (Appendix D). The cookbook uses Example 3, while our quantitative demonstration in Section 6 uses Example 3. The public code also shows how to combine the Jacobians of the HA-OLG block with the `sequence-jacobian` package to perform dynamic equilibrium analyses. Here, we give a limited overview with only the objects that are required to present the algorithm.

Our starting point is a life-cycle solver of the type that is typically found in partial equilibrium applications. In the representation from Section 3, there are fixed grids $\{\mathcal{G}_j\}_{j=0}^{J-1}$ that discretize the state space for every age. Age-specific solvers $\{\texttt{solve}_j(\cdot)\}_{j=0}^{J-1}$ are functions which, given the value vector for age $j+1$ and the aggregate inputs for age j, produce the value and policy vectors evaluated on $\mathcal{G}_j$, and the components of the transition equation,

$$\mathbf{y}_j(j),\, \mathbf{v}_j(j),\, \mathcal{L}_j(j),\, \Omega_j(j),\, \mathbf{F}_j(j) = \texttt{solve}_j\left(\mathbf{v}_{j+1}\left(j+1\right), \mathbf{X}_j\right).$$

We define auxiliary functions $\overline{\texttt{solve}}_j$ which, as is done in practice, chain backward applications of these single-period solvers to solve the model up to age j given the value vector at age $j+1$

$$\{\mathbf{y}_l(l),\, \mathbf{v}_l(l),\, \mathcal{L}_l(l),\, \Omega_l(l), \mathbf{F}_l(l)\}_{l=0}^{j} = \overline{\texttt{solve}}_j\left(\mathbf{v}_{j+1}\left(j+1\right), \{\mathbf{X}_l\}_{l=0}^{j}\right).$$

The steady-state solution $\{\mathbf{y}_{ss}(j),\, \mathbf{v}_{ss}(j),\, \mathcal{L}_{ss}(j),\, \Omega_{ss}(j), \mathbf{F}_{ss}(j)\}_{j=0}^{J-1}$ is that obtained by solving the model up to the terminal age $J-1$ and inputs $\{\mathbf{X}_{ss}\}_{j=0}^{J-1}$.[12]

5.1 From life-cycle solutions to building blocks

We now show that the steady-state solution $\{\mathbf{y}_{ss}(j),\, \mathbf{v}_{ss}(j),\, \mathcal{L}_{ss}(j),\, \Omega_{ss}(j), \mathbf{F}_{ss}(j)\}_{j=0}^{J-1}$ and partial solvers $\{\overline{\texttt{solve}}_j(\cdot)\}_{j=0}^{J-1}$ are sufficient to construct the building blocks of Theorem 1.

[11] If the maximum shock horizon is greater than the number of ages ($0 \leq t, s \leq L$ with $L > J$), the number of (t, s, j) combinations that satisfy $0 \leq j - t \leq J - 1 - s$ is $J \cdot (J+1) \cdot (2J+1)/6$.

[12] Since $J-1$ is the terminal age, neither $\texttt{solve}_{J-1}$ nor $\overline{\texttt{solve}}_{J-1}$ have a continuation value function as input. This is an advantage over infinite-horizon models that require an initial guess of the continuation value.

We continue to assume that there are no dynastic links (Assumption 3) and hence omit Ω for the remainder of this Section.

Note first that the expectation vectors $\mathcal{E}_t(j)$ in Definition 2 depend only on the steady-state survival transitions $\{\mathcal{L}_{ss}(j)\}_{j=0}^{J-1}$ and outcome vectors $\{\mathbf{y}_{ss}(j)\}_{j=0}^{J-1}$. Next, consider the policy and flow shifts that appear in Theorem 1, and the transition matrices required to calculate the distributional shifts that also appear. Using the policy vectors as examples, arrange the required elements in tables with shock horizon s increasing along rows and age j increasing along columns,

$$\begin{array}{cccc} \mathbf{y}_0^0(0) & \mathbf{y}_0^0(1) & \cdots & \mathbf{y}_0^0(J-2) & \mathbf{y}_0^0(J-1) \\ \mathbf{y}_0^1(0) & \mathbf{y}_0^1(1) & \cdots & \mathbf{y}_0^1(J-2) & \boldsymbol{\times} \\ \vdots & \vdots & \ddots & \vdots & \vdots \\ \mathbf{y}_0^{J-1}(0) & \boldsymbol{\times} & \cdots & \boldsymbol{\times} & \boldsymbol{\times} \end{array} . \tag{28}$$

The s-th row of these tables contains the response at time 0 to the announcement of a shock that occurs at time $s \geq 0$. The j-th column contains the responses of agents aged j at the announcement. Agents of age $j > J-1-s$ will be past the terminal age when the shock arrives and therefore do not respond; these are objects we need not calculate. The perturbed flow vectors that we need follow the same triangular pattern.

Now consider sequences of aggregate inputs of length j that equal the steady-state value $\mathbf{X}_{ss}$ in every period except the last (the j-th), where they equal $\mathbf{X}_{ss} + dx$. Solving the life cycle model up to age j with such sequences of aggregate inputs and assuming inputs revert to steady state afterwards yields

$$\left\{\mathbf{y}_l^j(l),\, \mathbf{v}_l^j(l),\, \mathcal{L}_l^j(l),\, \mathbf{F}_l^j(l)\right\}_{l=0}^{j} = \overline{\texttt{solve}}_j\left(\mathbf{v}_{ss}\left(j+1\right), \{\mathbf{X}_{ss} + \mathbf{1}_{t=j}dx\}_{t=0}^{j}\right). \tag{29}$$

This is the life-cycle solution of an agent that expects a shock to $\mathbf{X}$ at age j, and who has known about this shock from his birth. In (29), we use our partial solver and the steady state solution to avoid solving for ages greater than j.

Concentrating on the results of (29) other than the value vector, which does not appear in Theorem 1, Lemma 2 implies

$$\left\{\mathbf{y}_l^j(l),\, \mathcal{L}_l^j(l),\, \mathbf{F}_l^j(l)\right\}_{l=0}^{j} = \left\{\mathbf{y}_0^{j-l}(l),\, \mathcal{L}_0^{j-l}(l),\, \mathbf{F}_0^{j-l}(l)\right\}_{l=0}^{j}.$$

These are precisely the elements of the j-th "anti-diagonal" (bottom-left to top-right diagonals) of the tables in (28). Therefore, given the steady state solution and expectation vectors, we only have to evaluate each of the partial solvers $\{\overline{\texttt{solve}}_j(\cdot)\}_{j=0}^{J-1}$ once and apply Lemma 4 to get the remaining building blocks that we need for $\{\mathcal{F}(j)\}_{j=0}^{J-1}$. Since partial solver $\overline{\texttt{solve}}_j(\cdot)$ nests the evaluation of single-period solvers $\{\texttt{solve}_l(\cdot)\}_{l=0}^{j}$, this entails evaluating a total of $J \times (J+1)/2$ single-period solvers.

The reduced number of single period solutions contributes to the performance of our method. Return to the experiment in Table 1, which finds a 300-period Jacobian of an infinite-horizon household and compares its cost with those of finding the same Jacobian in

an analog life-cycle model with 75 possible ages. The infinite-horizon model (first row) and life-cycle model (third row) use the exact same single-period solver implementation and their single-period problems have the exact same number of idiosyncratic states. Applying the traditional SSJ method to the infinite-horizon model requires $H = 300$ solutions of the single-period problem. Applying our method to the life-cycle model requires $75 \times 76/2 = 2{,}850$ single period solutions. Therefore, the number of single-period problems that must be solved in the life-cycle version of the model grows only by a factor of $2{,}850/300 = 9.5$, which is close to the speed ratio we report in Table 1. The speed gains of the life-cycle model relative to the large-scale infinite-horizon model reflect that the (age-specific) single-period problems are much lower dimensional than corresponding (pooled) single-period problems.

5.2 Algorithm

Given the results of the previous subsection, one could first use partial solvers to obtain all the objects in (28), then use Lemma 4 to compute net distributional changes, and then use Theorem 1 to construct age-specific fake news matrices. This naive approach can become impractical even in moderately sized models. The number of points in age-specific state spaces can easily be in the thousands. As a result, each of the policy vectors ($\mathbf{y}$) and transition matrices ($\mathcal{L}$) in (28) can contain thousands and millions of elements, respectively.[13] Storing and manipulating the $J \times (J+1)/2$ policy vectors and transition matrices simultaneously can therefore become cumbersome even for moderate values of J and moderate state-space sizes. For such cases, this section presents an algorithm that constructs age-specific fake news matrices progressively, evaluating one partial solver at a time and updating the relevant matrix entries before calling the next solver, so that these objects need not all be stored in memory at once.

Algorithm 1 summarizes the routine. It takes the steady-state solution as its input and returns age-specific fake news matrices $\{\mathcal{F}(j)\}_{j=0}^{J-1}$ of shape $J \times J$. Without dynastic links, these are sufficient to calculate Jacobians for any shock horizon. After pre-computing expectation vectors, the main loop iterates over the $J-1$ required evaluations of partial solvers. Each evaluation yields a list of shocked transition matrices, policy vectors and flows. Using Lemma 2 these are interpreted as time-0 responses of age-l agents to shocks that happen at time $s-l$. Lines 5 to 13 use these shocked solutions iterating over the $t = 0$ age of agents, l. Line 6 updates $t = 0$ responses. For $t \geq 1$, fake news matrices propagate changes in $t = 1$ distributions ($\mathbf{\Xi}$) forward in time using expectation vectors. If $l = J-1$, $t = 0$ was the agents' last living period and there is no distributional shift in $t = 1$ (line 7 condition). Otherwise, lines 8 to 11 calculate and propagate the distributional shift.

The following lemma ensures the algorithm produces the complete fake news matrices described by Theorem 1.

[13] In practice, transition matrices are often sparse and could be stored using specialized representations. Exploiting this (different) form sparsity is useful to increase efficiency, but is independent from the efficiency gains provided by our algorithm.

Algorithm 1 Fake news matrices without dynastic links

Input: Steady state: $\{\mathbf{v}_{ss}, \mathcal{L}_{ss}(j), \mathbf{y}_{ss}(j), \mathbf{D}_{ss}(j), \mathbf{F}_{ss}(j)\}_{j=0}^{J-1}$ and $\mathbf{X}_{ss}$

Pre-compute: $\mathcal{E}_t(j)$ for $0 \leq j \leq J-1$ and $0 \leq t \leq J-1-j$ via Definition 2

Initialize: $\{\mathcal{F}(j)\}_{j=0}^{J-1} \in \mathbb{R}^{J \times J}$ with zeros

for $s = 0, \ldots, J-1$ **do** ▷ Shock horizon

$$\{\mathcal{L}_0^{s-l}(l), \mathbf{y}_0^{s-l}(l), \mathbf{F}_0^{s-l}(l)\}_{l=0}^{s} \leftarrow \begin{cases} \overline{\texttt{solve}}_s\left(\mathbf{v}_{ss}(s{+}1),\ \{\mathbf{X}_{ss} + \mathbf{1}_{j=s} dx\}_{j=0}^{s}\right), & s < J{-}1 \\ \overline{\texttt{solve}}_{J-1}\left(\{\mathbf{X}_{ss} + \mathbf{1}_{j=J-1} dx\}_{j=0}^{J-1}\right), & s = J{-}1 \end{cases}$$

  for $l = 0, \ldots, s$ **do** ▷ Age at $t = 0$

    $\mathcal{F}_{0,s-l}(l) \leftarrow d\mathbf{y}_0^{s-l}(l)^\intercal \mathbf{D}_{ss}(l) \ + \ \mathbf{y}_{ss}(l)^\intercal d\mathbf{F}_0^{s-l}(l)$

    if $l < J-1$ **then**

      $\boldsymbol{\Xi}^{s-l}(l+1) \leftarrow d\mathcal{L}_0^{s-l}(l)^\intercal \mathbf{D}_{ss}(l) \ + \ \mathcal{L}_{ss}(l)^\intercal d\mathbf{F}_0^{s-l}(l)$

      for $t = 1, \ldots, (J-1) - l$ **do** ▷ Time periods

        $\mathcal{F}_{t,s-l}(l+t) \leftarrow \mathcal{E}_{t-1}(l+1)^\intercal \boldsymbol{\Xi}^{s-l}(l+1)$

      end for

    end if

  end for

end for

Output: Fake news matrices $\{\mathcal{F}(j)\}_{j=0}^{J-1}$

Lemma 5. *For every $t, s, j \in \{0, \ldots, J-1\}$, Algorithm 1 produces the value of $\mathcal{F}_{t,s}(j)$ given by Theorem 1.*

Proof of Lemma 5. See Appendix A.4.

Appendix B.3 presents the version of the algorithm that allows for dynastic links, relaxing Assumption 3.

6 Application

Next, we demonstrate the usefulness of our method through an application: a dynamic general-equilibrium analysis of a permanent fall in births. We calibrate the motivating example model of Section 2 to reproduce the age pyramid and life-cycle profiles of income, wealth, and income risk in the United States. Then, we present examples of age-specific Jacobians of the household block in partial equilibrium. Finally, we calibrate the firm and government sectors, and simulate the effects of a permanent fall in the growth rate of newborn cohorts. We emphasize the effects of the transition on the natural rate of interest using the dynamic version of the aggregate asset supply and demand framework of Auclert et al. (2025b).

6.1 Household Block in Partial Equilibrium

We calibrate the household block to reproduce the distribution of income and assets in the 2019 wave of the U.S. Survey of Consumer Finances (SCF).[14] We describe this process in detail in Appendix C and only give a brief overview in this section.

Each model period corresponds to one year. Households enter the model at age 26, retire at age 65, and can live up to age 100 ($J = 75$). We use survival probabilities ψ from the life tables of the Social Security Administration. For income shocks, we use Janssens and McCrary's (2023) age-specific optimal discretization of the non-parametric process of Arellano, Blundell, and Bonhomme (2017). Newborns enter with zero wealth and labor productivity drawn from the ergodic distribution of this process at age 26. The total mass of newborns grows at an annual rate of 0.30%, so total population and aggregate quantities grow at the same rate. We refer to the fixed point of the detrended variables on this balanced growth path as the initial steady state. The warm-glow utility from bequeathing wealth $\phi(\cdot)$ has the same functional form as in Carroll (2002) and De Nardi (2004), implying that bequests are a luxury good, which helps us match the skewness of old-age wealth. Figure 1 depicts the age pyramid and the contributions of different age groups to labor supply, net taxes, and wealth in steady state.

[14] The steady-state calibration of the household block is very similar to that in Bardóczy, Savoia, and Velásquez-Giraldo (2024).

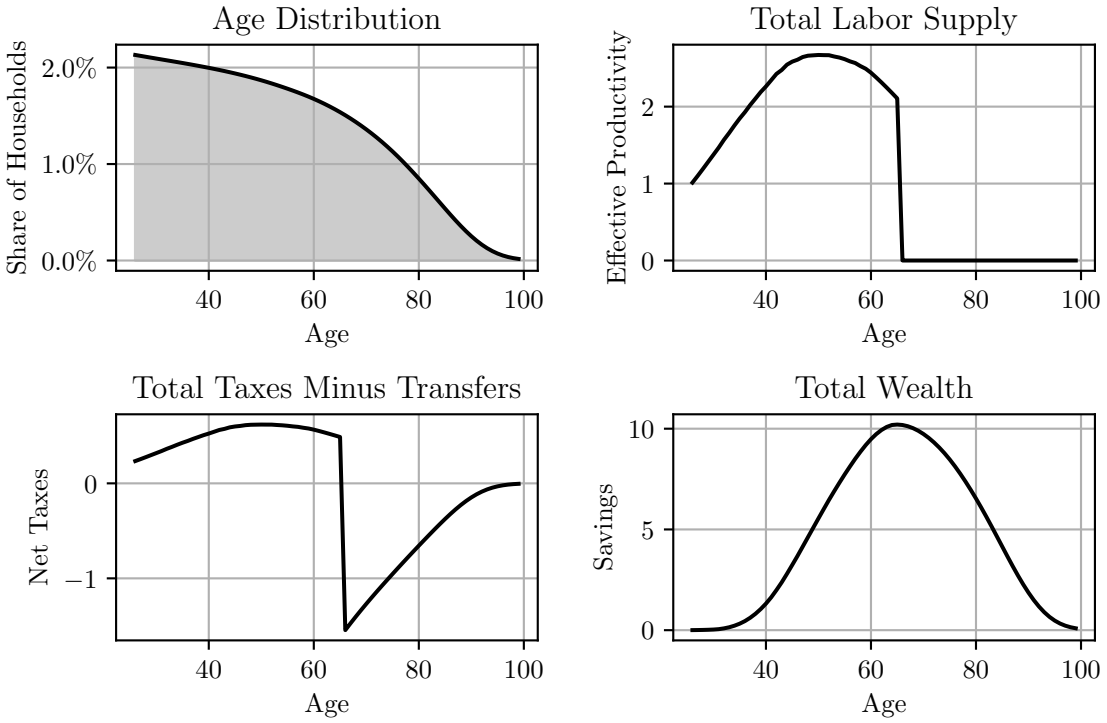

Figure 1: Age Structure and Life-Cycle Profiles in Steady State

Notes: the top left panel depicts the share of households of each age in the initial steady state of the model. The other panels depict the part of aggregate labor supply (N_t), net taxes T_t, and total savings A_t that is due to each age group in steady state.

Block representation. The core household block maps sequences of interest rates, tax rates, wages, aggregate inheritances, and newborn cohort growth rates into sequences of aggregate savings, bequests, consumption, labor supply, population, and net transfers. Because the size of newborn cohorts may grow over time, this application follows the framework of Example B in Section 3, where the distribution of households $\mathbf{D}_t$ is scaled by the size of the contemporaneous newborn cohort n_t. We continue to use hats to signify this normalization, and write the core household block as

$$\{R_t, \tau_t, w_t, I_t, \Upsilon_t\}_{t\geq 0} \to \{\hat{A}_t, \hat{B}_t, \hat{C}_t, \hat{N}_t, \hat{P}_t, \hat{T}_t\}_{t\geq 0} \tag{30}$$

Normalizing with the mass of newborns is convenient, because it is not affected by past demographic shocks. However, once we obtain the Jacobians of the core household block (30), it is straightforward to express the outputs in more intuitive per-capita terms. For each per-newborn output $\hat{X}_t \in \{\hat{A}_t, \hat{B}_t, \hat{C}_t, \hat{N}_t, \hat{P}_t, \hat{T}_t\}$, we may compute its per-capita analog and the population growth factor Γ_t as

$$X_t = \frac{\hat{X}_t}{\hat{P}_t}, \qquad \Gamma_t = \frac{\hat{P}_t}{\hat{P}_{t-1}}\Upsilon_t. \tag{31}$$

Before using the household block as a unit of economic analysis (e.g., to trace out asset demand as a function of interest rates), we solve for the fixed point between per-capita inheritance $\{I_t\}_{t\geq 0}$ (an input) and per-capita bequests $\{B_t\}_{t\geq 0}$ (an output). Thus, the final household block takes the form of

$$\{R_t, \tau_t, w_t, \Upsilon_t\}_{t\geq 0} \to \{A_t, B_t, C_t, N_t, P_t, T_t, \Gamma_t\}_{t\geq 0}. \tag{32}$$

In SSJ terminology, (32) is a solved block that nests an HA-OLG block (30) and a simple block (31).

Jacobians for age groups and cohorts. Because our method assembles block Jacobians from age-specific Jacobians, decomposing aggregate shock responses into the contributions of age groups or cohorts is immediate. Figure 2 showcases such a decomposition. The left panel shows the response of savings per capita to a 1 percentage point increase in the interest rate that occurs in year 10. This is, up to re-scaling, the tenth column of $\mathcal{J}^{A,R}$. Splitting $\mathcal{J}^{A,R}$ into $\sum_{j=0}^{J^{ret}-1} \mathcal{J}^{A,R}(j)$ and $\sum_{j=J^{ret}}^{J-1} \mathcal{J}^{A,R}(j)$ yields the contribution of working-age households and retirees to the total response. The distinction between age groups and cohorts is crucial to the interpretation of these decompositions. The age-specific Jacobians that we obtain with Algorithm 1 capture the contributions of groups whose composition changes over time. For example, in the left panel of Figure 2, most of the households that contribute to the response of workers in year 0 will be counted in the response of retirees in year 40, as they will have retired by then.[15]

[15] One may instead be interested in the responses of fixed cohorts of households over time. We can compute the elements of a Jacobian for the cohort of households that had age j in year 0 as

$$\mathcal{J}^{cohort}(j)_{t,s} = \begin{cases} \mathcal{J}(j+t)_{t,s}, & \text{if } j+t<J, \\ 0, & \text{otherwise,} \end{cases} \quad \forall\ t\geq 0, s\geq 0. \tag{33}$$

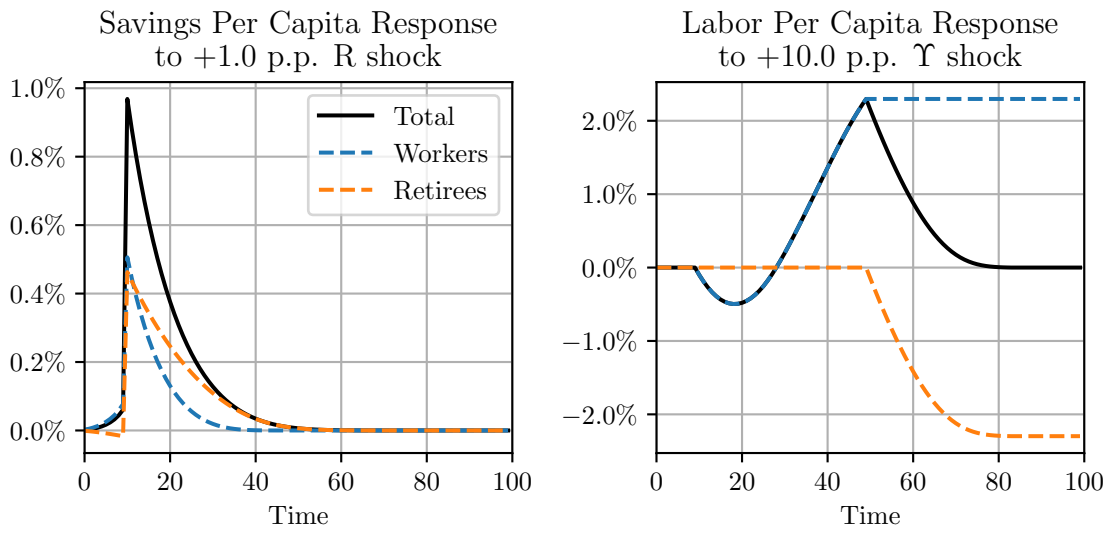

Figure 2: Examples of Life-Cycle Jacobians

Notes: The left panel shows the response to a one-time, anticipated increase in the real return of savings that occurs in year 10. The right panel shows the response to a one-time increase in the growth rate of newborn cohorts that occurs in year 10. In both panels, the total response is decomposed into the contributions of working-age households and retirees.

The responses of working-age and retired households are qualitatively different. In anticipation of the rise in the future interest rate, workers increase their savings while retirees reduce theirs. The interest-rate increase triggers two competing forces: a substitution effect, which encourages households to save more and take advantage of higher future returns, and an income effect, which encourages them to consume some of the future income gain. For working-age households, the substitution effect dominates, as is typical in infinite-horizon models. Retirees, by contrast, expect to live for only a short time after the shock and therefore smooth consumption over a shorter horizon, which amplifies the income effect relative to the substitution effect. After the shock, retirees' savings take much longer to return to steady state, because the retired population is progressively replenished by cohorts that were still working when the shock hit and accumulated extra savings in anticipation of it.

The right panel of Figure 2 shows how a 10 percentage point increase in the newborn growth rate Υ_t in year 10 affects aggregate labor supply per capita.[16] Recall that each working-age household supplies hours inelastically, so changes in aggregate labor supply are driven not by behavioral responses but by shifts in the population shares of cohorts with different levels of average productivity.[17]

Labor supply therefore does not respond until year 10, when the shock arrives and larger

Figure D.2 in Appendix D compares age and cohort Jacobians.

[16]Note that a one-time shock to the growth rate of newborn cohorts increases the mass of newborns and ultimately that of other cohorts forever.

[17]Because this shock shifts both the numerator and denominator of labor per capita (N_t/P_t), different additive decompositions could be constructed. We use $d(N_t/P_t) = dN_t/P_{ss} - N_{ss}/P_{ss} \cdot dP_t/P_{ss} = \sum_{j=0}^{75} [dN_t(j)/P_{ss} - N_{ss}/P_{ss} \cdot dP_t(j)/P_{ss}]$.

cohorts of young workers start entering the economy. Because these additional workers are initially young and inexperienced, their contribution to productivity-adjusted labor does not offset their contribution to total population, causing the initial drop in effective labor per capita.[18] As these larger cohorts age, their productivity increases and their contribution to effective labor per capita turns positive. In year 50, the last cohort unaffected by the shock retires; the workforce reaches its new steady state, and the working-age contribution stabilizes at a positive value because the shock permanently raises the number of working-age households. The retiree contribution is flat until year 50, when the first of the larger cohorts retires; it then declines secularly and stabilizes at a negative value in year 85, once the last unaffected cohort dies. The permanently larger mass of retirees exactly offsets the permanently larger mass of workers, so effective labor per capita returns to its initial steady-state value.

6.2 Demographic Transition in General Equilibrium

We conclude this section with a general-equilibrium analysis of a permanent fall in the birth rate. On the initial BGP, every new cohort is 0.30 percent larger than the previous cohort, and total population grows at the same rate. Our experiment assumes that newborn cohorts stop growing completely in period 0, and we use the sequence-space Jacobian method to compute the first-order approximation of the transition to the new steady state with zero population growth. We emphasize that the exercise in this section runs in a fraction of a minute on a laptop; this includes calculating all the required Jacobians.

Figure 3 shows the mechanical effects of the birth rate shock on the age structure of the population. The blue line on the left panel shows the exogenous growth rate of the newborn population, which drops from 0.30% to 0% in year 0. The orange line shows the resulting growth rate of total population, which approaches 0% gradually instead. Although the incoming cohorts are not growing after period 0, they are still larger than the outgoing cohorts that were born before the shock. The demographic transition is complete after 75 years, when the last households born before the shock die.

The right panel of Figure 3 shows three snapshots of the age structure of the population during the transition.[19] We distinguish three age groups: young workers aged 25–45, middle-aged workers aged 45–65, and retirees aged 65 and above. The blue bars represent the percentage point change in the population share of these groups relative to the initial steady state after 18 years, i.e. after a quarter into the demographic transition. The orange and green bars represent the same changes after 37 and 75 years, i.e. after two-thirds and the entirety of the transition, respectively.

On the initial balanced growth path, the population consists of 41.5 percent young workers, 35.5 percent middle-aged workers, and 23.0 percent retirees. In the terminal steady state with no population growth, these numbers are 39.6 percent, 35.8 percent, and 24.6

[18] Vandenbroucke (2021) documents a similar effect in the context of baby boomers' entry into the labor force.

[19] Note that the dynamics of the complete population pyramid for all ages is straightforward to compute using the age-specific Jacobians of the household block for output $P_{j,t}$, normalized population.

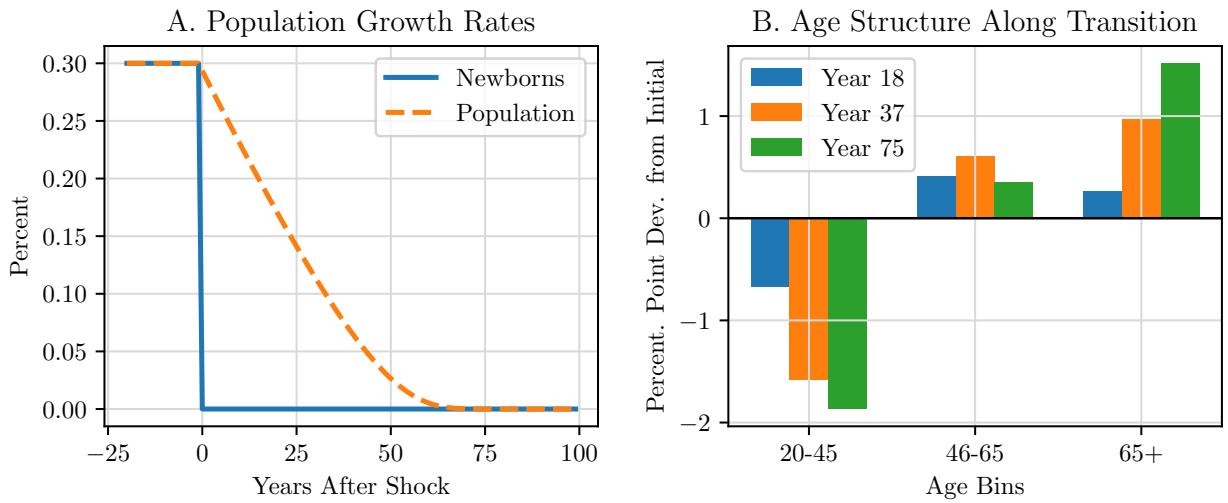

Figure 3: The Birth Rate Shock and its Mechanical Effects on Population

percent, respectively. The decline in the growth of new cohorts makes society older. The key takeaway, however, is that the transition is uneven across these broad age groups. The share of young workers drops most rapidly, reflecting that the shock affects them directly and immediately. The share of middle-aged workers increases in a hump-shaped pattern, peaking 37 years into the transition. By this time, the young and middle-aged groups have reached their final size, but the mass of retirees is still growing. Consistent with these facts, the share of retirees grows steadily, and the change is backloaded compared to the other two groups.

Prices and macroeconomic aggregates. The demographic transition induces changes in equilibrium prices and quantities. Figure 4 shows the paths of output, labor, capital, the income tax rate, the wage, and the interest rate from the initial steady state (black dotted line) to the terminal steady state (red dotted line). Output per capita rises initially, then falls and settles below its initial steady state. Because TFP is constant, this non-monotonic path is generated entirely by labor and capital per capita. Labor per capita rises at first because the working-age population shifts toward older, more productive workers, an effect that dominates the decline in the working-age share for the first 18 years. Eventually, however, labor per capita falls as the labor force of the older economy shrinks. Capital per capita also rises, peaks 37 years after the shock, then falls slightly and settles above its initial value. This path reflects both the mechanical effects of population aging and the endogenous response to changes in the interest rate, the wage, and the tax rate—channels we isolate formally below. The tax rate rises monotonically to finance social security payments at a higher dependency ratio. The wage rises and the interest rate falls, reflecting the growing scarcity of labor.

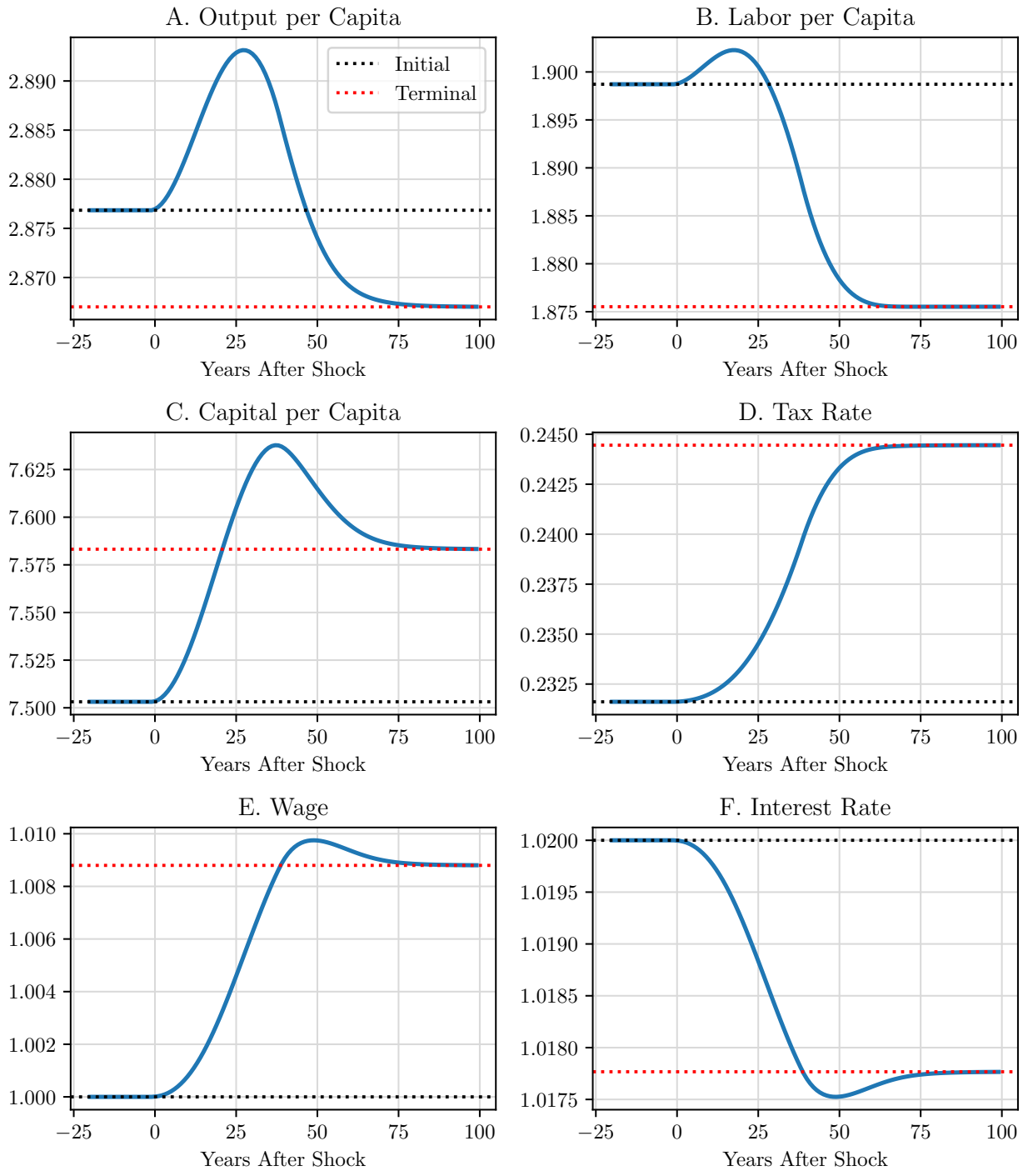

Figure 4: Equilibrium Responses to a Permanent Decline in the Birth Rate

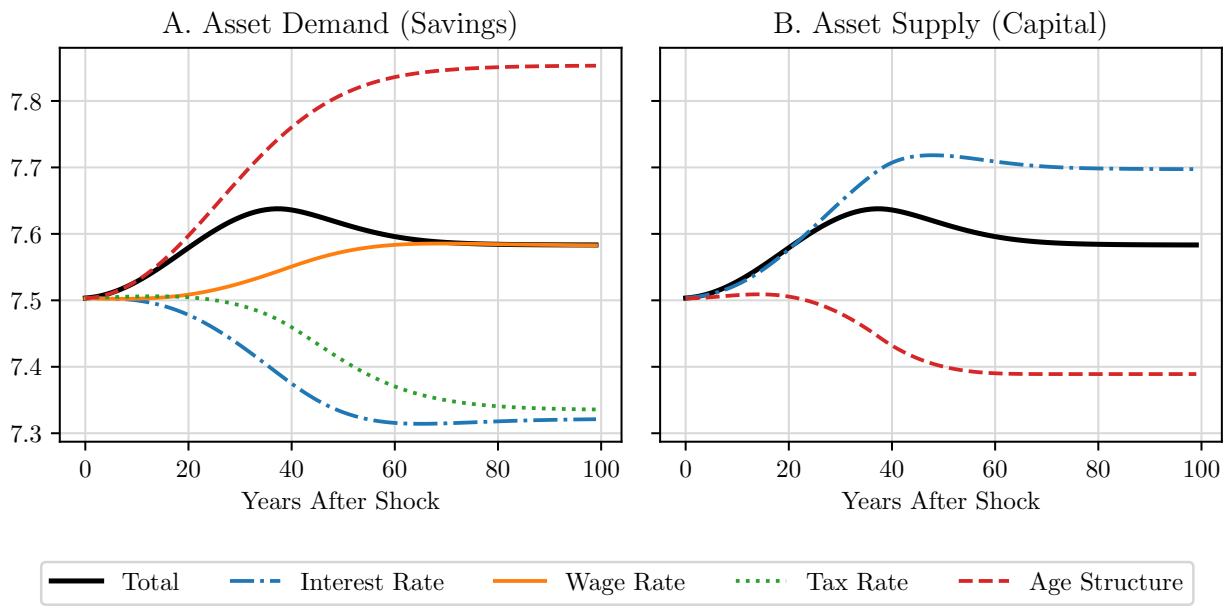

Figure 5: Dynamic Decomposition of Asset Demand and Supply

Asset demand and supply. Figure 5 decomposes the changes in asset demand (household savings) and asset supply (firms demand for capital). This decomposition is motivated by Auclert et al. (2025b), who compute the evolution of the natural rate of interest via shifts in the long-run (static) asset supply and demand curves in a heterogeneous-agent model with overlapping generations. Asset demand is a component of the household block (32)

$$\mathcal{A}_t^{demand}\big(\{R_t, w_t, \tau_t, \Upsilon_t\}_{t\geq 0}\big) \tag{34}$$

that we can differentiate using Algorithm 1. In this economy, the only asset in positive net supply is physical capital, and hence asset supply is

$$\mathcal{A}_t^{supply}(R_{t+1}, L_{t+1}, \Gamma_{t+1}) = \left(\frac{\alpha\Theta}{R_{t+1} - 1 + \delta}\right)^{\frac{1}{1-\alpha}} L_{t+1}\Gamma_{t+1} \tag{35}$$

which can be obtained by substituting the per-capita production function $Y_t = \Theta_t(K_{t-1}/\Gamma_t)^\alpha L_t^{1-\alpha}$ and rearranging it to express the firm's demand for capital.

Figure 5 shows how the $\mathcal{A}_t^{demand} = K_t = \mathcal{A}_t^{supply}$ equilibrium emerges from exogenous changes in age structure and endogenous changes in prices. Both panels show the equilibrium path of capital in black, with the contribution of a single factor overlaid in color. In the left panel, the strongest factor driving asset demand upward is population aging: in our calibrated model, as in the data, older workers save substantially more than younger households — for retirement and for luxury bequests, among other motives — so an older society saves more per capita. The wage contributes in the same direction: it rises as labor

becomes scarce, raising workers' incomes and encouraging them to save more for retirement. Two forces push the other way. First, the government must raise the income tax to sustain social security payments at the higher dependency ratio, a negative income effect for workers. Second, if the interest rate held steady, household asset demand would still exceed firms' capital needs, so the interest rate falls to clear the market.

This decomposition also reveals the reason for the hump-shaped path of capital. Each factor in isolation moves asset demand monotonically but the negative and positive effects play out at different speeds. Aging puts upward pressure on asset demand immediately, because young workers (whose population share falls most quickly) have the lowest savings. In contrast, the price adjustments that ultimately are driven by the scarcity of labor play out a bit more slowly, given that the increase in productivity per worker compensates for the decline in the labor force for a while.

Turning to asset supply, the initial rise and subsequent fall in labor per capita induces firms to pay a higher wage and demand less capital. The interest rate falls to boost the demand for capital, equating it with high savings from older households.

The finding that slower population growth can reduce the natural rate of interest is not new (see, e.g., Gagnon, Johannsen, and López-Salido 2021). Platzer and Peruffo (2022) and Auclert et al. (2025b) also quantify these mechanisms in rich heterogeneous-agent OLG models that have drawn substantial policy attention. Our adaptation of the sequence-space Jacobian method to life-cycle models greatly facilitates this type of analysis, including along the transition path. That matters because, as our application demonstrates, demographic shocks can produce long and non-trivial transitions even in a relatively simple model, where the only asset is physical capital.

7 Conclusion

This paper has two main goals. First, we want the derivations and algorithm we develop to serve the growing literature that uses models with overlapping generations of heterogeneous agents to tackle what we believe to be fundamental macroeconomic questions (see, for example, Auclert et al. 2021b; Platzer and Peruffo 2022; Gruss et al. 2025). We hope this will accelerate the development of existing models and lower the barriers to creating new ones. Second, we want this paper to serve as a bridge between fields in microeconomics that use life-cycle models—labor economics and household finance, for example—and the expanding sequence-space framework for macroeconomic modeling. Beyond the dynamic equilibrium analyses this framework facilitates, recent advances have extended it to incorporate imperfect expectations (Auclert, Rognlie, and Straub 2020; Bardóczy and Guerreiro 2024) and to study optimal policy (Auclert et al. 2024; Davila and Schaab 2025). The literature has prioritized modularity, often taking the sequence-space Jacobians of a block as its starting point. We hope that researchers will use our method to compute Jacobians for their own life-cycle models and leverage this growing toolkit.

Many technical advances we have not discussed here can further lower the computational burden of the models we consider. In particular, most techniques that speed up the mi-

croeconomic life-cycle problem or streamline its representation apply directly to our setup. Examples include sparse representations of transition matrices, sparse grids for age-specific state spaces (as in Brumm and Scheidegger 2017), and modeling decisions as sequences of stages (as in Carroll 2012; Druedahl 2021; Bardóczy 2022; Sun 2023). The results developed here can also be adapted to different or broader classes of models by altering our assumptions. We have provided explicit statements of these assumptions and the proofs behind our results to make that adaptation straightforward.

References

Arellano, Manuel, Richard Blundell, and Stéphane Bonhomme (2017). "Earnings and Consumption Dynamics: A Nonlinear Panel Data Framework". In: *Econometrica* 85.3, pp. 693–734.

Auclert, Adrien (2019). "Monetary Policy and the Redistribution Channel". In: *American Economic Review* 109.6, pp. 2333–2367.

Auclert, Adrien, Bence Bardóczy, Matthew Rognlie, and Ludwig Straub (2021a). "Using the Sequence-Space Jacobian to Solve and Estimate Heterogeneous-Agent Models". In: *Econometrica* 89.5, pp. 2375–2408.

Auclert, Adrien, Michael Cai, Matthew Rognlie, and Ludwig Straub (2024). *Optimal Long-Run Fiscal Policy with Heterogeneous Agents*. Pre-published.

Auclert, Adrien, Evan Majic, Matthew Rognlie, and Ludwig Straub (2025a). "Determinacy and Large-Scale Solutions in the Sequence Space". In: *Journal of Political Economy: Macroeconomics*. Forthcoming.

Auclert, Adrien, Hannes Malmberg, Frederic Martenet, and Matthew Rognlie (2021b). *Demographics, Wealth, and Global Imbalances in the Twenty-First Century*. Pre-published.

Auclert, Adrien, Hannes Malmberg, Matthew Rognlie, and Ludwig Straub (2025b). *The Race Between Asset Supply and Asset Demand*. Pre-published.

Auclert, Adrien, Matthew Rognlie, and Ludwig Straub (2020). *Micro Jumps, Macro Humps: Monetary Policy and Business Cycles in an Estimated HANK Model*. Pre-published.

— (2024). "The Intertemporal Keynesian Cross". In: *Journal of Political Economy* 132.12, pp. 4068–4121.

Azinovic-Yang, Marlon and Jan Žemlička (2025). *Deep Learning in the Sequence Space*. Pre-published.

Bardóczy, Bence (2022). "Spousal Insurance and the Amplification of Business Cycles". In.

Bardóczy, Bence and Joao Guerreiro (2024). *Unemployment Insurance in Macroeconomic Stabilization with Imperfect Expectations*. Pre-published.

Bardóczy, Bence, Ettore Savoia, and Mateo Velásquez-Giraldo (2024). *HANK Comes of Age: Monetary Policy with Heterogeneous Overlapping Generations*. Pre-published.

Beaudry, Paul, Paolo Cavallino, and Tim Willems (2024). *Life-Cycle Forces Make Monetary Policy Transmission Wealth-centric*. Pre-published.

Bhandari, Anmol, Thomas Bourany, David Evans, and Mikhail Golosov (2023). *A Perturbational Approach for Approximating Heterogeneous Agent Models*. Pre-published.

Bielecki, Marcin, Michał Brzoza-Brzezina, and Marcin Kolasa (2020). "Demographics and the Natural Interest Rate in the Euro Area". In: *European Economic Review* 129, p. 103535.

Blanchard, Olivier (2023). *Fiscal Policy under Low Interest Rates*. The MIT Press.

Boehl, Gregor (2023). *HANK on Speed: Robust Nonlinear Solutions Using Automatic Differentiation*. Pre-published.

Boppart, Timo, Per Krusell, and Kurt Mitman (2018). "Exploiting MIT Shocks in Heterogeneous-Agent Economies: The Impulse Response as a Numerical Derivative". In: *Journal of Economic Dynamics and Control*. Fed St. Louis-JEDC-SCG-SNB-UniBern Conference, Titled: "Fiscal and Monetary Policies". 89, pp. 68–92.

Brumm, Johannes and Simon Scheidegger (2017). "Using Adaptive Sparse Grids to Solve High-Dimensional Dynamic Models". In: *Econometrica* 85.5, pp. 1575–1612.

Cagetti, Marco and Mariacristina De Nardi (2006). "Entrepreneurship, Frictions, and Wealth". In: *Journal of Political Economy* 114.5, pp. 835–870.

Carroll, Christopher D. (2002). "Why Do the Rich Save So Much?" In: *Does Atlas Shrug? The Economic Consequences of Taxing the Rich*. Ed. by Joel B. Slemrod. Harvard University Press.

— (2006). "The Method of Endogenous Gridpoints for Solving Dynamic Stochastic Optimization Problems". In: *Economics Letters* 91.3, pp. 312–320.

— (2012). "Solution Methods for Microeconomic Dynamic Stochastic Optimization Problems".

Carvalho, Carlos, Andrea Ferrero, and Fernanda Nechio (2016). "Demographics and Real Interest Rates: Inspecting the Mechanism". In: *European Economic Review*. SI: The Post-Crisis Slump 88, pp. 208–226.

Castañeda, Ana, Javier Díaz-Giménez, and José-Víctor Ríos-Rull (2003). "Accounting for the U.S. Earnings and Wealth Inequality". In: *Journal of Political Economy* 111.4, pp. 818–857.

Davila, Eduardo and Andreas Schaab (2025). "Welfare Assessments with Heterogeneous Individuals". In: *Journal of Political Economy*.

De Nardi, Mariacristina (2004). "Wealth Inequality and Intergenerational Links". In: *The Review of Economic Studies* 71.3, pp. 743–768.

Dobrescu, Loretti and Akshay Shanker (2024). *Using Inverse Euler Equations to Solve Multidimensional Discrete-Continuous Dynamic Models: A General Method*. Pre-published.

Doepke, Matthias and Martin Schneider (2006). "Inflation and the Redistribution of Nominal Wealth". In: *Journal of Political Economy* 114.6, pp. 1069–1097.

Druedahl, Jeppe (2021). "A Guide on Solving Non-Convex Consumption-Saving Models". In: *Computational Economics* 58.3, pp. 747–775.

Evans, Richard W. and Kerk L. Phillips (2014). "OLG Life Cycle Model Transition Paths: Alternate Model Forecast Method". In: *Computational Economics* 43.1, pp. 105–131.

Fernández-Villaverde, Jesús, Gustavo Ventura, and Wen Yao (2025). "The Wealth of Working Nations". In: *European Economic Review* 173, p. 104962.

Gagnon, Etienne, Benjamin K. Johannsen, and David López-Salido (2021). "Understanding the New Normal: The Role of Demographics". In: *IMF Economic Review* 69.2, pp. 357–390.

Gruss, Bertrand, Eric Huang, Andresa Lagerborg, Diaa Noureldin, and Galip Kemal Ozhan (2025). "The Rise of the Silver Economy: Global Implications of

Population Aging". In: *IMF World Economic Outlook, April 2025: A Critical Juncture Amid Policy Shifts*. World Economic Outlook. International Monetary Fund.
Guvenen, Fatih, Gueorgui Kambourov, Burhan Kuruscu, Sergio Ocampo, and Daphne Chen (2023). "Use It or Lose It: Efficiency and Redistributional Effects of Wealth Taxation*". In: *The Quarterly Journal of Economics* 138.2, pp. 835–894.
Iacoviello, Matteo and Marina Pavan (2013). "Housing and Debt over the Life Cycle and over the Business Cycle". In: *Journal of Monetary Economics* 60.2, pp. 221–238.
Iskhakov, Fedor, Thomas H. Jørgensen, John Rust, and Bertel Schjerning (2017). "The Endogenous Grid Method for Discrete-Continuous Dynamic Choice Models with (or without) Taste Shocks". In: *Quantitative Economics* 8.2, pp. 317–365.
Janssens, Eva F. and Sean McCrary (2023). *Finite-State Markov-Chain Approximations: A Hidden Markov Approach*. Pre-published.
Kaplan, Greg, Benjamin Moll, and Giovanni L. Violante (2018). "Monetary Policy According to HANK". In: *American Economic Review* 108.3, pp. 697–743.
Krusell, Per and Jr. Smith Anthony A. (1998). "Income and Wealth Heterogeneity in the Macroeconomy". In: *Journal of Political Economy* 106.5, pp. 867–896.
Kübler, Felix and Simon Scheidegger (2025). "Self-Justified Equilibria: Existence and Computation". In: *Journal of the European Economic Association*, jvaf062.
Laibson, David (1997). "Golden Eggs and Hyperbolic Discounting*". In: *The Quarterly Journal of Economics* 112.2, pp. 443–478.
Luetticke, Ralph (2021). "Transmission of Monetary Policy with Heterogeneity in Household Portfolios". In: *American Economic Journal: Macroeconomics* 13.2, pp. 1–25.
Peterman, William B. and Erick Sager (2022). "Optimal Public Debt with Life Cycle Motives". In: *American Economic Journal: Macroeconomics* 14.4, pp. 404–437.
Platzer, Josef and Marcel Peruffo (2022). *Secular Drivers of the Natural Rate of Interest in the United States: A Quantitative Evaluation*. Pre-published.
Reiter, Michael (2009). "Solving Heterogeneous-Agent Models by Projection and Perturbation". In: *Journal of Economic Dynamics and Control* 33.3, pp. 649–665.
Straub, Ludwig (2019). "Consumption, Savings, and The Distribution of Permanent Income".
Sun, Jeffrey E (2023). *Continuation Value Is All You Need: A Deep Learning Method for Solving Heterogeneous-Agent Models*. Pre-published.
Vandenbroucke, Guillaume (2021). "The Baby Boomers and the Productivity Slowdown". In: *European Economic Review* 132, p. 103609.
Young, Eric R. (2010). "Solving the Incomplete Markets Model with Aggregate Uncertainty Using the Krusell–Smith Algorithm and Non-Stochastic Simulations". In: *Journal of Economic Dynamics and Control*. Computational Suite of Models with Heterogeneous Agents: Incomplete Markets and Aggregate Uncertainty 34.1, pp. 36–41.

A Proofs

A.1 Section 3 Proofs

The first proof, establishing the form of the steady-state distribution, is straightforward; we include it here for completeness.

Proof of Claim 1. A steady state of the model has $\mathbf{D}_t(j) = \mathbf{D}_{ss}(j)$ for all t and $0 \le j \le J-1$, with $\mathcal{L}_t(j) = \mathcal{L}_{ss}(j)$, $\Omega_t(j) = \Omega_{ss}(j)$, and $\mathbf{F}_{t+1}(j) = \mathbf{F}_{ss}(j)$. Substituting these identities into (16) yields, for $1 \le j \le J-1$,

$$\mathbf{D}_{ss}(j) = \mathcal{L}_{ss}(j-1)^{\mathsf{T}}\, \mathbf{D}_{ss}(j-1) + \mathbf{F}_{ss}(j),$$

and for $j = 0$,

$$\mathbf{D}_{ss}(0) = \sum_{l=0}^{J-1} \Omega_{ss}(l)^{\mathsf{T}}\, \mathbf{D}_{ss}(l) + \mathbf{F}_{ss}(0).$$

□

Common setup for Lemmas 1–3. Apply the recursive definitions in (20) until the terminal age to arrive at, for $0 \le j < J-1$ and $t, s \ge 0$,

$$\begin{aligned}
\mathbf{v}_t^s(j) &= v[j]\big(\mathbf{v}_{t+1}^s(j+1),\, \mathbf{X}_t^s\big) \\
&= v[j]\big(v[j+1]\big(\mathbf{v}_{t+2}^s(j+2),\, \mathbf{X}_{t+1}^s\big),\, \mathbf{X}_t^s\big) \\
&\equiv v[j](\mathbf{X}_t^s) \circ v[j+1](\mathbf{X}_{t+1}^s) \circ \mathbf{v}_{t+2}^s(j+2) \\
&\cdots \\
&= v[j](\mathbf{X}_t^s) \circ v[j+1](\mathbf{X}_{t+1}^s) \circ \cdots \circ v[J-1](\mathbf{X}_{t+J-1-j}^s),
\end{aligned}$$

and, likewise,

$$\begin{aligned}
\mathbf{y}_t^s(j) &= y[j](\mathbf{X}_t^s) \circ v[j+1](\mathbf{X}_{t+1}^s) \circ \cdots \circ v[J-1](\mathbf{X}_{t+J-1-j}^s), \\
\mathcal{L}_t^s(j) &= \mathcal{L}[j](\mathbf{X}_t^s) \circ v[j+1](\mathbf{X}_{t+1}^s) \circ \cdots \circ v[J-1](\mathbf{X}_{t+J-1-j}^s), \\
\Omega_t^s(j) &= \Omega[j](\mathbf{X}_t^s) \circ v[j+1](\mathbf{X}_{t+1}^s) \circ \cdots \circ v[J-1](\mathbf{X}_{t+J-1-j}^s), \\
\mathbf{F}_t^s(j) &= F[j](\mathbf{X}_t^s) \circ v[j+1](\mathbf{X}_{t+1}^s) \circ \cdots \circ v[J-1](\mathbf{X}_{t+J-1-j}^s).
\end{aligned} \tag{A.1}$$

At the boundary $j = J-1$, the second part of Assumption 2 gives the no-continuation forms $\mathbf{v}_t^s(J-1) = v[J-1](\mathbf{X}_t^s)$, $\mathbf{y}_t^s(J-1) = y[J-1](\mathbf{X}_t^s)$, and analogously for Ω and $\mathbf{F}$.

Recall that $\mathbf{X}^s$ is the sequence with $\mathbf{X}_{ss} + dx$ in entry s and $\mathbf{X}_{ss}$ in every other entry. Equivalently, $\mathbf{X}_\tau^s = \mathbf{X}_{ss} + dx \cdot \mathbf{1}\{\tau = s\}$. The set of $\mathbf{X}^s$-entries appearing on the right-hand side of (A.1) at age j and time t is defined by

$$S_{t,j} := \{\mathbf{X}_t^s, \mathbf{X}_{t+1}^s, \ldots, \mathbf{X}_{t+J-1-j}^s\}.$$

The three lemmas now follow by checking when $\mathbf{X}_{ss} + dx$ does or does not appear in $S_{t,j}$.

Proof of Lemma 1. Assume $t > s$. Every element of $S_{t,j}$ has time index in $\{t, t+1, \ldots, t+J-1-j\}$, all strictly greater than s, so every entry equals $\mathbf{X}_{ss}$. Substituting into (A.1) yields, for each $0 \leq j < J-1$,

$$\mathbf{y}_t^s(j) = y[j](\mathbf{X}_{ss}) \circ v[j+1](\mathbf{X}_{ss}) \circ \cdots \circ v[J-1](\mathbf{X}_{ss}) = \mathbf{y}_{ss}(j),$$

and identically $\mathcal{L}_t^s(j) = \mathcal{L}_{ss}(j)$, $\Omega_t^s(j) = \Omega_{ss}(j)$, and $\mathbf{F}_t^s(j) = \mathbf{F}_{ss}(j)$. At $j = J-1$, the same substitution into the boundary statement gives $\mathbf{y}_t^s(J-1) = y[J-1](\mathbf{X}_{ss}) = \mathbf{y}_{ss}(J-1)$, and likewise for $\mathbf{v}$, Ω, and $\mathbf{F}$. □

Proof of Lemma 2. Fix $k \geq 0$. For every $l \geq 0$, $\mathbf{X}_{t+l}^s = \mathbf{X}_{ss} + dx \cdot \mathbf{1}\{t+l = s\} = \mathbf{X}_{ss} + dx \cdot \mathbf{1}\{t+k+l = s+k\} = \mathbf{X}_{t+k+l}^{s+k}$, so each input on the right-hand side of (A.1) for (t, s) at age j equals the corresponding input for $(t+k, s+k)$ at the same age. Since the function family $\{v[j], y[j], \mathcal{L}[j], \Omega[j], F[j]\}_{j=0}^{J-1}$ is time-invariant by Assumption 2, the right-hand sides of (A.1) agree at (t, s) and $(t+k, s+k)$. Hence

$$\mathbf{y}_t^s(j) = \mathbf{y}_{t+k}^{s+k}(j), \quad \mathcal{L}_t^s(j) = \mathcal{L}_{t+k}^{s+k}(j), \quad \Omega_t^s(j) = \Omega_{t+k}^{s+k}(j), \quad \mathbf{F}_t^s(j) = \mathbf{F}_{t+k}^{s+k}(j),$$

for all $0 \leq j < J-1$ and $k \geq 0$. At $j = J-1$ the identities $\mathbf{v}_t^s(J-1) = \mathbf{v}_{t+k}^{s+k}(J-1)$ (and analogously for $\mathbf{y}$, Ω, and $\mathbf{F}$) follow from $\mathbf{X}_t^s = \mathbf{X}_{t+k}^{s+k}$ applied to the boundary statement. □

Proof of Lemma 3. Assume $s - t > J-1-j$, equivalently $s > t+J-1-j$. The largest time index appearing in $S_{t,j}$ is $t+J-1-j < s$, so every element of $S_{t,j}$ has time index strictly less than s and equals $\mathbf{X}_{ss}$. Substituting into (A.1) for $0 \leq j < J-1$, and into the boundary statement for $j = J-1$, gives the required result. □

A.2 Section 4 Proofs

We first prove the lemma characterizing distributional shifts without dynastic links.

Proof of Lemma 4. By Definition 4, $\boldsymbol{\Xi}^s(j) = d\mathbf{D}_1^s(j) - d\mathbf{F}_1^s(j)$. The fixed initial condition $\mathbf{D}_0 - \mathbf{F}_0 = \mathbf{D}_{ss} - \mathbf{F}_{ss}$ gives

$$d\mathbf{D}_0^s(j) = d\mathbf{F}_0^s(j), \qquad 0 \leq j \leq J-1. \tag{A.2}$$

Case $1 \leq j \leq J-1$ (eq. (25)). Applying (16) at $t = 0$ and $j \geq 1$,

$$\mathbf{D}_1^s(j) = \mathcal{L}_0^s(j-1)^\mathsf{T}\, \mathbf{D}_0^s(j-1) + \mathbf{F}_1^s(j).$$

Linearizing around the steady state,

$$d\mathbf{D}_1^s(j) = d\mathcal{L}_0^s(j-1)^\mathsf{T}\, \mathbf{D}_{ss}(j-1) \;+\; \mathcal{L}_{ss}(j-1)^\mathsf{T}\, d\mathbf{D}_0^s(j-1) \;+\; d\mathbf{F}_1^s(j).$$

Substituting (A.2) and subtracting $d\mathbf{F}_1^s(j)$ yields (25). By Lemma 3 at $t = 0$ and age $j-1$, $d\mathcal{L}_0^s(j-1) = \mathbf{0}$ and $d\mathbf{F}_0^s(j-1) = \mathbf{0}$ for $s > J-j$, so $\boldsymbol{\Xi}^s(j) = \mathbf{0}$ in that range.

Case $j = 0$ (eq. (26)). Under Assumption 3, $\Omega_t^s(j) = \Omega_{ss}(j) = \mathbf{0}$ for all t, s, j. Applying (16) at $t = 0$ and $j = 0$ collapses to $\mathbf{D}_1^s(0) = \mathbf{F}_1^s(0)$, so $d\mathbf{D}_1^s(0) = d\mathbf{F}_1^s(0)$ and $\boldsymbol{\Xi}^s(0) = \mathbf{0}$. □

The remainder of this subsection proves Theorem 1. Throughout, we maintain Assumption 3 ($\Omega_{ss}(\cdot) \equiv d\Omega_0^s(\cdot) \equiv \mathbf{0}$), so that $\boldsymbol{\Xi}^s(0) = \mathbf{0}$ by Lemma 4.

For $t \geq 1$ define the *fake-news residual*

$$\mathbf{Q}_{t,s}(j) \;:=\; \begin{cases} d\mathbf{D}_t^s(j) \;-\; d\mathbf{D}_{t-1}^{s-1}(j), & s \geq 1, \\ d\mathbf{D}_t^0(j), & s = 0, \end{cases} \tag{A.3}$$

the time-t response of the age-j distribution to a date-s shock, net (when $s \geq 1$) of the time-$(t-1)$ response to a date-$(s-1)$ shock. The two-case form parallels Definition 1, which sets $\mathcal{F}_{t,0}(j) = \mathcal{J}_{t,0}(j)$ at $s = 0$ and $\mathcal{F}_{t,s}(j) = \mathcal{J}_{t,s}(j) - \mathcal{J}_{t-1,s-1}(j)$ at $s \geq 1$.

The following lemma handles the $t = 0$ case of Theorem 1.

Lemma 6 (Initial period, $t = 0$)**.** *For $s \geq 0$ and $0 \leq j \leq J-1$,*

$$\mathcal{F}_{0,s}(j) = \begin{cases} d\mathbf{y}_0^s(j)^\mathsf{T}\mathbf{D}_{ss}(j) \;+\; \mathbf{y}_{ss}(j)^\mathsf{T} d\mathbf{F}_0^s(j), & s \leq J-1-j, \\ 0, & s > J-1-j. \end{cases}$$

Proof. By Definition 1 and (22), $\mathcal{F}_{0,s}(j) = \mathcal{J}_{0,s}(j) = d\mathbf{y}_0^s(j)^\mathsf{T}\mathbf{D}_{ss}(j) + \mathbf{y}_{ss}(j)^\mathsf{T} d\mathbf{D}_0^s(j)$. The initial condition $\mathbf{D}_0 - \mathbf{F}_0$ is fixed at steady state, so $d\mathbf{D}_0^s(j) = d\mathbf{F}_0^s(j)$, giving the first case. For $s > J-1-j$, Lemma 3 at $t = 0$ gives $d\mathbf{y}_0^s(j) = \mathbf{0}$ and $d\mathbf{F}_0^s(j) = \mathbf{0}$, so $\mathcal{F}_{0,s}(j) = 0$. □

To prove Theorem 1 for $t \geq 1$, we characterize the fake-news residual recursively, beginning with the base case $t = 1$.

Claim 2. *For $s \geq 0$ and $0 \leq j \leq J-1$, $\mathbf{Q}_{1,s}(j) = \boldsymbol{\Xi}^s(j)$.*

Proof. For $s \geq 1$, (A.3) gives $\mathbf{Q}_{1,s}(j) = d\mathbf{D}_1^s(j) - d\mathbf{D}_0^{s-1}(j)$. The fixed initial condition makes $d\mathbf{D}_0^{s-1}(j) = d\mathbf{F}_0^{s-1}(j)$, and Lemma 2 (at $k = 1$) gives $d\mathbf{F}_0^{s-1}(j) = d\mathbf{F}_1^s(j)$, so $\mathbf{Q}_{1,s}(j) = d\mathbf{D}_1^s(j) - d\mathbf{F}_1^s(j) = \boldsymbol{\Xi}^s(j)$ by Definition 4.

For $s = 0$, the $s = 0$ branch of (A.3) gives $\mathbf{Q}_{1,0}(j) = d\mathbf{D}_1^0(j)$. Lemma 1 at $t = 1 > 0 = s$ gives $d\mathbf{F}_1^0(j) = \mathbf{0}$, so $\mathbf{Q}_{1,0}(j) = d\mathbf{D}_1^0(j) - d\mathbf{F}_1^0(j) = \boldsymbol{\Xi}^0(j)$ by Definition 4. □

The next result gives a recursive form of the fake-news residual.

Lemma 7 (Fake-news residual: survivor recursion)**.** *For $s \geq 0$:*

(i) $\mathbf{Q}_{t,s}(0) = \mathbf{0}$ *for every* $t \geq 1$*;*

(ii) $\mathbf{Q}_{t,s}(j) = \mathcal{L}_{ss}(j-1)^\mathsf{T}\, \mathbf{Q}_{t-1,s}(j-1)$ *for every* $t \geq 2$ *and* $1 \leq j \leq J-1$.

Proof. **Part (i),** $j = 0$**.** For $t = 1$, Claim 2 and $\boldsymbol{\Xi}^s(0) = \mathbf{0}$ (Lemma 4) give $\mathbf{Q}_{1,s}(0) = \boldsymbol{\Xi}^s(0) = \mathbf{0}$. For $t \geq 2$, Assumption 3 collapses the $j = 0$ branch of (16) to $\mathbf{D}_t^s(0) = \mathbf{F}_t^s(0)$, and likewise at $(t-1, s-1)$. For $s \geq 1$, linearizing and subtracting,

$$\mathbf{Q}_{t,s}(0) = d\mathbf{F}_t^s(0) - d\mathbf{F}_{t-1}^{s-1}(0) = \mathbf{0}$$

by Lemma 2 (at $k = 1$). For $s = 0$, the $s = 0$ branch of (A.3) together with the same collapse gives $\mathbf{Q}_{t,0}(0) = d\mathbf{D}_t^0(0) = d\mathbf{F}_t^0(0) = \mathbf{0}$ by Lemma 1 (at $t \geq 2 > 0 = s$).

Part (ii), $1 \leq j \leq J-1$. Applying (16) and linearizing around steady state, for any (t, s),

$$d\mathbf{D}_t^s(j) = d\mathcal{L}_{t-1}^s(j-1)^\mathsf{T}\,\mathbf{D}_{ss}(j-1) \;+\; \mathcal{L}_{ss}(j-1)^\mathsf{T}\,d\mathbf{D}_{t-1}^s(j-1) \;+\; d\mathbf{F}_t^s(j). \tag{A.4}$$

For $s \geq 1$, write (A.4) at (t, s) and at $(t-1, s-1)$ and subtract:

$$\mathbf{Q}_{t,s}(j) = \left[d\mathcal{L}_{t-1}^s(j-1) - d\mathcal{L}_{t-2}^{s-1}(j-1)\right]^\mathsf{T}\mathbf{D}_{ss}(j-1) + \mathcal{L}_{ss}(j-1)^\mathsf{T}\,\mathbf{Q}_{t-1,s}(j-1) + d\mathbf{F}_t^s(j) - d\mathbf{F}_{t-1}^{s-1}(j).$$

Lemma 2 (at $k = 1$) collapses both the $d\mathcal{L}$ bracket and the $d\mathbf{F}$ difference to $\mathbf{0}$, leaving $\mathbf{Q}_{t,s}(j) = \mathcal{L}_{ss}(j-1)^\mathsf{T}\,\mathbf{Q}_{t-1,s}(j-1)$.

For $s = 0$, the $s = 0$ branch of (A.3) gives $\mathbf{Q}_{t,0}(j) = d\mathbf{D}_t^0(j)$ and $\mathbf{Q}_{t-1,0}(j-1) = d\mathbf{D}_{t-1}^0(j-1)$. Apply Lemma 1 at $t \geq 2 > 0 = s$ to zero out $d\mathcal{L}_{t-1}^0(j-1)$ and $d\mathbf{F}_t^0(j)$ in (A.4):

$$\mathbf{Q}_{t,0}(j) = \mathcal{L}_{ss}(j-1)^\mathsf{T}\,d\mathbf{D}_{t-1}^0(j-1) = \mathcal{L}_{ss}(j-1)^\mathsf{T}\,\mathbf{Q}_{t-1,0}(j-1).$$

□

Iterating this recursion in age then yields the closed form below.

Lemma 8 (Fake-news residual: closed form)**.** *For $t \geq 1$, $s \in \{0, \ldots, J-1\}$, and $0 \leq j \leq J-1$,*

$$\mathbf{Q}_{t,s}(j) = \begin{cases} \left(\prod_{r=j-t+1}^{j-1} \mathcal{L}_{ss}(r)\right)^\mathsf{T} \boldsymbol{\Xi}^s(j-t+1), & j \geq t, \\ \mathbf{0}, & j < t, \end{cases} \tag{A.5}$$

where the product is taken left-to-right in increasing r, with the convention that the empty product equals the identity matrix; this case arises at $t = 1$, where the index set $\{j-t+1, \ldots, j-1\} = \{j, \ldots, j-1\}$ is empty. Moreover, $\mathbf{Q}_{t,s}(j) = \mathbf{0}$ whenever $j - t > J - 1 - s$.

Proof. We prove (A.5) by induction on t.

Base case ($t = 1$). For $j \geq 1 = t$, Claim 2 gives $\mathbf{Q}_{1,s}(j) = \boldsymbol{\Xi}^s(j)$, which matches the first branch of (A.5): the product $\prod_{r=j}^{j-1} \mathcal{L}_{ss}(r)$ is empty and equal to the identity. For $j = 0 < t = 1$, Claim 2 and $\boldsymbol{\Xi}^s(0) = \mathbf{0}$ (Lemma 4) give $\mathbf{Q}_{1,s}(0) = \boldsymbol{\Xi}^s(0) = \mathbf{0}$, matching the second branch.

Inductive step ($t \geq 2$). Assume (A.5) holds at $t-1$.

Case 1 ($j \geq t$). Then $j - 1 \geq t - 1$, so the inductive hypothesis at $(t-1, s, j-1)$ gives

$$\mathbf{Q}_{t-1,s}(j-1) = \Big(\prod_{r=j-t+1}^{j-2} \mathcal{L}_{ss}(r)\Big)^\mathsf{T} \boldsymbol{\Xi}^s(j-t+1).$$

Lemma 7(ii) and the rule $(AB)^\mathsf{T} = B^\mathsf{T}A^\mathsf{T}$ yield

$$\mathbf{Q}_{t,s}(j) = \mathcal{L}_{ss}(j-1)^\mathsf{T}\,\mathbf{Q}_{t-1,s}(j-1) = \Big(\prod_{r=j-t+1}^{j-1} \mathcal{L}_{ss}(r)\Big)^\mathsf{T} \boldsymbol{\Xi}^s(j-t+1).$$

Case 2 ($j < t$). If $j = 0$, Lemma 7(i) gives $\mathbf{Q}_{t,s}(0) = \mathbf{0}$ directly. If $1 \le j < t$, then $j-1 < t-1$, so the inductive hypothesis gives $\mathbf{Q}_{t-1,s}(j-1) = \mathbf{0}$, and Lemma 7(ii) yields $\mathbf{Q}_{t,s}(j) = \mathcal{L}_{ss}(j-1)^{\mathsf{T}}\,\mathbf{0} = \mathbf{0}$. Either way, $\mathbf{Q}_{t,s}(j) = \mathbf{0}$, matching the second branch.

Truncation. Suppose $j-t > J-1-s$. If $j < t$, the second branch of (A.5) gives $\mathbf{Q}_{t,s}(j) = \mathbf{0}$ directly. If $j \ge t$, set $l := j-t+1$; then $1 \le l \le J-1$ (since $j \le J-1$ and $t \ge 1$), and $j-t > J-1-s$ gives $l > J-s$. Lemma 4 then yields $\boldsymbol{\Xi}^s(l) = \mathbf{0}$, so substituting into the first branch of (A.5),

$$\mathbf{Q}_{t,s}(j) = \Big(\prod_{r=j-t+1}^{j-1} \mathcal{L}_{ss}(r)\Big)^{\mathsf{T}} \boldsymbol{\Xi}^s(l) = \mathbf{0}.$$

□

We now combine these results to prove Theorem 1.

Proof of Theorem 1. **Case 1 ($t = 0$).** The condition $j-t \le J-1-s$ reduces to $s \le J-1-j$, and Lemma 6 gives both the non-vanishing formula in that range and $\mathcal{F}_{0,s}(j) = 0$ when $s > J-1-j$ (i.e., $j-t > J-1-s$).

Case 2 ($t \ge 1$). For $s \ge 1$, Definition 1 and (22) give

$$\mathcal{F}_{t,s}(j) = \mathcal{J}_{t,s}(j) - \mathcal{J}_{t-1,s-1}(j) = \big(d\mathbf{y}_t^s(j) - d\mathbf{y}_{t-1}^{s-1}(j)\big)^{\mathsf{T}}\mathbf{D}_{ss}(j) \;+\; \mathbf{y}_{ss}(j)^{\mathsf{T}}\,\mathbf{Q}_{t,s}(j),$$

and the policy difference vanishes by Lemma 2 (at $k = 1$). For $s = 0$, Definition 1 and (22) give

$$\mathcal{F}_{t,0}(j) = \mathcal{J}_{t,0}(j) = d\mathbf{y}_t^0(j)^{\mathsf{T}}\,\mathbf{D}_{ss}(j) \;+\; \mathbf{y}_{ss}(j)^{\mathsf{T}}\,d\mathbf{D}_t^0(j),$$

in which the first term vanishes by Lemma 1 (at $t \ge 1 > 0 = s$) and the second equals $\mathbf{y}_{ss}(j)^{\mathsf{T}}\,\mathbf{Q}_{t,0}(j)$ by the $s = 0$ branch of (A.3). In either case,

$$\mathcal{F}_{t,s}(j) = \mathbf{y}_{ss}(j)^{\mathsf{T}}\,\mathbf{Q}_{t,s}(j), \qquad t \ge 1,\; 0 \le j \le J-1. \tag{A.6}$$

Case 2.1 ($j \ge t$, $j-t \le J-1-s$). Lemma 8 gives

$$\mathbf{Q}_{t,s}(j) = \Big(\prod_{r=j-t+1}^{j-1} \mathcal{L}_{ss}(r)\Big)^{\mathsf{T}} \boldsymbol{\Xi}^s(j-t+1).$$

Substituting into (A.6) and using $(AB)^{\mathsf{T}} = B^{\mathsf{T}}A^{\mathsf{T}}$,

$$\mathcal{F}_{t,s}(j) = \Big(\prod_{r=j-t+1}^{j-1} \mathcal{L}_{ss}(r)\,\mathbf{y}_{ss}(j)\Big)^{\mathsf{T}} \boldsymbol{\Xi}^s(j-t+1).$$

Iterating Definition 2 from start age $j-t+1$ for $t-1$ further steps (the iteration is empty at $t = 1$, in which case $\mathcal{E}_0(j-t+1) = \mathcal{E}_0(j) = \mathbf{y}_{ss}(j)$),

$$\mathcal{E}_{t-1}(j-t+1) = \mathcal{L}_{ss}(j-t+1)\,\mathcal{L}_{ss}(j-t+2)\cdots\mathcal{L}_{ss}(j-1)\,\mathbf{y}_{ss}(j) = \prod_{r=j-t+1}^{j-1} \mathcal{L}_{ss}(r)\,\mathbf{y}_{ss}(j).$$

Therefore $\mathcal{F}_{t,s}(j) = \mathcal{E}_{t-1}(j-t+1)^{\mathsf{T}}\,\boldsymbol{\Xi}^{s}(j-t+1)$, which is case (ii) of Theorem 1.

Case 2.2 ($j < t$ or $j - t > J - 1 - s$). Both clauses of Lemma 8 give $\mathbf{Q}_{t,s}(j) = \mathbf{0}$ (the second branch when $j < t$, the truncation clause when $j - t > J - 1 - s$). Hence by (A.6), $\mathcal{F}_{t,s}(j) = 0$. □

A.3 Fake News Matrices for Growth Shocks in Example B

Throughout this subsection we work with the normalized block of (19): $\hat{\mathbf{D}}$ and $\hat{\mathbf{F}}$ denote the normalized distributions and flows (including their steady-state versions), while $\mathcal{L}$ denotes the non-normalized survival transition matrices delivered by the agent's dynamic problem.

For newborn-growth shocks the fixed initial object is the non-normalized incoming distribution $\mathbf{m}_0$; its normalized counterpart $\hat{\mathbf{m}}_0 = \mathbf{m}_0/n_0$ varies with the shocked cohort size $n_0 = n_{-1}\Upsilon_0$. Adding the stationary normalized flows yields the initial condition

$$\hat{\mathbf{D}}_0(j) = \begin{cases} \eta, & j = 0 \\ \frac{1}{\Upsilon_0}\,\mathcal{L}_{ss}(j-1)^{\mathsf{T}}\hat{\mathbf{D}}_{ss}(j-1) + \hat{\mathbf{F}}_{ss}(j), & 0 < j \le J-1, \end{cases} \tag{A.7}$$

where steady-state objects are still defined in the absence of shocks.

First, we prove an intermediate claim that will be useful in characterizing the fake news matrix.

Claim 3 (Distributional shift invariance for growth shocks)**.** *In the setting of Example B, changes in distributions induced by shocks to $1/\Upsilon$ satisfy, for all $0 \le j \le J-1$ and for all $t \ge 1$, $s \ge 1$,*

$$d\hat{\mathbf{D}}_t^s(j) = d\hat{\mathbf{D}}_{t-1}^{s-1}(j).$$

Proof of Claim 3. Start by differentiating (19) at an arbitrary $t \ge 1$, $s \ge 0$. Because this shock induces no behavioral response and no change in normalized flows, we have $d\mathcal{L}_{t-1}^{s}(j-1) = \mathbf{0}$ and $d\hat{\mathbf{F}}_t^s(j) = \mathbf{0}$. Therefore, we obtain

$$d\hat{\mathbf{D}}_t^s(j) = \begin{cases} \mathbf{0}, & j = 0 \\ \mathcal{L}_{ss}(j-1)^{\mathsf{T}}\left(\mathbf{1}_{t=s}\cdot d\left(\frac{1}{\Upsilon}\right)\,\hat{\mathbf{D}}_{ss}(j-1) + \frac{1}{\Upsilon_{ss}}\,d\hat{\mathbf{D}}_{t-1}^{s}(j-1)\right), & 0 < j \le J-1. \end{cases} \tag{A.8}$$

Now we prove the actual claim by induction over age $0 \le j \le J-1$.

Base case ($j = 0$). Differentiating (A.7), we get $d\hat{\mathbf{D}}_0^s(0) = \mathbf{0}$ for all $s \ge 0$. Together with (A.8) this implies that for any $s \ge 0$ and $t \ge 0$, $d\hat{\mathbf{D}}_t^s(0) = \mathbf{0}$ and, therefore, for any $s \ge 1$ and $t \ge 1$, $d\hat{\mathbf{D}}_t^s(0) = d\hat{\mathbf{D}}_{t-1}^{s-1}(0)$.

Inductive step ($j \ge 1$). Assume $d\hat{\mathbf{D}}_{\tilde{t}}^{\tilde{s}}(j-1) = d\hat{\mathbf{D}}_{\tilde{t}-1}^{\tilde{s}-1}(j-1)$ for any $\tilde{s} \ge 1$ and $\tilde{t} \ge 1$.

Consider an arbitrary $s \geq 1$. For $t \geq 2$, using (A.8) we have

$$\begin{aligned} d\hat{\mathbf{D}}_t^s(j) - d\hat{\mathbf{D}}_{t-1}^{s-1}(j) =& \mathcal{L}_{ss}(j-1)^\intercal d\left(\frac{1}{\Upsilon}\right) \hat{\mathbf{D}}_{ss}(j-1) \cdot (\mathbf{1}_{t=s} - \mathbf{1}_{t-1=s-1}) + \\ & \mathcal{L}_{ss}(j-1)^\intercal \frac{1}{\Upsilon_{ss}} \left(d\hat{\mathbf{D}}_{t-1}^s(j-1) - d\hat{\mathbf{D}}_{t-2}^{s-1}(j-1)\right) \\ =& \mathcal{L}_{ss}(j-1)^\intercal \frac{1}{\Upsilon_{ss}} \left(d\hat{\mathbf{D}}_{t-1}^s(j-1) - d\hat{\mathbf{D}}_{t-2}^{s-1}(j-1)\right) \end{aligned} \tag{A.9}$$

The first term on the right hand side vanishes because $t = s$ if and only if $t - 1 = s - 1$.

Now consider subcases over t.

Case 1 ($t = 1$). Differentiating (A.7) for $j \geq 1$ we have

$$d\hat{\mathbf{D}}_0^{s-1}(j) = \mathbf{1}_{s=1} \cdot d\left(\frac{1}{\Upsilon}\right) \mathcal{L}_{ss}(j-1)^\intercal \hat{\mathbf{D}}_{ss}(j-1).$$

Hence, subtracting from (A.8) we have

$$\begin{aligned} d\hat{\mathbf{D}}_1^s(j) - d\hat{\mathbf{D}}_0^{s-1}(j) =& \mathcal{L}_{ss}(j-1)^\intercal \left(\mathbf{1}_{s=1} \cdot d\left(\frac{1}{\Upsilon}\right) \hat{\mathbf{D}}_{ss}(j-1) + \frac{1}{\Upsilon_{ss}} d\hat{\mathbf{D}}_0^s(j-1)\right) - \\ & \mathcal{L}_{ss}(j-1)^\intercal \mathbf{1}_{s=1} \cdot d\left(\frac{1}{\Upsilon}\right) \hat{\mathbf{D}}_{ss}(j-1) \\ =& \mathcal{L}_{ss}(j-1)^\intercal \left(\frac{1}{\Upsilon_{ss}} d\hat{\mathbf{D}}_0^s(j-1)\right) = \mathbf{0}, \end{aligned}$$

where the last equality follows from differentiating (A.7) and noting that $d\hat{\mathbf{D}}_0^s(j-1) = \mathbf{0}$ for $s \geq 1$.

Case 2 ($t \geq 2$). The inductive hypothesis implies $d\hat{\mathbf{D}}_{t-1}^s(j-1) = d\hat{\mathbf{D}}_{t-2}^{s-1}(j-1)$ and hence (A.9) becomes $d\hat{\mathbf{D}}_t^s(j) - d\hat{\mathbf{D}}_{t-1}^{s-1}(j) = \mathbf{0}$. □

We now prove the main claim.

Claim 4 (Newborn growth fake news matrices)**.** *In the setting of Example B, the age-specific fake news matrices for shocks to $1/\Upsilon$ satisfy, for all $t, s \geq 0$ and $0 \leq j \leq J-1$,*

$$\mathcal{F}_{t,s}(j) = \mathbf{0} \quad \textit{for all } s \geq 1,$$

and

$$\mathcal{F}_{t,0}(j) = \begin{cases} \Upsilon_{ss}\, \mathcal{E}_t(j-t)^\intercal \big(\hat{\mathbf{D}}_{ss}(j-t) - \hat{\mathbf{F}}_{ss}(j-t)\big), & \textit{if } j \geq t+1, \\ \mathbf{0}, & \textit{otherwise,} \end{cases}$$

where $\mathcal{E}_t$ is constructed as in Definition 2 from the normalized survival transitions $(1/\Upsilon_{ss})\,\mathcal{L}_{ss}$ of (19).

Proof of Claim 4. The newborn growth factor Υ does not enter the dynamic optimization problem, hence, realized and anticipated shocks to it do not elicit a response in policy functions, non-normalized transition matrices, or normalized flows: $d\mathbf{y}_t^s(j) = \mathbf{0}$ and $d\mathcal{L}_t^s(j) = \mathbf{0}$ for all j, and $d\hat{\mathbf{F}}_t^s(j) = \mathbf{0}$ for $j \geq 1$.

Applying the definition of age-specific Jacobians and using the fact that $d\mathbf{y}_t^s(j) = \mathbf{0}$, we have

$$\mathcal{J}_{t,s}(j) \cdot d(1/\Upsilon) = d\mathbf{y}_t^s(j)^\mathsf{T} \hat{\mathbf{D}}_{ss}(j) + \mathbf{y}_{ss}(j)^\mathsf{T} d\hat{\mathbf{D}}_t^s(j) = \mathbf{y}_{ss}(j)^\mathsf{T} d\hat{\mathbf{D}}_t^s(j).$$

Hence, for $t, s \geq 1$ the fake news matrix entries satisfy

$$\mathcal{F}_{t,s}(j) = \mathcal{J}_{t,s}(j) - \mathcal{J}_{t-1,s-1}(j) = \frac{1}{d(1/\Upsilon)} \mathbf{y}_{ss}(j)^\mathsf{T} \left(d\hat{\mathbf{D}}_t^s(j) - d\hat{\mathbf{D}}_{t-1}^{s-1}(j) \right) = \mathbf{0},$$

with the last equality implied by Claim 3.

Elements in the first row of the fake news matrices are

$$\mathcal{F}_{0,s}(j) = \mathcal{J}_{0,s}(j) = \frac{1}{d(1/\Upsilon)} \mathbf{y}_{ss}(j)^\mathsf{T} d\hat{\mathbf{D}}_0^s(j).$$

Differentiating (A.7) we find $d\hat{\mathbf{D}}_0^s(j) = \mathbf{0}$ for $s \geq 1$ and, therefore, $\mathcal{F}_{0,s}(j) = \mathbf{0}$ for $s \geq 1$.

This establishes that all non-zero elements of age-specific fake news matrices for newborn growth shocks must be located in their first columns. To characterize these elements, iterate (A.8) at $s = 0$ for t steps: the indicator term vanishes at every step (the time index runs over $\{1, \ldots, t\}$ while $s = 0$), each step contributes a factor $\frac{1}{\Upsilon_{ss}} \mathcal{L}_{ss}(\cdot)^\mathsf{T}$, and the resulting product of normalized transitions $(1/\Upsilon_{ss}) \mathcal{L}_{ss}(\cdot)$ applied to $\mathbf{y}_{ss}(j)$ equals $\mathcal{E}_t(j-t)$: the expectation vectors of Definition 2 built from these normalized transitions. Hence

$$\mathcal{F}_{t,0}(j) \cdot d(1/\Upsilon) = \mathbf{y}_{ss}(j)^\mathsf{T} d\hat{\mathbf{D}}_t^0(j) = \begin{cases} \mathcal{E}_t(j-t)^\mathsf{T} \, d\hat{\mathbf{D}}_0^0(j-t), & \text{if } j \geq t, \\ \mathbf{0}, & \text{otherwise.} \end{cases} \tag{A.10}$$

Finally, differentiating (A.7) we get

$$d\hat{\mathbf{D}}_0^0(j_0) = \begin{cases} \mathbf{0}, & j_0 = 0, \\ \mathcal{L}_{ss}(j_0 - 1)^\mathsf{T} \hat{\mathbf{D}}_{ss}(j_0 - 1) \, d(1/\Upsilon), & 1 \leq j_0 \leq J - 1. \end{cases}$$

which, by the steady-state version of (19), is

$$d\hat{\mathbf{D}}_0^0(j_0) = \begin{cases} \mathbf{0}, & j_0 = 0, \\ \Upsilon_{ss} (\hat{\mathbf{D}}_{ss}(j_0) - \hat{\mathbf{F}}_{ss}(j_0)) \, d(1/\Upsilon), & 1 \leq j_0 \leq J - 1. \end{cases}$$

Substituting this expression into (A.10), we obtain

$$\mathcal{F}_{t,0}(j) = \begin{cases} \Upsilon_{ss} \cdot \mathcal{E}_t(j-t)^\mathsf{T} \left(\hat{\mathbf{D}}_{ss}(j-t) - \hat{\mathbf{F}}_{ss}(j-t) \right), & \text{if } j - t \geq 1, \\ \mathbf{0}, & \text{otherwise.} \end{cases}$$

□

A.4 Section 5 Proofs

We continue to work under the absence-of-dynastic-links assumption, so the non-dynastic Theorem 1 applies and the auxiliary results of Appendix A.2 are available.

Proof of Lemma 5. Theorem 1 restricts the non-zero entries of $\{\mathcal{F}(j)\}_{j=0}^{J-1}$ to the triples (t, s, j) with $0 \le j - t \le J - 1 - s$. Algorithm 1 initializes these matrices to $\mathbf{0}$. Then, it iterates over the shock horizon s, the age-at-shock l, and time t to fill these non-zero entries. We verify that the algorithm assigns the correct value at every non-zero triplet identified by Theorem 1 and that the remaining entries are left at their initialized value 0.

Initialization, $t = 0$. For each shock horizon $s \in \{0, \dots, J-1\}$ and each $l \in \{0, \dots, s\}$, line 6 of the algorithm sets

$$\mathcal{F}_{0,s-l}(l) \;\leftarrow\; d\mathbf{y}_0^{s-l}(l)^{\mathsf{T}}\, \mathbf{D}_{ss}(l) \;+\; \mathbf{y}_{ss}(l)^{\mathsf{T}}\, d\mathbf{F}_0^{s-l}(l).$$

Reindex $s' := s - l$ and $j := l$. The loop bounds $0 \le l \le s \le J - 1$ cover precisely the pairs (s', j) with $s' \le J - 1 - j$, and the right-hand side equals the non-vanishing branch of Lemma 6. For (s', j) with $s' > J - 1 - j$ no admissible (s, l) exists, so $\mathcal{F}_{0,s'}(j)$ remains at 0, matching the vanishing branch.

Survivor case, $t \ge 1$ *and* $j \ge t$. Inside the outer-s loop, for each $l \in \{0, \dots, \min\{s, J-2\}\}$ (the bound $l \le J-2$, which is enforced by line 7, ensures the next age $l+1$ lies in $\{1, \dots, J-1\}$, the range of Lemma 4) the algorithm sets

$$\mathbf{\Xi}^{s-l}(l+1) \;\leftarrow\; d\mathcal{L}_0^{s-l}(l)^{\mathsf{T}}\, \mathbf{D}_{ss}(l) \;+\; \mathcal{L}_{ss}(l)^{\mathsf{T}}\, d\mathbf{F}_0^{s-l}(l),$$

matching case (i) of Lemma 4 at age $l+1 \ge 1$, so the assigned value equals $\mathbf{\Xi}^{s-l}(l+1)$. The inner t-loop on $\{1, \dots, (J-1) - l\}$ then sets

$$\mathcal{F}_{t,s-l}(l+t) \;\leftarrow\; \mathcal{E}_{t-1}(l+1)^{\mathsf{T}}\, \mathbf{\Xi}^{s-l}(l+1).$$

Reindex $s' := s - l$ and $j := l + t$, equivalently $l = j - t$ and $s = s' + j - t$. The update becomes

$$\mathcal{F}_{t,s'}(j) \;\leftarrow\; \mathcal{E}_{t-1}(j-t+1)^{\mathsf{T}}\, \mathbf{\Xi}^{s'}(j-t+1),$$

which is the $t \ge 1$ case of Theorem 1. The loop bounds cover precisely the triples (t, s', j) with $t \ge 1$, $j \ge t$, and $j - t \le J - 1 - s'$: given such a triple, the choice $l := j - t$, $s := s' + l$ satisfies $0 \le l \le J - 2$, $l \le s \le J - 1$, and $1 \le t \le (J-1) - l$, so the update is performed once.

Remaining entries. An entry $\mathcal{F}_{t,s'}(j)$ with $t \ge 1$ is reached by the inner loop only if $l := j - t \ge 0$ and $s := s' + l \le J - 1$. The two complementary cases are:

- $j < t$ (equivalently $l < 0$): no admissible l exists, so $\mathcal{F}_{t,s'}(j)$ remains at 0, matching the "otherwise" branch of Theorem 1 (the condition $0 \le j - t$ fails).
- $j \ge t$ but $j - t > J - 1 - s'$ (equivalently $s = s' + l > J - 1$): no admissible outer-loop s exists, so $\mathcal{F}_{t,s'}(j)$ remains at 0, again matching the "otherwise" branch (the condition $j - t \le J - 1 - s'$ fails).

The algorithm therefore produces the value of $\mathcal{F}_{t,s'}(j)$ prescribed by Theorem 1 on every triple $(t, s', j) \in \{0, \ldots, J-1\}^3$. $\square$

B Dynastic Links

This appendix relaxes Assumption 3 (absence of dynastic links, $\Omega_t^s(j) = \Omega_{ss}(j) = \mathbf{0}$) used throughout Sections 4 and 5 of the main text. We characterize age-specific fake news matrices, present an algorithm to compute them, and provide proofs of our results without this assumption.

With dynastic links, dying agents' idiosyncratic states pass to entering newborns through the steady-state death-to-birth matrix $\Omega_{ss}(j)$, and shocks to inputs propagate through $d\Omega_0^s(j)$. Two results from Section 4 require generalization. First, Lemma 4, which characterizes shifts in distributions right after a shock, gains a non-trivial $j = 0$ case. Second, our characterization of fake news matrices in Theorem 1 acquires a third case covering cohorts born after the announcement date 0. Both changes come from the possibility that, even if newborns do not react to past shocks, their distribution over states may be shifted as a result of their parents' behavior. To express the third case of our fake news matrices we also need a new object, the *distributional shift propagator* $\mathbf{\Phi}_{t,s}(j)$, which carries the time-1 shift forward through both survival and death-rebirth.

Subsection B.1 introduces these objects and states the main result in the case with dynastic links; Subsection B.2 gives their proofs. Algorithm 1 is generalized in Subsection B.3.

B.1 Fake News Matrices with Dynastic Links

The definition of the endogenous distributional shift carries over verbatim from the main text; we restate it for convenience.

Definition 5 (Endogenous Distributional Shifts)**.** *For shock date $s \geq 0$ and $l \in \{0, \ldots, J-1\}$, the endogenous distributional shift is*

$$\mathbf{\Xi}^s(l) \;:=\; d\mathbf{D}_1^s(l) - d\mathbf{F}_1^s(l).$$

The next lemma generalizes Lemma 4: case (i), which involves only the survivor branch, is unchanged; case (ii), which involves newborns, becomes a sum over shifts in inflows from all possible parent ages that react to the shock.

Lemma 9 (Distributional Shifts With Dynastic Links)**.** *Let $s \geq 0$. Then:*

(i) If $1 \leq j \leq J-1$, then

$$\mathbf{\Xi}^s(j) \;=\; d\mathcal{L}_0^s(j-1)^\mathsf{T}\mathbf{D}_{ss}(j-1) \;+\; \mathcal{L}_{ss}(j-1)^\mathsf{T} d\mathbf{F}_0^s(j-1). \tag{B.1}$$

(ii) If $j = 0$, then

$$\mathbf{\Xi}^s(0) \;=\; \sum_{j_0=0}^{J-1-s} \Big(d\Omega_0^s(j_0)^\mathsf{T}\mathbf{D}_{ss}(j_0) \;+\; \Omega_{ss}(j_0)^\mathsf{T} d\mathbf{F}_0^s(j_0) \Big). \tag{B.2}$$

Moreover, $\mathbf{\Xi}^s(j) = \mathbf{0}$ whenever $j > J - s$ (with $1 \leq j \leq J-1$).

$\boldsymbol{\Xi}$ gives the time-1 change in the age-j distribution net of the direct response of the exogenous age-j inflow. As in the case without dynastic links, and in Auclert et al. (2021a), entries of fake news matrices propagate these time-1 shifts forward in time. The difference with respect to our baseline algorithm is that now the time-1 shift $\boldsymbol{\Xi}^s(\cdot)$ must be propagated forward through **both** survival and death-rebirth. The next definition does this recursively.

Definition 6 (Distributional Shift Propagator)**.** *For shock date $s \geq 0$ and $j \in \{0, \ldots, J-1\}$, set*

$$\boldsymbol{\Phi}_{0,s}(j) \;:=\; \boldsymbol{\Xi}^s(j),$$

and for $t \geq 1$,

$$\boldsymbol{\Phi}_{t,s}(j) \;:=\; \begin{cases} \mathcal{L}_{ss}(j-1)^{\mathsf{T}}\, \boldsymbol{\Phi}_{t-1,s}(j-1), & 1 \leq j \leq J-1, \\ \displaystyle\sum_{r=0}^{J-1} \Omega_{ss}(r)^{\mathsf{T}}\, \boldsymbol{\Phi}_{t-1,s}(r), & j = 0. \end{cases}$$

The m-th entry of $\boldsymbol{\Phi}_{t,s}(j)$ is the time-$(t+1)$ distributional shift at age j and grid point m, propagated t periods forward from the time-1 shift $\boldsymbol{\Xi}^s(\cdot)$ through the steady-state transition matrices. Under the absence-of-dynastic-links assumption the second branch collapses to $\mathbf{0}$ and only survivor paths matter, which is why Definition 6 is not needed for the main-text statement of Theorem 1.

We can now state the full version of Theorem 1, in which case (iii) covers cohorts born after date 0 via the propagator. Unlike the case without dynastic links, the non-zero elements of fake news matrices are not confined to their upper $0 \leq t \leq J-1$ region. Hence, as is the case in the infinite-horizon fake news algorithm, we must define a truncation horizon N.

Theorem 2 (Structure of Age-Specific Fake News Matrices with Dynastic Links)**.** *Let $t \in \{0, \ldots, N-1\}$ and $s, j \in \{0, \ldots, J-1\}$. If $j - t \leq J - 1 - s$, then*

$$\mathcal{F}_{t,s}(j) = \begin{cases} d\mathbf{y}_0^s(j)^{\mathsf{T}}\mathbf{D}_{ss}(j) \;+\; \mathbf{y}_{ss}(j)^{\mathsf{T}} d\mathbf{F}_0^s(j), & \text{if } t = 0, \\ \mathcal{E}_{t-1}(j-t+1)^{\mathsf{T}}\boldsymbol{\Xi}^s(j-t+1), & \text{if } t \geq 1 \text{ and } j \geq t, \\ \mathbf{y}_{ss}(j)^{\mathsf{T}}\boldsymbol{\Phi}_{t-1,s}(j), & \text{if } t \geq 1 \text{ and } j < t, \end{cases} \tag{B.3}$$

and $\mathcal{F}_{t,s}(j) = 0$ otherwise.

Cases (i) and (ii) reduce to Theorem 1 of the main text under $\Omega_{ss}(\cdot) \equiv \mathbf{0}$ (since then $\boldsymbol{\Xi}^s(0) = \mathbf{0}$ by Lemma 9). Case (iii) is genuinely new: it concerns agents who are born after date 0, whose age-j distribution at time $t+1$ inherits perturbations from their ancestors, encoded in $\boldsymbol{\Phi}_{t-1,s}(j)$.

Unlike the non-dynastic Theorem 1, the row index t here runs up to the truncation horizon $N-1$, not just to $J-1$. To see why, recall that the theorem sets an entry to zero only when the clause $j - t \leq J - 1 - s$ fails. In case (iii) we have $j < t$, hence $j - t < 0 \leq J - 1 - s$, so the clause holds for every such entry; these case (iii) entries are therefore never truncated

and need not vanish at any t. Only the survivor entries of case (ii), which require $j \geq t$ and hence $t \leq J-1$, can be zeroed by the clause. The truncation horizon N is therefore the only bound on t; the shock date s and the age j stay in $\{0, \ldots, J-1\}$ because the household's planning horizon is only J periods.

Remark 2 (The shock date stops at $J-1$). Extending the shock date to $s \geq J$ would only append zero columns, which is why we index s in $\{0, \ldots, J-1\}$. To see why, fix $s \geq J$. The newborn shift then vanishes, because the sum in case (ii) of Lemma 9 runs up to $J-1-s < 0$ and is empty, and the survivor shifts vanish by the same lemma since $j > J-s$ for every $j \geq 1$. With $\boldsymbol{\Xi}^s(\cdot) \equiv \mathbf{0}$ the propagator of Definition 6 stays at zero, as it is seeded at $\boldsymbol{\Phi}_{0,s} = \boldsymbol{\Xi}^s$ and advanced by a homogeneous recursion. Cases (ii) and (iii) of Theorem 2 therefore vanish, and case (i) vanishes by Lemma 3, which forces $d\mathbf{y}_0^s(j) = d\mathbf{F}_0^s(j) = \mathbf{0}$ once $j > J-1-s$. Hence $\mathcal{F}_{t,s}(j) = \mathbf{0}$ for all t and j whenever $s \geq J$. The last column carrying non-zero mass is $s = J-1$, where the newborn sum keeps its $j_0 = 0$ term.

B.2 Proofs

Proof of Lemma 9. The proof of (B.1) (case (i)) is identical to that in Appendix A.2 and does not use the absence-of-dynastic-links assumption.

Case $j = 0$. Applying (16) at $t = 1$ and $j = 0$,

$$\mathbf{D}_1^s(0) = \sum_{j_0=0}^{J-1} \Omega_0^s(j_0)^\mathsf{T} \, \mathbf{D}_0^s(j_0) + \mathbf{F}_1^s(0).$$

Taking the difference around steady state, substituting (A.2), and dropping $O(dx^2)$ terms,

$$d\mathbf{D}_1^s(0) = \sum_{j_0=0}^{J-1} \Big[d\Omega_0^s(j_0)^\mathsf{T} \, \mathbf{D}_{ss}(j_0) \; + \; \Omega_{ss}(j_0)^\mathsf{T} \, d\mathbf{F}_0^s(j_0) \Big] \; + \; d\mathbf{F}_1^s(0).$$

By Lemma 3 at $t = 0$ and age j_0, $d\Omega_0^s(j_0) = \mathbf{0}$ and $d\mathbf{F}_0^s(j_0) = \mathbf{0}$ for $j_0 > J-1-s$, so the bracketed terms vanish in that range and the j_0-sum truncates to $\{0, \ldots, J-1-s\}$. Subtracting $d\mathbf{F}_1^s(0)$ yields (B.2). □

The remaining proofs below use an auxiliary object, the path transition matrix $\bar{\Lambda}_{t,l}(j)$: the t-step steady-state transition matrix from age l to age j, i.e. the sum, over every path of length t that starts at age l and ends at age j, of the products of the one-step survival and death-rebirth transitions along the path.

Definition 7 (Path Transition Matrix)**.** *For $l, j \in \{0, \ldots, J-1\}$, set $\bar{\Lambda}_{0,l}(j) := I$ if $j = l$ and $\bar{\Lambda}_{0,l}(j) := \mathbf{0}$ otherwise, where I is the identity matrix on the age-l idiosyncratic grid. For $t \geq 1$,*

$$\bar{\Lambda}_{t,l}(j) := \begin{cases} \mathcal{L}_{ss}(j-1)^\mathsf{T} \bar{\Lambda}_{t-1,l}(j-1), & 1 \leq j \leq J-1, \\ \displaystyle\sum_{r=0}^{J-1} \Omega_{ss}(r)^\mathsf{T} \bar{\Lambda}_{t-1,l}(r), & j = 0. \end{cases}$$

We use two pieces of additional local notation within this subsection. First, we define

$$\bar{\mathcal{E}}_{t,l}(j) \;:=\; \bar{\Lambda}_{t,l}(j)^{\mathsf{T}}\,\mathbf{y}_{ss}(j).$$

Remark 3. Note that $\mathcal{E}_t(j) = \bar{\mathcal{E}}_{t,j}(j+t)$ for $j+t \le J-1$, recovering the main-text $\mathcal{E}$ of Definition 2.

Second, to lighten notation, we also define

$$\bar{\boldsymbol{\Xi}}^s(j_0) \;:=\; d\Omega_0^s(j_0)^{\mathsf{T}}\mathbf{D}_{ss}(j_0) \;+\; \Omega_{ss}(j_0)^{\mathsf{T}}d\mathbf{F}_0^s(j_0).$$

With this shorthand the dynastic birth shift (B.2) reads $\boldsymbol{\Xi}^s(0) = \sum_{j_0=0}^{J-1-s}\bar{\boldsymbol{\Xi}}^s(j_0)$. The proofs also use the fake-news residual $\mathbf{Q}_{t,s}(j)$ of (A.3). Because its definition does not involve the death-to-birth map, it carries over unchanged to the dynastic setting.

The following lemma records the relationship between the propagator $\boldsymbol{\Phi}_{t,s}(j)$ and the path matrix, expressing the propagator as a sum of path-transition-weighted time-1 shifts.

Lemma 10 (Propagator via path matrices)**.** *For $t \ge 0$, $s \in \{0,\dots,J-1\}$, and $0 \le j \le J-1$,*

$$\boldsymbol{\Phi}_{t,s}(j) \;=\; \sum_{l=0}^{J-s}\bar{\Lambda}_{t,l}(j)\,\boldsymbol{\Xi}^s(l). \tag{B.4}$$

Proof. We proceed by induction on t.

Base case $t=0$. Definition 6 gives $\boldsymbol{\Phi}_{0,s}(j) = \boldsymbol{\Xi}^s(j)$, while Definition 7 gives $\bar{\Lambda}_{0,l}(j) = I$ when $l=j$ and $\mathbf{0}$ otherwise. Hence the right-hand side of (B.4) reduces to $\boldsymbol{\Xi}^s(j)$ when $j \le J-s$, and to $\mathbf{0}$ when $j > J-s$. In the latter range Lemma 4 also gives $\boldsymbol{\Xi}^s(j) = \mathbf{0}$: the constraint $j > J-s$ together with $s \le J-1$ forces $j \ge 2$, so in particular $j \ne 0$, and clause (i) of the lemma applies.

Inductive step. Suppose (B.4) holds at $t-1$. For $1 \le j \le J-1$, Definition 6 and the inductive hypothesis give

$$\boldsymbol{\Phi}_{t,s}(j) = \mathcal{L}_{ss}(j-1)^{\mathsf{T}}\boldsymbol{\Phi}_{t-1,s}(j-1) = \sum_{l=0}^{J-s}\mathcal{L}_{ss}(j-1)^{\mathsf{T}}\,\bar{\Lambda}_{t-1,l}(j-1)\,\boldsymbol{\Xi}^s(l).$$

The summand equals $\bar{\Lambda}_{t,l}(j)\,\boldsymbol{\Xi}^s(l)$ by the survival branch of Definition 7.

For $j=0$, Definition 6 and the inductive hypothesis give

$$\boldsymbol{\Phi}_{t,s}(0) = \sum_{r=0}^{J-1}\Omega_{ss}(r)^{\mathsf{T}}\boldsymbol{\Phi}_{t-1,s}(r) = \sum_{r=0}^{J-1}\sum_{l=0}^{J-s}\Omega_{ss}(r)^{\mathsf{T}}\,\bar{\Lambda}_{t-1,l}(r)\,\boldsymbol{\Xi}^s(l).$$

Swapping the finite r- and l-sums and applying the rebirth branch of Definition 7 at $j=0$,

$$\boldsymbol{\Phi}_{t,s}(0) = \sum_{l=0}^{J-s}\Big(\sum_{r=0}^{J-1}\Omega_{ss}(r)^{\mathsf{T}}\,\bar{\Lambda}_{t-1,l}(r)\Big)\,\boldsymbol{\Xi}^s(l) = \sum_{l=0}^{J-s}\bar{\Lambda}_{t,l}(0)\,\boldsymbol{\Xi}^s(l).$$

□

The next claim establishes the $t = 0$ case of Theorem 2.

Claim 5 (Initial period, $t = 0$)**.** *For $s \geq 0$ and $0 \leq j \leq J-1$,*

$$\mathcal{F}_{0,s}(j) = \begin{cases} d\mathbf{y}_0^s(j)^\mathsf{T}\mathbf{D}_{ss}(j) \;+\; \mathbf{y}_{ss}(j)^\mathsf{T} d\mathbf{F}_0^s(j), & s \leq J-1-j, \\ 0, & s > J-1-j. \end{cases}$$

Proof. At $t = 0$ the distribution $\mathbf{D}_0$ is the fixed initial condition, so $d\mathbf{D}_0^s(j) = d\mathbf{F}_0^s(j)$ for all j by (A.2), independently of Ω_{ss}. The proof of Lemma 6 then applies verbatim: Definition 1 and (22) give the first case, and Lemma 3 at $t = 0$ the second. □

The $t \geq 1$ entries of Theorem 2 follow from a closed form for the residual $\mathbf{Q}_{t,s}$ (Lemma 12), which we establish by induction on t; the next claim supplies the base case at $t = 1$.

Claim 6 (Base case, $t = 1$)**.** *For $s \geq 0$ and $0 \leq j \leq J-1$,*

$$\mathbf{Q}_{1,s}(j) = \begin{cases} \boldsymbol{\Xi}^s(j), & 1 \leq j \leq J-1, \\ \displaystyle\sum_{j_0=0}^{J-1-s} \bar{\boldsymbol{\Xi}}^s(j_0), & j = 0. \end{cases}$$

Proof. For $s \geq 1$, (A.3) gives $\mathbf{Q}_{1,s}(j) = d\mathbf{D}_1^s(j) - d\mathbf{D}_0^{s-1}(j)$. The fixed initial condition $\mathbf{D}_0 - \mathbf{F}_0 = \mathbf{D}_{ss} - \mathbf{F}_{ss}$ gives $d\mathbf{D}_0^{s-1}(j) = d\mathbf{F}_0^{s-1}(j)$, and Lemma 2 (at $k = 1$) gives $d\mathbf{F}_0^{s-1}(j) = d\mathbf{F}_1^s(j)$, so $\mathbf{Q}_{1,s}(j) = d\mathbf{D}_1^s(j) - d\mathbf{F}_1^s(j) = \boldsymbol{\Xi}^s(j)$ by Definition 5. For $s = 0$, the $s = 0$ branch of (A.3) gives $\mathbf{Q}_{1,0}(j) = d\mathbf{D}_1^0(j)$, and Lemma 1 at $t = 1 > 0 = s$ gives $d\mathbf{F}_1^0(j) = \mathbf{0}$, so $\mathbf{Q}_{1,0}(j) = d\mathbf{D}_1^0(j) - d\mathbf{F}_1^0(j) = \boldsymbol{\Xi}^0(j)$ by Definition 5. This gives $\mathbf{Q}_{1,s}(j) = \boldsymbol{\Xi}^s(j)$ for all j; for $j = 0$, (B.2) of Lemma 9 re-expresses $\boldsymbol{\Xi}^s(0)$ as $\sum_{j_0=0}^{J-1-s} \bar{\boldsymbol{\Xi}}^s(j_0)$. □

The next lemma is the dynastic-links version of Lemma 7: the survivor branch ($1 \leq j \leq J-1$) is unchanged, but the age-0 residual is no longer zero and instead aggregates the residuals of all dying cohorts through the steady-state death-to-birth map Ω_{ss}.

Lemma 11 (Fake-news residual: recursion)**.** *For $t \geq 2$ and $0 \leq j \leq J-1$,*

$$\mathbf{Q}_{t,s}(j) = \begin{cases} \mathcal{L}_{ss}(j-1)^\mathsf{T}\, \mathbf{Q}_{t-1,s}(j-1), & 1 \leq j \leq J-1, \\ \displaystyle\sum_{r=0}^{J-1} \Omega_{ss}(r)^\mathsf{T}\, \mathbf{Q}_{t-1,s}(r), & j = 0. \end{cases} \tag{B.5}$$

Proof. We take $s \geq 1$ in the two cases below; the case $s = 0$ is treated at the end.

Case $1 \leq j \leq J-1$. Applying (16) at (t, s) and $(t-1, s-1)$,

$$\begin{aligned} \mathbf{D}_t^s(j) &= \mathcal{L}_{t-1}^s(j-1)^\mathsf{T}\, \mathbf{D}_{t-1}^s(j-1) + \mathbf{F}_t^s(j), \\ \mathbf{D}_{t-1}^{s-1}(j) &= \mathcal{L}_{t-2}^{s-1}(j-1)^\mathsf{T}\, \mathbf{D}_{t-2}^{s-1}(j-1) + \mathbf{F}_{t-1}^{s-1}(j). \end{aligned}$$

Linearizing around steady state,

$$d\mathbf{D}_t^s(j) = d\mathcal{L}_{t-1}^s(j-1)^\mathsf{T}\,\mathbf{D}_{ss}(j-1) \;+\; \mathcal{L}_{ss}(j-1)^\mathsf{T}\,d\mathbf{D}_{t-1}^s(j-1) \;+\; d\mathbf{F}_t^s(j),$$
$$d\mathbf{D}_{t-1}^{s-1}(j) = d\mathcal{L}_{t-2}^{s-1}(j-1)^\mathsf{T}\,\mathbf{D}_{ss}(j-1) \;+\; \mathcal{L}_{ss}(j-1)^\mathsf{T}\,d\mathbf{D}_{t-2}^{s-1}(j-1) \;+\; d\mathbf{F}_{t-1}^{s-1}(j).$$

By Lemma 2, $d\mathcal{L}_{t-1}^s(j-1) = d\mathcal{L}_{t-2}^{s-1}(j-1)$ and $d\mathbf{F}_t^s(j) = d\mathbf{F}_{t-1}^{s-1}(j)$, so subtracting the two displays gives

$$\mathbf{Q}_{t,s}(j) = \mathcal{L}_{ss}(j-1)^\mathsf{T}\big[d\mathbf{D}_{t-1}^s(j-1) - d\mathbf{D}_{t-2}^{s-1}(j-1)\big] = \mathcal{L}_{ss}(j-1)^\mathsf{T}\,\mathbf{Q}_{t-1,s}(j-1).$$

Case $j = 0$. Applying (16) at (t,s) and $(t-1,s-1)$,

$$\mathbf{D}_t^s(0) = \sum_{r=0}^{J-1} \Omega_{t-1}^s(r)^\mathsf{T}\,\mathbf{D}_{t-1}^s(r) + \mathbf{F}_t^s(0),$$
$$\mathbf{D}_{t-1}^{s-1}(0) = \sum_{r=0}^{J-1} \Omega_{t-2}^{s-1}(r)^\mathsf{T}\,\mathbf{D}_{t-2}^{s-1}(r) + \mathbf{F}_{t-1}^{s-1}(0).$$

Linearizing around steady state and subtracting yields

$$\begin{aligned}\mathbf{Q}_{t,s}(0) = \sum_{r=0}^{J-1} \Big[&\big(d\Omega_{t-1}^s(r) - d\Omega_{t-2}^{s-1}(r)\big)^\mathsf{T}\mathbf{D}_{ss}(r) \\ &+\; \Omega_{ss}(r)^\mathsf{T}\big(d\mathbf{D}_{t-1}^s(r) - d\mathbf{D}_{t-2}^{s-1}(r)\big)\Big] \\ &+\; d\mathbf{F}_t^s(0) - d\mathbf{F}_{t-1}^{s-1}(0).\end{aligned}$$

By Lemma 2, $d\Omega_{t-1}^s(r) = d\Omega_{t-2}^{s-1}(r)$ and $d\mathbf{F}_t^s(0) = d\mathbf{F}_{t-1}^{s-1}(0)$, so the $d\Omega$ and $d\mathbf{F}$ terms vanish, leaving $\mathbf{Q}_{t,s}(0) = \sum_{r=0}^{J-1} \Omega_{ss}(r)^\mathsf{T}\mathbf{Q}_{t-1,s}(r)$.

Case $s = 0$. Here (A.3) gives $\mathbf{Q}_{t,0}(j) = d\mathbf{D}_t^0(j)$. Linearizing (16) at $(t,0)$ and applying Lemma 1 (at $t \geq 2 > 0$) to drop $d\mathcal{L}_{t-1}^0$, $d\Omega_{t-1}^0$, and $d\mathbf{F}_t^0$ leaves $\mathbf{Q}_{t,0}(j) = \mathcal{L}_{ss}(j-1)^\mathsf{T}\,\mathbf{Q}_{t-1,0}(j-1)$ for $1 \leq j \leq J-1$ and $\mathbf{Q}_{t,0}(0) = \sum_{r=0}^{J-1} \Omega_{ss}(r)^\mathsf{T}\,\mathbf{Q}_{t-1,0}(r)$. □

Remark 4 (Path matrix support). For $k \geq 0$ and $0 \leq l, j \leq J-1$, $\bar{\Lambda}_{k,l}(j) = \mathbf{0}$ unless $j = l+k$ or $0 \leq j \leq k-1$.

Proof. Induction on k. For $k = 0$, $\bar{\Lambda}_{0,l}(j) = I$ if $j = l$ and $\mathbf{0}$ otherwise; the allowed support $\{l\}$ matches (the second branch $[0,-1]$ is empty).

For the inductive step, assume the claim at $k-1 \geq 0$. For $1 \leq j \leq J-1$, Definition 7 gives $\bar{\Lambda}_{k,l}(j) = \mathcal{L}_{ss}(j-1)^\mathsf{T}\bar{\Lambda}_{k-1,l}(j-1)$, and by the inductive hypothesis $\bar{\Lambda}_{k-1,l}(j-1)$ is non-zero only if $j-1 = l+(k-1)$ (i.e., $j = l+k$) or $0 \leq j-1 \leq k-2$ (i.e., $1 \leq j \leq k-1$); in either case $j \in \{l+k\} \cup [0, k-1]$. For $j = 0$ and $k \geq 1$, $0 \in [0, k-1]$, so the claim imposes no restriction. □

The next lemma is the dynastic-links version of Lemma 8: the survivor entries ($j \geq t$) are unchanged, but the entries with $j < t$ are no longer zero and instead collect the death-rebirth contributions of all dying cohorts, propagated through the path transition matrix $\bar{\Lambda}$.

Lemma 12 (Fake-news residual: closed form)**.** *For $t \geq 1$, $s \geq 0$, and $0 \leq j \leq J-1$,*

$$\mathbf{Q}_{t,s}(j) = \begin{cases} \bar{\Lambda}_{t-1,j-t+1}(j)\, \boldsymbol{\Xi}^s(j-t+1), & j \geq t, \\ \displaystyle\sum_{j_0=0}^{J-1-s} \left[\bar{\Lambda}_{t-1,j_0+1}(j)\, \boldsymbol{\Xi}^s(j_0+1) + \bar{\Lambda}_{t-1,0}(j)\, \bar{\boldsymbol{\Xi}}^s(j_0)\right], & j < t, \end{cases} \tag{B.6}$$

where $\bar{\Lambda}$ is from Definition 7. Moreover, $\mathbf{Q}_{t,s}(j) = \mathbf{0}$ whenever $j - t > J - 1 - s$.

Proof. We proceed by induction on t.

Base case ($t = 1$). For $j \geq 1 = t$, Claim 6 gives $\mathbf{Q}_{1,s}(j) = \boldsymbol{\Xi}^s(j)$, which matches (B.6) since $\bar{\Lambda}_{0,j}(j) = I$ by Definition 7. For $j = 0 < t = 1$, Claim 6 gives $\sum_{j_0=0}^{J-1-s} \bar{\boldsymbol{\Xi}}^s(j_0)$, matching (B.6) since $\bar{\Lambda}_{0,j_0+1}(0) = \mathbf{0}$ (as $j_0 + 1 \neq 0$) and $\bar{\Lambda}_{0,0}(0) = I$.

Inductive step ($t \geq 2$). Assume (B.6) holds at $t-1$. We verify it at t by expanding $\mathbf{Q}_{t,s}(j)$ through Lemma 11 in three subcases.

Case 1 ($j \geq t$). Here $j-1 \geq t-1$, so by the inductive hypothesis $\mathbf{Q}_{t-1,s}(j-1) = \bar{\Lambda}_{t-2,j-t+1}(j-1)\, \boldsymbol{\Xi}^s(j-t+1)$. Definition 7 at $j \geq 1$ gives $\bar{\Lambda}_{t-1,j-t+1}(j) = \mathcal{L}_{ss}(j-1)^{\mathsf{T}} \bar{\Lambda}_{t-2,j-t+1}(j-1)$, so

$$\mathbf{Q}_{t,s}(j) = \mathcal{L}_{ss}(j-1)^{\mathsf{T}}\, \bar{\Lambda}_{t-2,j-t+1}(j-1)\, \boldsymbol{\Xi}^s(j-t+1) = \bar{\Lambda}_{t-1,j-t+1}(j)\, \boldsymbol{\Xi}^s(j-t+1).$$

Case 2 ($1 \leq j < t$). Here $j - 1 < t - 1$, so by the inductive hypothesis $\mathbf{Q}_{t-1,s}(j-1) = \sum_{j_0=0}^{J-1-s} [\bar{\Lambda}_{t-2,j_0+1}(j-1)\, \boldsymbol{\Xi}^s(j_0+1) + \bar{\Lambda}_{t-2,0}(j-1)\, \bar{\boldsymbol{\Xi}}^s(j_0)]$. The same recursion gives $\bar{\Lambda}_{t-1,l}(j) = \mathcal{L}_{ss}(j-1)^{\mathsf{T}} \bar{\Lambda}_{t-2,l}(j-1)$ for $l \in \{j_0+1, 0\}$, so

$$\mathbf{Q}_{t,s}(j) = \sum_{j_0=0}^{J-1-s} \left[\bar{\Lambda}_{t-1,j_0+1}(j)\, \boldsymbol{\Xi}^s(j_0+1) + \bar{\Lambda}_{t-1,0}(j)\, \bar{\boldsymbol{\Xi}}^s(j_0)\right].$$

Case 3 ($j = 0$). By Lemma 11, $\mathbf{Q}_{t,s}(0) = \sum_{r=0}^{J-1} \Omega_{ss}(r)^{\mathsf{T}} \mathbf{Q}_{t-1,s}(r)$. Split the sum on r at $r = t-1$ and apply the inductive hypothesis at $t-1$:

- For $r \geq t-1$, $\mathbf{Q}_{t-1,s}(r) = \bar{\Lambda}_{t-2,r-t+2}(r)\, \boldsymbol{\Xi}^s(r-t+2)$. Reindexing $j_0 := r-t+1 \in [0, J-t]$ gives the contribution $\Omega_{ss}(j_0+t-1)^{\mathsf{T}} \bar{\Lambda}_{t-2,j_0+1}(j_0+t-1)\, \boldsymbol{\Xi}^s(j_0+1)$.
- For $r \leq t-2$, $\mathbf{Q}_{t-1,s}(r) = \sum_{j_0=0}^{J-1-s} [\bar{\Lambda}_{t-2,j_0+1}(r)\, \boldsymbol{\Xi}^s(j_0+1) + \bar{\Lambda}_{t-2,0}(r)\, \bar{\boldsymbol{\Xi}}^s(j_0)]$.

We show that, for each $j_0 \in [0, J-1-s]$, the coefficient of $\boldsymbol{\Xi}^s(j_0+1)$ in $\mathbf{Q}_{t,s}(0)$ equals $\bar{\Lambda}_{t-1,j_0+1}(0)$ and the coefficient of $\bar{\boldsymbol{\Xi}}^s(j_0)$ equals $\bar{\Lambda}_{t-1,0}(0)$.

We treat each $j_0 \in [0, J-1-s]$ in three regimes.

Case 3.1 ($j_0 + t - 1 \leq J-1$). The rebirth branch supplies $\sum_{r=0}^{t-2} \Omega_{ss}(r)^{\mathsf{T}} \bar{\Lambda}_{t-2,j_0+1}(r)$ and the survivor branch adds the single term $\Omega_{ss}(j_0+t-1)^{\mathsf{T}} \bar{\Lambda}_{t-2,j_0+1}(j_0+t-1)$. By Remark 4 with

$k = t-2$ and $l = j_0+1$, $\bar{\Lambda}_{t-2,j_0+1}(r) = \mathbf{0}$ for $r \in [t-1, J-1] \setminus \{j_0+t-1\}$, so the two contributions extend to $\sum_{r=0}^{J-1} \Omega_{ss}(r)^\top \bar{\Lambda}_{t-2,j_0+1}(r) = \bar{\Lambda}_{t-1,j_0+1}(0)$ by Definition 7 at $j=0$.

Case 3.2 ($j_0+t-1 > J-1$, $j_0+1 \le J-1$). The survivor reindex falls outside $[0, J-1]$ and contributes nothing. Remark 4 still gives $\bar{\Lambda}_{t-2,j_0+1}(r) = \mathbf{0}$ for all $r \in [t-1, J-1]$, and the same extension to $\sum_{r=0}^{J-1}$ identifies the rebirth sum with $\bar{\Lambda}_{t-1,j_0+1}(0)$.

Case 3.3 ($j_0 = J-1$, $s=0$). Here $l = j_0+1 = J$ lies just outside the index range of Definition 7. Set $\bar{\Lambda}_{0,J}(j) := \mathbf{0}$ for $j \in [0, J-1]$ (the natural extension, since $j \neq J$); the survival and rebirth recursions propagate $\bar{\Lambda}_{k,J}(j) = \mathbf{0}$ to all $k \ge 0$ and $j \in [0, J-1]$. Both the rebirth sum $\sum_{r=0}^{t-2} \Omega_{ss}(r)^\top \bar{\Lambda}_{t-2,J}(r)$ and $\bar{\Lambda}_{t-1,J}(0)$ vanish identically, so the $\bar{\Xi}^0(J)$ coefficients on either side of (B.6) match (both $\mathbf{0}$) regardless of the value assigned to $\bar{\Xi}^0(J)$.

For the $\bar{\Xi}^s(j_0)$ coefficient: only the rebirth branch contributes, giving $\sum_{r=0}^{t-2} \Omega_{ss}(r)^\top \bar{\Lambda}_{t-2,0}(r) = \sum_{r=0}^{J-1} \Omega_{ss}(r)^\top \bar{\Lambda}_{t-2,0}(r) = \bar{\Lambda}_{t-1,0}(0)$, using $\bar{\Lambda}_{t-2,0}(r) = \mathbf{0}$ for $r \ge t-1$ (Remark 4).

For $j_0 \in (J-1-s, J-t]$ (non-empty only when $s \ge t$), the survivor reindex would supply terms with $\bar{\Xi}^s(j_0+1)$, but $\bar{\Xi}^s(j_0+1) = \mathbf{0}$ by Lemma 4 (since $j_0+1 > J-s$), so the closing sum truncates at $j_0 = J-1-s$. Hence

$$\mathbf{Q}_{t,s}(0) = \sum_{j_0=0}^{J-1-s} \left[\bar{\Lambda}_{t-1,j_0+1}(0)\, \bar{\Xi}^s(j_0+1) + \bar{\Lambda}_{t-1,0}(0)\, \bar{\Xi}^s(j_0)\right],$$

matching (B.6) for $t \ge 2$ at $j=0$.

Truncation. For $s \le J-1$, $j-t > J-1-s$ requires $j \ge t$ (otherwise $j-t \le -1$ forces $s > J-1$), hence $s > J-(j-t+1)$. Lemma 4 then gives $\bar{\Xi}^s(j-t+1) = \mathbf{0}$, so the survivor branch of (B.6) vanishes. □

Proof of Theorem 2. **Case 1 ($t=0$).** The result is Claim 5.

Case 2 ($t \ge 1$). For $s \ge 1$, Definition 1 and (22) give $\mathcal{F}_{t,s}(j) = \left(d\mathbf{y}_t^s(j) - d\mathbf{y}_{t-1}^{s-1}(j)\right)^\top \mathbf{D}_{ss}(j) + \mathbf{y}_{ss}(j)^\top \mathbf{Q}_{t,s}(j)$, and the policy difference vanishes by Lemma 2 (at $k=1$). For $s=0$, Definition 1 and (22) give $\mathcal{F}_{t,0}(j) = \mathcal{J}_{t,0}(j) = d\mathbf{y}_t^0(j)^\top \mathbf{D}_{ss}(j) + \mathbf{y}_{ss}(j)^\top d\mathbf{D}_t^0(j)$, in which the first term vanishes by Lemma 1 (at $t \ge 1 > 0 = s$) and the second equals $\mathbf{y}_{ss}(j)^\top \mathbf{Q}_{t,0}(j)$ by the $s=0$ branch of (A.3). In either case, $\mathcal{F}_{t,s}(j) = \mathbf{y}_{ss}(j)^\top \mathbf{Q}_{t,s}(j)$ for every $j \in \{0, \dots, J-1\}$.

For the remainder of the proof, suppose $j-t \le J-1-s$. Since the theorem assumes $s \in \{0, \dots, J-1\}$, the precondition of Lemma 10 is also satisfied. Combining the identity above with Lemma 12 and the shorthand $\bar{\mathcal{E}}_{t-1,l}(j) = \bar{\Lambda}_{t-1,l}(j)^\top \mathbf{y}_{ss}(j)$ yields

$$\mathcal{F}_{t,s}(j) = \begin{cases} \bar{\mathcal{E}}_{t-1,j-t+1}(j)^\top\, \bar{\Xi}^s(j-t+1), & j \ge t, \\ \displaystyle\sum_{j_0=0}^{J-1-s} \left[\bar{\mathcal{E}}_{t-1,j_0+1}(j)^\top\, \bar{\Xi}^s(j_0+1) + \bar{\mathcal{E}}_{t-1,0}(j)^\top\, \bar{\Xi}^s(j_0)\right], & j < t. \end{cases} \tag{B.7}$$

Case 2.1 ($j \ge t$). Iterating the survival branch of Definition 7 $t-1$ times (each application takes place at an age in $\{j-t+2, \dots, j\}$, all positive; the product is empty when $t=1$),

$$\bar{\Lambda}_{t-1,j-t+1}(j) = \mathcal{L}_{ss}(j-1)^\top\, \mathcal{L}_{ss}(j-2)^\top \cdots \mathcal{L}_{ss}(j-t+1)^\top\, \bar{\Lambda}_{0,j-t+1}(j-t+1).$$

Since $\bar{\Lambda}_{0,j-t+1}(j-t+1) = I$, transposing both sides and multiplying by $\mathbf{y}_{ss}(j)$ gives

$$\bar{\mathcal{E}}_{t-1,j-t+1}(j) = \mathcal{L}_{ss}(j-t+1)\,\mathcal{L}_{ss}(j-t+2)\cdots\mathcal{L}_{ss}(j-1)\,\mathbf{y}_{ss}(j) = \mathcal{E}_{t-1}(j-t+1)$$

by Definition 2. The first branch of (B.7) therefore equals $\mathcal{E}_{t-1}(j-t+1)^{\mathsf{T}}\,\boldsymbol{\Xi}^s(j-t+1)$.

Case 2.2 ($j < t$). Since $\bar{\mathcal{E}}_{t-1,0}(j)^{\mathsf{T}}$ does not depend on j_0, factoring it out of the second piece and applying (B.2),

$$\sum_{j_0=0}^{J-1-s} \bar{\mathcal{E}}_{t-1,0}(j)^{\mathsf{T}}\,\bar{\boldsymbol{\Xi}}^s(j_0) = \bar{\mathcal{E}}_{t-1,0}(j)^{\mathsf{T}} \sum_{j_0=0}^{J-1-s} \bar{\boldsymbol{\Xi}}^s(j_0) = \bar{\mathcal{E}}_{t-1,0}(j)^{\mathsf{T}}\,\boldsymbol{\Xi}^s(0).$$

Reindexing $l := j_0 + 1$ in the survivor piece sends $\{0,\dots,J-1-s\}$ onto $\{1,\dots,J-s\}$. Adding the two contributions,

$$\sum_{j_0=0}^{J-1-s} \left[\bar{\mathcal{E}}_{t-1,j_0+1}(j)^{\mathsf{T}}\,\boldsymbol{\Xi}^s(j_0+1) + \bar{\mathcal{E}}_{t-1,0}(j)^{\mathsf{T}}\,\bar{\boldsymbol{\Xi}}^s(j_0)\right] = \sum_{l=0}^{J-s} \bar{\mathcal{E}}_{t-1,l}(j)^{\mathsf{T}}\,\boldsymbol{\Xi}^s(l).$$

Substituting $\bar{\mathcal{E}}_{t-1,l}(j)^{\mathsf{T}} = \mathbf{y}_{ss}(j)^{\mathsf{T}}\,\bar{\Lambda}_{t-1,l}(j)$ and factoring $\mathbf{y}_{ss}(j)^{\mathsf{T}}$ out of the l-sum,

$$\sum_{l=0}^{J-s} \bar{\mathcal{E}}_{t-1,l}(j)^{\mathsf{T}}\,\boldsymbol{\Xi}^s(l) = \mathbf{y}_{ss}(j)^{\mathsf{T}} \sum_{l=0}^{J-s} \bar{\Lambda}_{t-1,l}(j)\,\boldsymbol{\Xi}^s(l) = \mathbf{y}_{ss}(j)^{\mathsf{T}}\,\boldsymbol{\Phi}_{t-1,s}(j)$$

by Lemma 10. The second branch of (B.7) therefore equals $\mathbf{y}_{ss}(j)^{\mathsf{T}}\,\boldsymbol{\Phi}_{t-1,s}(j)$.

Case 2.3 (truncation, $j - t > J - 1 - s$). If $j - t > J - 1 - s$, then $j \geq t$ (otherwise $j - t \leq -1 \leq J - 1 - s$ contradicts the case hypothesis), and the truncation case of Lemma 12 gives $\mathbf{Q}_{t,s}(j) = \mathbf{0}$, so $\mathcal{F}_{t,s}(j) = 0$. Combined with the $s > J - 1 - j$ branch of Claim 5 at $t = 0$, the theorem follows. □

B.3 Algorithm with Dynastic Links

Algorithm 1 assumes no dynastic links ($\Omega_{ss}(\cdot) \equiv \mathbf{0}$). Reinstating them takes only two additions, and both fit inside its single outer loop. First, the newborn shift $\boldsymbol{\Xi}^s(0)$ is no longer zero: by case (ii) of Lemma 9 it accumulates the shocked death-rebirth contributions $\{d\Omega^s_0(j_0)\}_{j_0=0}^{J-1-s}$, which Algorithm 2 builds up in its solver-batch loop (one call to $\overline{\texttt{solve}}_s$ returns a *batch* of shocked objects for all ages $l = 0,\dots,s$). Second, by case (iii) of Theorem 2 the fake news matrices gain entries $\mathcal{F}_{t,s}(j)$ with $j < t$, obtained by propagating the time-1 shift $\boldsymbol{\Xi}^s(\cdot)$ forward through the propagator $\boldsymbol{\Phi}_{t,s}(j)$ of Definition 6.

Both additions fit inside one traversal of the existing outer loop, with no separate sweep to first assemble the shifts and then propagate them, provided that the loop visits the shock horizons starting from the largest, $s = J - 1$, and working down to $s = 0$. To see why this order suffices, note that the seeding step $\boldsymbol{\Phi}_{0,s}(j) \leftarrow \boldsymbol{\Xi}^s(j)$ reads the entire shift vector $\boldsymbol{\Xi}^s(\cdot)$, so we need every entry of that vector in hand by the time the loop reaches s. The

newborn entry $\Xi^s(0)$ is ready because it accumulates contributions from the solver batches at horizons $s, s+1, \ldots, J-1$, and visiting the larger horizons first runs all of those batches no later than iteration s. Each survivor entry $\Xi^s(j)$ with $1 \le j \le J-s$ is ready for the same reason, since the batch at horizon $s+j-1 \ge s$ writes it and that batch too runs before the loop reaches s. The only entries the seeding step never receives from a batch are those with $j > J-s$, and these vanish by Lemma 9, so leaving them at zero is correct. The vector $\Xi^s(\cdot)$ is therefore complete when the loop arrives at s, ready for the death-rebirth propagation.

Up to the newborn accumulation $\Xi^{s-l}(0)$, the solver-batch loop is a literal copy of Algorithm 1; once the descending sweep completes $\Xi^s(\cdot)$, the algorithm seeds $\mathbf{\Phi}_{0,s} \leftarrow \Xi^s$ and propagates it via Definition 6 to write the case-(iii) death-rebirth entries.

Memory. The propagator is advanced in place: computing $\mathbf{\Phi}_{t,s}(\cdot)$ via Definition 6 uses only the previous time slice $\{\mathbf{\Phi}_{t-1,s}(j)\}_{j=0}^{J-1}$, so the algorithm keeps $O(J)$ propagator vectors resident at any instant, independent of the horizon N and the shock date s. It never materializes the full family $\{\mathbf{\Phi}_{t,s}(j)\}_{t,s,j}$, nor the path matrices $\bar{\Lambda}_{t,l}(j)$ of Lemma 10 through which it could equivalently be expressed; each death-rebirth entry is read off as $\mathbf{y}_{ss}(j)^\mathsf{T}\mathbf{\Phi}_{t-1,s}(j)$ and the slice is overwritten as t advances.

Algorithm 2 is correct in the sense of the following lemma.

Lemma 13 (Algorithm correctness with dynastic links)**.** *For every $t \in \{0, \ldots, N-1\}$, $s \in \{0, \ldots, J-1\}$, and $j \in \{0, \ldots, J-1\}$, Algorithm 2 produces the value of $\mathcal{F}_{t,s}(j)$ given by Theorem 2.*

Proof of Lemma 13. Up to the newborn accumulation $\Xi^{s-l}(0)$, the solver-batch loop coincides with Algorithm 1; by the proof of Lemma 5 it therefore writes the $t = 0$ entries (Claim 5), the survivor shifts $\Xi^{s-l}(l+1)$ (case (i) of Lemma 9), and the survivor entries $\mathcal{F}_{t,s}(j) = \mathcal{E}_{t-1}(j-t+1)^\mathsf{T}\Xi^s(j-t+1)$ for $j \ge t$ (case (ii) of Theorem 2), leaving the remaining $t = 0$ and survivor entries at $\mathbf{0}$. It remains to verify the two dynastic additions.

The newborn shift $\Xi^s(0)$ is complete when it is used. For each l the algorithm adds $d\Omega_0^{s-l}(l)^\mathsf{T}\mathbf{D}_{ss}(l) + \Omega_{ss}(l)^\mathsf{T}d\mathbf{F}_0^{s-l}(l)$ to $\Xi^{s-l}(0)$. Writing $\sigma := s - l$, the contributions to $\Xi^\sigma(0)$ arrive at outer iterations $s = \sigma, \sigma+1, \ldots, J-1$; since the loop visits s in descending order, all precede or coincide with iteration σ, so by the end of that iteration $\Xi^\sigma(0) = \sum_{j_0=0}^{J-1-\sigma}\left[d\Omega_0^\sigma(j_0)^\mathsf{T}\mathbf{D}_{ss}(j_0) + \Omega_{ss}(j_0)^\mathsf{T}d\mathbf{F}_0^\sigma(j_0)\right]$, which is case (ii) of Lemma 9.

Case $t \ge 1$, $j < t$. By the previous paragraph $\Xi^s(\cdot)$ is final when iteration s reaches the propagation step, so the algorithm seeds $\mathbf{\Phi}_{0,s}(j) \leftarrow \Xi^s(j)$ and advances $\mathbf{\Phi}_{t-1,s} \to \mathbf{\Phi}_{t,s}$ by the recursions of Definition 6; by induction on t its $\mathbf{\Phi}_{t,s}(j)$ equals the value of Definition 6. The death-rebirth line then sets $\mathcal{F}_{t,s}(j) \leftarrow \mathbf{y}_{ss}(j)^\mathsf{T}\mathbf{\Phi}_{t-1,s}(j)$ for $j < t$, which is case (iii) of Theorem 2 by Lemma 10 (the constraint $j - t \le J - 1 - s$ is automatic for $j < t$). Under $\Omega_{ss}(\cdot) \equiv \mathbf{0}$ this case is vacuous and Lemma 13 reduces to Lemma 5. □

Algorithm 2 Fake news matrices with dynastic links

Input: Steady state: $\{\mathbf{v}_{ss}, \mathcal{L}_{ss}(j), \Omega_{ss}(j), \mathbf{y}_{ss}(j), \mathbf{D}_{ss}(j), \mathbf{F}_{ss}(j)\}_{j=0}^{J-1}$, $\mathbf{X}_{ss}$, and time horizon $N \geq 1$

Pre-compute: $\mathcal{E}_t(j)$ for $0 \leq j \leq J-1$ and $0 \leq t \leq J-1-j$ via Definition 2

Initialize: $\{\mathcal{F}(j)\}_{j=0}^{J-1} \in \mathbb{R}^{N \times J}$ with zeros and $\boldsymbol{\Xi}^s(j) \leftarrow \mathbf{0}$ for $s, j = 0, \ldots, J-1$

for $s = J-1, \ldots, 0$ **do** ▷ Shock horizon, descending

$$\begin{Bmatrix} \mathcal{L}_0^{s-l}(l), & \Omega_0^{s-l}(l), \\ \mathbf{y}_0^{s-l}(l), & \mathbf{F}_0^{s-l}(l) \end{Bmatrix}_{l=0}^{s} \leftarrow \begin{cases} \overline{\texttt{solve}}_s\left(\mathbf{v}_{ss}(s{+}1),\ \{\mathbf{X}_{ss} + \mathbf{1}_{j=s} dx\}_{j=0}^{s}\right), & s < J{-}1 \\ \overline{\texttt{solve}}_{J-1}\left(\{\mathbf{X}_{ss} + \mathbf{1}_{j=J-1} dx\}_{j=0}^{J-1}\right), & s = J{-}1 \end{cases}$$

  for $l = 0, \ldots, s$ **do** ▷ Age at $t = 0$

    $\mathcal{F}_{0,s-l}(l) \leftarrow d\mathbf{y}_0^{s-l}(l)^\intercal \mathbf{D}_{ss}(l) \ + \ \mathbf{y}_{ss}(l)^\intercal d\mathbf{F}_0^{s-l}(l)$

    $\boldsymbol{\Xi}^{s-l}(0) \mathrel{+}= d\Omega_0^{s-l}(l)^\intercal \mathbf{D}_{ss}(l) \ + \ \Omega_{ss}(l)^\intercal d\mathbf{F}_0^{s-l}(l)$ ▷ Accumulate newborn shift

    if $l < J-1$ **then**

      $\boldsymbol{\Xi}^{s-l}(l+1) \leftarrow d\mathcal{L}_0^{s-l}(l)^\intercal \mathbf{D}_{ss}(l) \ + \ \mathcal{L}_{ss}(l)^\intercal d\mathbf{F}_0^{s-l}(l)$

      for $t = 1, \ldots, (J-1) - l$ **do** ▷ Survivor entries

        $\mathcal{F}_{t,s-l}(l+t) \leftarrow \mathcal{E}_{t-1}(l+1)^\intercal \boldsymbol{\Xi}^{s-l}(l+1)$

      end for

    end if

  end for

  $\boldsymbol{\Phi}_{0,s}(j) \leftarrow \boldsymbol{\Xi}^s(j),\ j = 0, \ldots, J-1$

  for $t = 1, \ldots, N-1$ **do** ▷ Death-rebirth, $j < t$

    for $j = 0, \ldots, \min\{t-1, J-1\}$ **do**

      $\mathcal{F}_{t,s}(j) \leftarrow \mathbf{y}_{ss}(j)^\intercal \boldsymbol{\Phi}_{t-1,s}(j)$

    end for

    $\boldsymbol{\Phi}_{t,s}(0) \leftarrow \sum_{r=0}^{J-1} \Omega_{ss}(r)^\intercal \boldsymbol{\Phi}_{t-1,s}(r)$

    for $j = 1, \ldots, J-1$ **do**

      $\boldsymbol{\Phi}_{t,s}(j) \leftarrow \mathcal{L}_{ss}(j-1)^\intercal \boldsymbol{\Phi}_{t-1,s}(j-1)$

    end for

  end for

end for

Output: Fake news matrices $\{\mathcal{F}(j)\}_{j=0}^{J-1}$ of shape $N \times J$

C Application Details

This appendix provides additional details on the application in Section 6. Functional forms follow standard choices in the literature, and the calibration is based on Bardóczy, Savoia, and Velásquez-Giraldo (2024). We begin by fixing externally calibrated parameters, then estimate features of the income process and of household preferences to match income and wealth patterns in the 2019 Survey of Consumer Finances (SCF), and finally calibrate the firm and government sectors. Finally, we present the dynamic acyclic graph representation of the model.

C.1 Functional Forms

Utility from consumption is isoelastic, $u(c) = c^{1-\rho}/(1-\rho)$, where ρ is the coefficient of relative risk aversion. Utility from bequests takes the form proposed by Carroll (2002) and De Nardi (2004):

$$\phi(a) = b\,\frac{(a+\xi)^{1-\rho}}{1-\rho}.$$

This specification makes bequests a luxury good: they are a relatively more important driver of saving for richer households than for poorer ones. The parameter ξ controls this luxuriousness and b the overall intensity of the motive.

Let z denote household productivity. Log-productivity is the sum of an individual fixed effect κ, a deterministic age profile $\{f_j\}_{j=0}^{J-1}$, and an idiosyncratic shock η,

$$\ln(z_{i,t}) = \kappa_i + f_{j(i,t)} + \eta_{i,t}. \tag{C.1}$$

During working years, the shock follows an age-specific Markov process; at retirement, it is fixed at its final working-age value:

$$\eta_{i,t+1} \sim \Pi_{j(i,t)}(\eta_{i,t}) \text{ for } j(i,t) < J^{ret} - 1, \quad \text{and} \quad \eta_{i,t+1} = \eta_{i,t} \text{ for } j(i,t) \geq J^{ret} - 1.$$

C.2 Calibration

The top panel of Table C.1 lists the parameters and processes we fix externally. The steady-state wage rate is normalized to 1.0. For income shocks, we use the persistent component of Janssens and McCrary's (2023) optimal discretization of the nonparametric process estimated by Arellano, Blundell, and Bonhomme (2017). Arellano, Blundell, and Bonhomme estimated the process using the Panel Study of Income Dynamics and reported it for ages 25 to 60; we extend it to age 65 by replicating the last grid and transition matrix. The discretization has 18 states with age-varying grid values and transition probabilities.

We calibrate the remaining household-side parameters to match the life-cycle dynamics of income and wealth in the 2019 SCF and to satisfy equilibrium conditions in steady state.

We proceed in three steps. First, we calibrate the individual fixed effects κ and age intercepts $\{f_j\}$ of the income process in Equation C.1. The age intercepts come from fitting

Table C.1: Calibration of the application model

Quantity	Symbol	Value
Externally calibrated		
Birth age	$j = 0$	26
Retirement age	$j = J_{Ret}$	65
Maximum age	$j = J - 1$	100
Real interest rate	R_{ss}	1.02
Cohort growth factor	Υ_{ss}	1.003
Wage rate	w_{ss}	1.0
Hours	h_{ss}	1.0
Capital share of production	α	0.34
Survival probabilities	$\{\psi(j)\}_{j=0}^{J-1}$	SSA Life tables[a]
Productivity shock distribution	$\eta_{i,j}$	Arellano, Blundell, and Bonhomme (2017) and Janssens and McCrary (2023)
Productivity age-intercepts	$\{f_j\}_{j=0}^{J-1}$	Age polynomial in SCF 2019
Internally calibrated		
Productivity FE dispersion	σ_κ	0.62
Income tax rate	τ_{ss}	0.23
Relative risk aversion	ρ	2.17
Discount factor	β	0.92
Bequest intensity	b	400.82
Bequest shifter	ξ	11.48
Inheritances per capita	I_{ss}	0.29[b]
Capital depreciation	δ	0.11

[a] We use cross-sectional probabilities for the year 2004.
[b] Compare the inheritance number to an average wealth of 7.50.

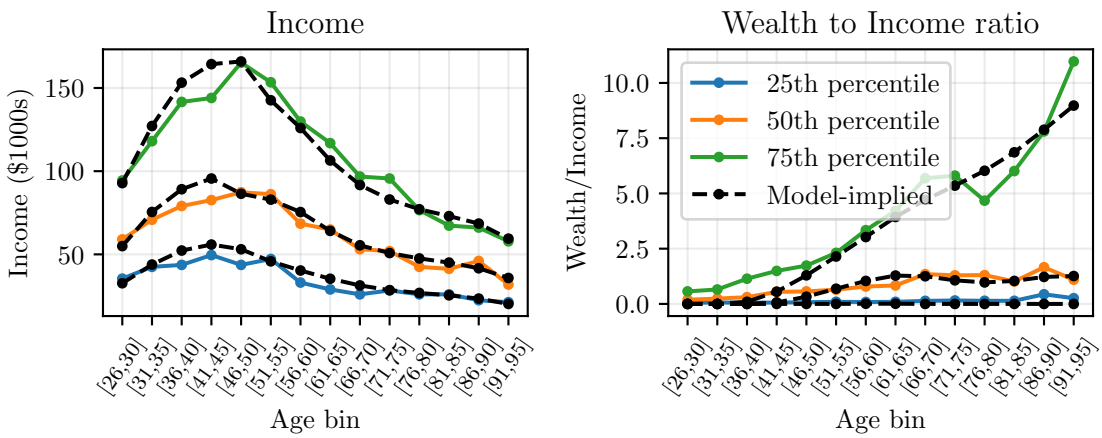

Figure C.1: Household Model Fit of Life-Cycle Income and Wealth

a fifth-degree polynomial in age to log earnings (wage income plus social security and retirement income) of SCF respondents. We assume $\kappa \sim \mathcal{N}(0, \sigma_\kappa)$ and discretize this distribution with three equiprobable points. To pin down σ_κ, we split SCF respondents into five-year age bins ($[26, 30]$, $[31, 35]$, $\ldots$, $[91, 95]$) and compute the 25th, 50th, and 75th percentiles of earnings within each bin. We choose σ_κ to minimize the sum of squared differences between these moments and their model-implied counterparts, taking η and $\{f_j\}$ as given.

Second, with the income process in hand, we find the steady-state tax rate τ that balances the government budget by setting aggregate net transfers T_{ss} to zero. This step is independent of household decisions because the tax and pension-benefit schedules are exogenous to the household.

Third, we estimate the preference parameters $\{\beta, \rho, b, \xi\}$ to match the age profile of savings in the SCF while ensuring that bequests of the dead equal inheritances of the living. We define the wealth-to-income ratio as financial assets over income for respondents with positive income, use the same five-year age bins as before, and target the 25th, 50th, and 75th percentiles within each bin. We search for the values of $\{\beta, \rho, b, \xi\}$ that minimize the weighted sum[20] of squared differences between these moments and their model-implied counterparts, where the model-implied ratio is $a_{i,t}/y_{i,t}$. For each candidate preference vector, we solve for the per-capita inheritance I_{ss} that satisfies

$$\sum_{j=0}^{J-1} \int I_{ss}\, dD^{(3)}_{j,ss}(z, a_{-1}) = \underbrace{\sum_{j=0}^{J-1} \int (1 - \psi_j)\, a_{-1}\, dD^{(1)}_{j,ss}(z_{-1}, a_{-1})}_{B_{ss}}.$$

This is a fixed-point problem: the right-hand side—total bequeathed wealth—depends on the wealth distribution, which in turn depends on per-capita inheritances.

[20]The weights rescale the moments to a common scale by expressing them as relative deviations.

Finally, we set the capital depreciation rate δ to the value consistent with capital demand (10), our assumed 2% real interest rate, and the production implied by the savings and labor supply of households in steady state ($A_{ss} = K_{ss}$ and $N_{ss} = L_{ss}$).

The bottom panel of Table C.1 shows the resulting values for internally calibrated parameters. Figure C.1 shows the fit of the income and wealth to income ratio percentiles targeted in the calibration.

C.3 DAG Representation

To solve for the transition dynamics, we evaluate the model blocks along the following dynamic acyclic graph.

- Unknowns: $\{L_t, K_t, \tau_t, \Gamma_t^{\text{guess}}\}$. Exogenous: $\{\Theta_t, \Upsilon_t\}$.
- Evaluate firm block $\{L_t, K_t, \Gamma_t^{\text{guess}}, \Theta_t\} \to \{Y_t, R_t, w_t\}$.
- Solve household block $\{R_t, \tau_t, w_t, \Upsilon_t\} \to \{C_t, A_t, N_t, T_t, \Gamma_t\}_{t \geq 0}$.
- Targets: $\{T_t, A_t - K_t, N_t - L_t, \Gamma_t - \Gamma_t^{\text{guess}}\}$.
- Verify Walras's law: $\{C_t + K_t - (1 - \delta)K_{t-1} - Y_t\}$.

D Life-Cycle Jacobians Cookbook

This appendix gives a detailed account of how to calculate and use life-cycle Jacobians in practice. Our target audience is readers with a life-cycle model they can solve, and which they would like to integrate into a simulation or policy exercise with equilibrium effects. We want to give users concrete descriptions and visualizations of what each object in our algorithm is and does. We use a simplified version of the household model from Section 6 without population growth, bequests, or individual productivity fixed effects. This appendix covers only how to obtain Jacobians from a life-cycle solver, but we provide public code with examples of how to use these Jacobians in the `sequence-jacobian` toolkit for equilibrium analyses. The public code with these interactive examples and reproductions of all the results in this appendix is available at https://github.com/Mv77/LC-SSJ_public.

Simplified demonstration model. We use a version of the household model in Section 6 with no income fixed effects (κ), no utility from bequests, no population growth ($\Upsilon = 1$) or demographic flows ($\mathbf{F}_t(a) = 0$) and a much simpler productivity shock process (η). This model is not estimated. We set $\rho = 2.0$, $\beta = 0.99$, $\tau = 0.3$, $R = 1.02$. We use the same income age intercepts $\{f_j\}$ and death probabilities $\{\delta_j\}$ as in the main text example. The shock process for η is an AR(1) with an autocorrelation of 0.97 and a standard deviation of 0.2 in its innovations; we discretize it with 9 points. As in the main text example, productivity becomes constant when the household retires.

Standard implementation of life-cycle models. Our starting point to apply the algorithm introduced in Section 5 is a life-cycle model solved by backward induction with aggregate variables taken as given. A partial equilibrium implementation makes no distinction between time and age: it represents the problem of a cohort that has age 0 at time 0, age 1 at time 1, and so on. Such an implementation commonly has the following structure:

- There are age-specific grids that discretize the state space of every age $\{\mathcal{G}_j\}_{j=0}^{J-1}$.[21]
- There are age-varying parameters that affect the agent's problem, for example, an age-profile of productivity or a sequence of tax rates. We separate the input with respect to which we want to compute Jacobians, $\mathbf{X}$, and write the sequence of age-varying parameters as $\{\vartheta_j, \mathbf{X}_j\}_{j=0}^{J-1}$, where ϑ collects the rest of parameters.
- There are age-specific solvers $\{\texttt{solve}_j(\cdot)\}_{j=0}^{J-1}$ which, given the solution of age $j+1$, find the solution of age j. To lighten the notation, we incorporate the auxiliary parameters $\{\vartheta_j\}$ into the definition of these solvers and stop writing them. The "solution" of an age comprises its policy function $\mathbf{y}(j)$, value function $\mathbf{v}(j)$, survival transition matrix $\mathcal{L}(j)$, death-to-birth transition matrix $\Omega(j)$, and flow vector $\mathbf{F}(j)$.

$$\mathbf{y}_j(j),\, \mathbf{v}_j(j),\, \mathcal{L}_j(j),\, \Omega_j(j),\, \mathbf{F}_j(j) = \texttt{solve}_j\left(\mathbf{v}_{j+1}\left(j+1\right), \mathbf{X}_j\right).$$

[21] A reason why grids might be age-varying is that certain states might disappear after certain ages. For example, income shocks to a household might be turned off after retirement.

The vectors $\mathbf{y}_j(j)$ and $\mathbf{v}_j(j)$ are defined on grid $\mathcal{G}_j$, and transition matrices $\mathcal{L}_j(j)$ and $\Omega_j(j)$ have dimensions $|\mathcal{G}_j| \times |\mathcal{G}_{j+1}|$ and $|\mathcal{G}_j| \times |\mathcal{G}_0|$, respectively.

With this implementation, we define two additional objects:

- Auxiliary functions that solve the dynamic problem up to an age j. These functions, which we will denote with $\overline{\texttt{solve}}$, take as input the continuation value function $\mathbf{v}_{j+1}(j+1)$ and parameters up to age j:

$$\{\mathbf{y}_l(l),\, \mathbf{v}_l(l),\, \mathcal{L}_l(l),\, \Omega_l(l),\, \mathbf{F}_l(l)\}_{l=0}^{j} = \overline{\texttt{solve}}_j \left(\mathbf{v}_{j+1}(j+1), \{\mathbf{X}_l\}_{l=0}^{j}\right).$$

  Each function $\overline{\texttt{solve}}_j$ chains backward applications of single-period solvers $\{\texttt{solve}_l\}_{l=0}^{j}$.

- The steady-state solution is that obtained when the aggregate input is at its steady-state value $\mathbf{X} = \mathbf{X}_{ss}$ at every age

$$\{\mathbf{y}_{ss}(j),\, \mathbf{v}_{ss}(j),\, \mathcal{L}_{ss}(j),\, \Omega_{ss}(j),\, \mathbf{F}_{ss}(j)\}_{j=0}^{J-1} = \overline{\texttt{solve}}_{J-1} \left(\{\mathbf{X}_{ss}\}_{j=0}^{J-1}\right).$$

  Since $J-1$ is the terminal age, $\overline{\texttt{solve}}_{J-1}$ does not have a continuation value function as input.

Instantiation of our demo model. For the demonstration model in this appendix, the specific instantiation of these objects is the following.

- Each age-specific grid $\mathcal{G}_j$ contains every combination of persistent income shock η and start-of-period savings a_{-1}. We use 9 points for η and 51 for a_{-1}. Hence, $\mathcal{G}_j$ has 459 elements for every j and we represent them as two-dimensional tensors, one dimension for each variable.
- The parameters that are not aggregate inputs $\{\vartheta_j\}_{j=0}^{J-1}$ include preferences like ρ and β, the age-fixed effects that trace the life-cycle profile of productivity f_j, and the transition matrix for the income shock, among others. The aggregate inputs are $\{R_j, \tau_j, w_j\}_{j=0}^{J-1}$, plus a pension multiplier that we use for our equilibrium demonstration in the public code.
- The outputs of age-specific solvers are as follows
  - $\mathbf{y}_j(j)$ are vectors evaluating the idiosyncratic outcomes of interest in every point of $\mathcal{G}_j$. These outcomes include the consumption and savings of surviving households, the bequests left by dying households, and the supplied effective units of labor among others.
  - $\mathbf{v}_j(j)$ must be vectors with all the properties of the value function that are necessary for the solution of the model, evaluated on every point of $\mathcal{G}_j$. This particular model can be solved with Carroll's (2006) method of endogenous gridpoints (EGM), which requires only the derivative of the value function with respect to assets,

$$\frac{\partial}{\partial a_{-1}} V_j(\eta, a_{-1}) = R_j \cdot (1-\delta_j) \times [c_a^*(\eta, a_{-1})]^{-\rho}.$$

where $c_a^*(\cdot)$ is the optimal consumption function for age a. More complex models can require tracking more properties of the value function.[22]

- $\mathcal{L}_j(j)$ transform measures over (η_j, a_{j-1}) to measures over (η_{j+1}, a_j). This entails applying survival probability $(1-\delta_j)$, using the solved consumption function to find savings, and applying the income shock transition. This could be achieved with a 459×459 transition matrix. Instead, we build a more efficient representation of these matrices that exploits the fact that the income shock transition is conditionally independent from the savings choice.
- $\Omega_j(j)$ are zero-matrices because this example does not consider explicit intergenerational links.
- $\mathbf{F}_0(0) = \eta$ to represent the entry of newborns; $\mathbf{F}_j(j) = 0$ for $j > 0$.

Practically, the age-specific solver for this model $\texttt{solve}_j\left(\mathbf{v}_{j+1}\left(j+1\right), \mathbf{X}_j\right)$ has four steps. First, it applies EGM to find optimal consumption on an endogenous grid that does not match $\mathcal{G}_j$. Second, it interpolates consumption onto $\mathcal{G}_j$. Third, it uses on-grid consumption to evaluate the marginal value function and any relevant outcome points needed to construct $\mathbf{v}_j(j)$ and $\mathbf{y}_j(j)$. Fourth, it uses on-grid savings and the lottery/histogram method of Young (2010), survival probabilities, and the income process to find the transition probabilities in $\mathcal{L}(j)$.

D.1 Inspecting fake news matrices and Jacobians

We now depict and narrate the outputs of Algorithm 1 in the main text, and of the age- and cohort-specific Jacobians that we use throughout the paper. For this example, we apply the algorithm to the simplified demonstration model.

The main outputs of the algorithm are age-specific fake news matrices. Theorem 1 says that, without dynastic links, $\mathcal{F}_{t,s}(j)$ can be different from zero only if $0 \leq j - t \leq J - 1 - s$. This restriction isolates the agents who were alive when the shock was announced $(0 \leq j - t)$ and who would still be living when the announced shock hits $(j - t \leq J - 1 - s)$. Figure D.1 depicts these non-zero regions of the fake news matrices associated with various different ages. This representation communicates why our algorithm is efficient: most of the (t, s, j) combinations are zero, we can safely skip them, and we do.

To solve for macroeconomic equilibrium dynamics, we use aggregate Jacobians. We obtain them using $\mathcal{F} = \sum_{j=0}^{J-1} \mathcal{F}(j)$ and then $\mathcal{J}_{t,s} = \sum_{k=0}^{\min\{t,s\}} \mathcal{F}_{t-k,s-k}$. Other sectors of the economy interact with the household sector through these aggregate Jacobians, just like in Auclert et al. (2021a).

After we have found the equilibrium dynamics of household block inputs, we can easily explore the behavior of different age groups and cohorts. We start with age-specific Jacobians, $\mathcal{J}(j)$, which we construct from age-specific fake news matrices using (23). The dynamic response of households aged j to input shift $d\mathbf{X}$ is $\mathcal{J}(j) \cdot d\mathbf{X}$. The responses are additive; for example, the response of working-age households (like we show in Figure 2) is

[22] For example solution methods for discrete-continuous problems can require both the level and derivative of the value function (see, for example, Iskhakov et al. 2017; Dobrescu and Shanker 2024)

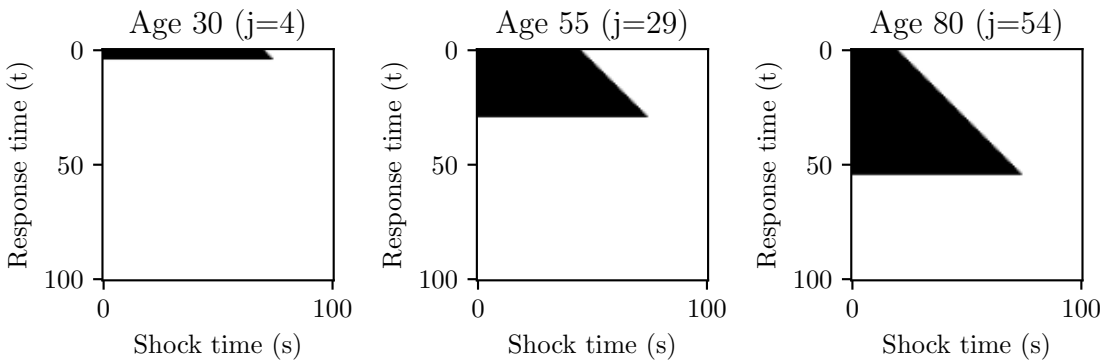

Notes: each panel depicts the zero and non-zero elements of $\mathcal{F}(j)$ for different values of j. Non-zero elements are black and zero elements are white. The depicted matrices correspond to the response of consumption (C) to the interest factor R.

Figure D.1: Non-Zero Elements of Age-Specific Fake News Matrices $\mathcal{F}_{t,s}(j)$

$\left(\sum_{j=0}^{40} \mathcal{J}(j)\right) \cdot d\mathbf{X}$. The groups of households that compose these dynamic responses shift over time—newborns enter and 65-year-olds exit the group of working-age households every year. One might instead be interested in the responses of a fixed cohort of households over time. Cohort Jacobians $\mathcal{J}^{cohort}(j)$, defined in (33), conveniently track these responses. The dynamic response of the cohort of households that had age j at time 0 to input shift $d\mathbf{X}$ is $\mathcal{J}^{cohort}(j) \cdot d\mathbf{X}$. Figure D.2 compares the age and cohort Jacobians associated with the consumption response to interest rate increases that happen at different horizons.

a) Consumption Response to 1 p.p. increase in R, by age groups

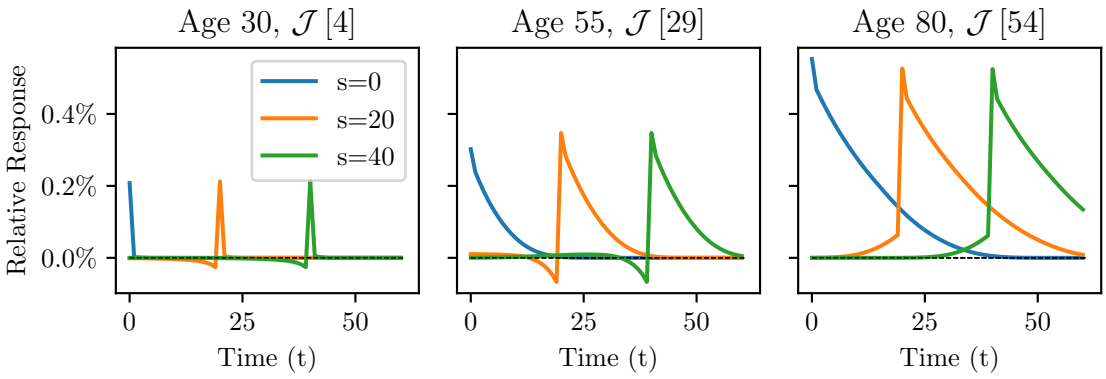

b) Consumption Response to 1 p.p. increase in R, by cohorts

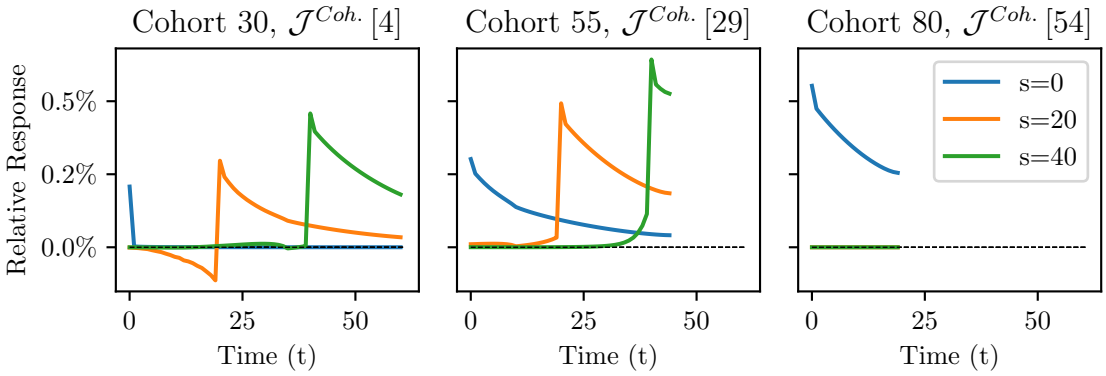

Notes: t denotes the time since the shock was announced and s denotes the time when the shock occurs. Responses are normalized by steady-state aggregate consumption of the relevant age group or cohort at the given time. Panel a) shows the dynamic responses of different age groups; a given household can move across groups as time advances. Panel b) shows the dynamic responses of different cohorts of households; cohorts are indexed by their age at time 0. These responses are cut short when the cohorts exit the model, as they reach age 100.

Figure D.2: Age- and Cohort-Specific Jacobians of Consumption